Investigation of the Effects of a Pulsed Electrode on a Magnetized Plasma

A Thesis
Presented to
The Academic Faculty

by

Richard Logan

In Partial Fulfillment
of the requirements for the Degree
Doctor of Philosophy in Nuclear Engineering

Georgia Institute of Technology
April 1995

Investigation of the Effects of a Pulsed Electrode on a Magnetized Plasma

Approved:

Weston M. Stacey, Chairman

A. V. Larson

Glenn Smith

Richard Browner

John Mandrekas

Date Approved 3/15/95

Acknowledgments

This work was made possible through the efforts of a number of people. Dr. Mike Hayes, the first of my three advisors at Tech, encouraged my interest in plasma physics when I was just another unsupported graduate student. Mike welcomed me into his lab and, most significantly, played a major role in the development of the proposal that won a NASA Graduate Student Researchers Fellowship at the Lewis Research Center. Mike remains a Good and supportive friend.

Dr. Bruce Dewald made me aware of the NASA fellowship program. Through the years, Bruce supported my work in the lab and always listened to my late night tirades when experiments weren't going well.

Dr. Joe Shonka has supported me since my fellowship ran out. Without Joe, there is no way this work could have been completed and I would not have my Ph.D. Joe, a Georgia Tech graduate, is always willing to help out graduate students in need. The world needs more people like Joe.

I need to thank Jerry , Peter, Dr. John Mandrekas, Regen, Heping, Drew and most especially Danika for helping me through many tough spots.

Finally, I need to thank my family. My mother and father, brother and sister, grandparents, aunts and uncles and cousins all contributed in major ways to my desire to learn and succeed. The experiences of my childhood (walks on the beech with Mary, gardening with Aunt Rose and Aunt Sophie, summer trips to New Hampshire with my parents) made me want to learn more about the natural world and have resulted in this degree.

This thesis is a shade of what I wanted it to be. The complete freedom I had as a graduate student was paid for with the many hours spent in the library trying to find the most basic information about experimental techniques. The search for the basics (how do you get the signal out from an emissive probe?) ate up most of the short time I had as a NASA fellow. When everything finally came together, it was time to move on. So, I apologize to any reader for the short descriptions and lack of detail. The phenomenon I am about to describe is really more interesting than this work makes it seem.

Table of Contents

List of Tables

List of Figures

Summary

The electrodynamic tether is a device proposed to provide power to space vehicles in near earth orbit. The interaction of the tether with the ambient ionospheric plasma is still being investigated and is not well understood. Several models of this interaction are reviewed in this thesis. One model, the anisotropic contactor model, predicts the formation of electrostatic double layers near a current collecting plasma contactor. Detailed experiments performed at UCLA indicate the tether interaction with the ionosphere is more complicated than the anisotropic model predicts. In particular, it was found not to be possible to collect a steady state current from the laboratory plasma and no evidence of collected current levels above the electron saturation current was observed. This thesis reports results of experiments performed in a magnetized plasma with parameter ratios characteristic of the ionosphere. Current collecting probes, capacitive probes and magnetic loop probes were used to investigate the effects of a pulsed disc probe on the plasma. The results of this work indicate the pulsed electrode creates a complicated potential structure in the magnetized plasma and is also responsible for initiating a high frequency electrostatic instability in the plasma. In addition, observations of fluctuations in the current collected from the plasma support the idea that a steady state current can not be collected in the ionosphere.

CHAPTER I

Introduction

The electrodynamic tether is being considered as a power source for orbiting spacecraft[1]. In principle, a long conducting wire, the tether, traveling across the Earth's geomagnetic field can generate a substantial potential difference across its two ends. The magnitude of this potential difference is determined by Faraday's law which relates the electromotive force around an electrical circuit to the time rate of change of the magnetic flux through the circuit. If the tether can also be made to draw an electric current from its surroundings then it can be used as a power source by a spacecraft. The objects that collect charge from the ionosphere and transfer it to the tether are called contactors. Recent theoretical and experimental work suggests the most effective contactors are clouds of plasma emitted from plasma sources at each end of the tether. These plasma clouds are called plasma contactors[2].

In the past few years, substantial work has gone into predicting the maximum current that can be coaxed out of the ionosphere. Some of this interest has been generated by the anticipated deployment of a scale model of the electrodynamic tether from the space shuttle while other work has been motivated by a desire to protect satellites from destructive plasma discharges. Satellite potential exceeding 19,000 volts have been recorded[3]. Arcing from high-voltage solar arrays is also a problem that requires a better understanding of current collection by orbiting structures[4]. Finally, the interaction of the space shuttle with its environment[5], through the current collected by its exposed engine nozzles, is suspected of causing broad band electrostatic noise[6] and other electrodynamic effects[7] [8] that can potentially interfere with

orbiting plasma experiments. It turns out that estimating this current is not a simple matter because of the complexity of the tethers plasma environment[9]. Recent theoretical work has attempted to study this interaction by employing models of ever greater sophistication. However, novel ground based experiments have once again shown that plasmas behave in quite unexpected ways.

Early work on current flow between biased conductors

Investigations of current collection by orbiting spacecraft have their roots in the pioneering work done by Irving Langmuir in the 1920's on current flow in gas discharge tubes. Langmuir discovered that the maximum current that can be emitted by a hot filament in a vacuum tube was limited by the very current it emitted. In addition, he discovered the limiting effect of probe geometry on current collection in ionized gases. The concept of space-charge limited current and the limiting effects of probe geometry are as applicable to spacecraft as they are to vacuum tubes.

Langmuir's studies began with the investigation of the current emitting properties of tungsten filaments in vacuum tubes. Previous work on thermionic current emission suggested that the current emitted by a heated tungsten filament should increase dramatically as the filament temperature increases:

$$i = a\sqrt{T}\,\mathrm{e}^{-\frac{b}{T}}$$

This is Richardson's equation: a and b are constants, T is the absolute temperature of the material and i is referred to as the saturation current. Langmuir's own investigations, however, showed that the current becomes independent of the filament temperature if the filament is heated above a critical temperature that depends on the filament voltage. This result is presented in Figure 1[10].

Langmuir's experiments were conducted by studying the electric current collected by a positively biased conducting plate placed in the vicinity of the electron emitting filament. He idealized these experiments by considering the electrons to be emitted by one infinite plane conductor and collected by another infinite plane conductor. The collecting plane is biased at a positive potential with respect to the emitting plane. This bias produces an electric field between that plates that varies linearly with position and causes the emitted electrons to accelerate toward the positive plane. Langmuir realized that as the electron current increased a situation could arise where the density of electrons traveling between the plates was so great it would significantly alter the electric field between the plates and prevent the further emission of electrons. He then derived an expression for the maximum current that can pass between the two electrodes. A complete account of the derivation is given beginning on page 8 of the previous reference but the important result is that the maximum current that can be collected by the positive electrode varies as the 3/2 power of the potential difference:

$$i = \frac{\sqrt{2}}{9\pi}\sqrt{\frac{e}{m}}\frac{V^{3/2}}{x^2}$$

where e and m are the charge and mass of the particles emitted from the cathode. Langmuir called the charge density between the plates space charge. The value of the space charge limited current depends only on the potential difference between the conductors, their separation and on their geometry. The effects of space charge have since been seen in a wide variety of situations including the thermal emission of electrons from metals[11], the breakdown of neutral gas in electric fields[12] and many other circumstances.[13]

A probe in a plasma is surrounded by a sheath, a region where the normally neutral plasma becomes charged because the probe is collecting either the positive or negative constituent of the plasma and repelling the other. For large probes (those that have a sheath thickness small compared to the physical dimension of the probe), the situation is analogous to the two planes used by Langmuir to discuss space

charge limited current flow. The plasma acts as a source of charged particles with some distribution of initial velocities. These particles travel through the non-neutral probe sheath and, for sufficiently high probe biases, play a dominant role in determining the current collecting ability of the probe. The current collectors used to supply current to the electrodynamic tether can be thought of as large plasma probes. Therefor, to produce maximum possible power, the tether current should be space-charge limited.

Let it be mentioned in passing that the characteristic current plateau that occurs when using wire probes in thermal, unmagnetized plasmas is not necessarily a space charge limited current. In this case the sheath dimension is large compared to the dimension of the probe and it is possible for charged particles to scatter out of the sheath rather than be collected by the probe. For instance, the maximum current collected by a cylindrical wire probe increases as $v^{1/2}$ rather than $v^{3/2}$. Langmuir termed this probe current limited by orbital motion[14]. It is possible that the current collected by small tether plasma contactors will be limited to this smaller value.

A simple model of current collection in a magnetic field

Parker and Murphy[15], in their study of electron collection by orbiting satellites, studied an analogous situation when they investigated the effect strong electric fields have on current collection from magnetized plasmas. A charged particle in a magnetic field cannot move very far in a direction perpendicular to the direction of the field. Such motion produces a force on the particle that alters its velocity in such a way that the particle is forced back to its initial position. A plasma is said to be magnetized when the motion of its constituents is significantly affected by this force. An estimate of the importance of this effect in a particular situation can be had by comparing the Larmor radius (also called the gyro or cyclotron radius):

Table 1. *Drift equation solutions for a Coulomb potential*

Sphere potential (volts)	collection area ratio $(r_0/a)^2$	$(dr/dz)_{max}$
1	1.0025	0.0011
10	1.025	0.011
10^2	1.246	0.097
10^3	3.107	0.60
10^4	13.58	2.2
10^5	69.92	7.2
10^6	292.0	22.8
10^7	1355	72.1
10^8	6303	228

The data for this table is taken from the paper by Parker and Murphy. Notice the extremely high voltages that are necessary to collect current across the geomagnetic field.

$$r_L = \frac{mv}{eB}$$

(where m and e are the particle mass and charge, v is its velocity, and B is the magnitude of the magnetic field, all in MKS units) to other dimensions characteristic to the problem. Thus, a plasma can be considered magnetized at one scale length and unmagnetized on another.

Parker and Murphy considered the plasma electrons to initially be magnetized and neglected any perturbing effects electron collection would have on the plasma environment. The authors considered the effect a large satellite potential (defined with respect to the ionospheric plasma potential) would have on current collection. This potential gives rise to a radial drift of electrons toward the satellite

$$v_r = -\left(v_z / m\omega^2\right)\frac{\partial^2 \phi}{\partial r \partial z}$$

where z and r are directions along and across the magnetic field, m is the mass of the electron, ω is the electron cyclotron frequency and Φ is the electrostatic potential energy of the electron in the field produced by the satellite. All units are in the MKS system. Note that this is not the ExB drift discussed in most textbooks on plasma physics. Rather, this is a drift caused by the variation of the electric field with distance from the satellite and is orders of magnitude smaller than the ExB drift. The equation can be integrated and used to find the maximum radius from which current can be collected. This then gives an estimate of the maximum current that can be collected by the satellite. The results are summarized in Table 1.

These results are valid as long as $v_r < v_z$ or, equivalently, $dr/dz > 1$. Rewriting the previous equation using the potential function for the coulomb potential and equating the result to 1

$$\frac{dr}{dz} = 1 = \frac{3\phi_0}{m\omega_c^2 a^2} \frac{a^3 rz}{\left(r^2 + z^2\right)^{5/2}}$$

(a is the satellite radius, Φ_0 is the magnitude of the potential energy of an electron at the surface of the satellite) leads to the identification of a potential above which this drift approximation is invalid

$$v < 4200\left(aB\right)^2$$

For satellite potentials above this value a rigorous bound on the collected current can still be found by studying the equations of motion of the electrons. Following much the same procedure used, the authors find the limiting current to be

$$\frac{I}{I_0} = \frac{r_0^2}{a^2} < 1 + \left[8\Phi_0 \Big/ \left(m\omega_c^2 a^2 \right) \right]^{1/2}$$

(r_0 is the maximum distance across the magnetic field from which the satellite can collect electrons) which, for high potentials, predicts a smaller value for the collected current than that found using the drift approximation. These results suggested that very large satellite potentials are required to enhance the current collected by the satellite to an order of magnitude above the saturation current to the satellite. Note that the maximum current increases as $v^{1/2}$ indicating the current is limited by the geometry of the system. This suggests that relying solely on very large electric fields to collect current is not particularly efficient.

Current collection using plasma clouds

Wei and Wilbur[16] investigated the possibility of collecting significant currents from the ionosphere using gaseous electrodes. Since the magnitude of the collected current scales directly with the size of the current collecting electrode it is advantageous to have as large a collector as possible. However large collectors, such as metallized balloons, have a large drag coefficient so they are undesirable if an extended stay in space is anticipated. Gaseous collectors, consisting of ionized plasma clouds, have the advantages of a lower drag coefficient, an adjustable current collecting area (adjustable by varying plasma density and temperature) and the possibly current enhancing effects of emitting charged particles directly into the ionosphere.

The problem studied Wei and Wilbur can be described as an investigation of current flow in a spherically symmetric double sheath. A double sheath is formed by charged particle emission from two particle sources. The sources are of different polarity so that the source-emitting electrons, say, also

collects the ions emitted by the other source. Each source is enclosed in a non-neutral sheath so the system is described as having a double sheath. The spherically symmetric sources are biased so that a current flows between the concentric shells.

The authors solve Poison's equation in spherical coordinates using the boundary conditions required for space-charge limited emission: $dv/dr = 0$ at each surface. When this condition holds the charge density between the spheres has become so great that the electric field driving the current flow at the surface of each source is reduced to zero. If the charge density were to increase above this critical value, the surface electric fields would reverse direction and actually act to inhibit further particle emission. An excellent discussion of this topic begins on page 8 of the first reference.

By integrating Poison's equation across the region separating the two spheres a condition relating the ratio of the electron to ion current, a, to the normalized electron current, j_0, is found. The result is presented as a graph of the current ratio as a function of the ratio of the sphere radii. The current ratio increases almost linearly with radius ratio suggesting that plasma contactor clouds need to be very large in order to draw significant space charge limited current from the ionosphere. In addition, the current collected from the ionosphere is found to scale as the 3/2 power of the applied potential, emphasizing the superior performance of the plasma cloud over the passive collectors studied by Parker and Murphy.

A more detailed study of the interaction of a plasma source with the ionosphere was performed by Iess and Dobrowolny[17]. The authors consider a three species plasma consisting of plasma contactor ions, ionospheric ions and ionospheric electrons. Plasma contactor electrons are not considered because the plasma cloud is assumed to be biased to collect electrons. The effect of the geomagnetic field is neglected because the authors assume the effect of the plasma contactor electric field will be orders of magnitude greater than any possible magnetic field effects. They reach this conclusion simply by comparing the relative strengths of the electric and magnetic fields.

The object is to solve Poison's equation

$$\frac{1}{\hat{r}^2}\frac{d}{d\hat{r}}\left(\hat{r}^2\frac{\partial\hat{\phi}}{\partial r}\right) = A\left(\frac{n_{i1}}{n_1}+\frac{n_{i2}}{n_1}+\frac{n_{e11}}{n_1}\right)$$

$$A = -\left(\frac{r_0}{\lambda_{de}}\right)^2\frac{n_1}{n_2}\frac{1}{\hat{\phi}_0}$$

$$\hat{r} = r/r_0 \qquad \hat{\phi} = \phi/\phi_0$$

by eliminating the density variables (n_{i1}, n_{i2}, n_{e1})through the use of appropriate conservation equations. In the equation above, Poisson's equation has been written in dimensionless form using spherical coordinates. The subscripts e and i refer to electron and ion quantities, n_1 is the plasma density at r_0 and f is the electrostatic potential at position r. The parameter r_0 is loosely defined as 1) the distance at which the source electron density has dropped to zero and 2) the expansion of the plasma cloud into the ambient plasma has become spherically symmetric. The conservation equations that need to be solved are:

Ion energy conservation

$$\frac{m_{i1}}{2}\left(v_{i1}^2 - v_0^2\right) = e\left(\phi_0 - \phi\right)$$

where f_0 is the electrostatic potential at r_0 and the v's refer to the ion velocity. This equation equates the energy gained by the contactor ions as they are pushed out of the contactor cloud with their gain in potential energy.

Ion mass conservation.

$$v_{i1}n_{i1}r^2 = v_0 n_1 r_0^2$$

This says the outward ion flux at a position r in the cloud must be equal to the ion flux at the source.

Electron momentum conservation.

$$\frac{e}{m_e}\frac{d\phi}{dr} = \frac{kT_{c2}}{m_e}\frac{d\ln n_{c2}}{dr} + v_{c2}\frac{dv_{c2}}{dr} + \nu^{[1]}\left(v_{c2} - v_{i1}\right) + \nu^{[2]}v_{c2}$$

The possible effects of plasma turbulence are include in this equation through terms proportional to the relative velocities of the particles.

Electron mass conservation

$$v_{c2}n_{c2}r^2 = v_{c0}n_0r_0^2$$

The subscript s refers to the population of electrons at the source position r_0.

Poison's equation is solved separately for the dense plasma contactor cloud and the ambient plasma. A normalized electron flux is defined

$$\Psi_s = \frac{n_s v_s r_s^2}{n_0 v_0 r_0^2}$$

and considered to be an eigenvalue of the problem used to match the solutions in the two separate regions. The subscripts s and 0 refer to quantities measured at the (arbitrary) position s and the position r_0. n and v are the electron density and velocity at these two positions.

The results of this work indicate plasma clouds can significantly increase the amount of current collected from the ionosphere and that this enhancement factor is

$$i = jAv$$

a decrease in v due to the turbulent fields will reduce the total current (A is the area of the charge collecting surface).

Finally, a parameter regime is identified in which electrostatic double layers form. Double layers are similar to the sheaths that surround probes in that they are regions of non-neutral plasma. However, unlike sheaths, which are found only near current collecting electrodes, double layers are not associated with a material boundary. Double layers are relatively common laboratory objects and are frequently associated with charged particle acceleration and enhanced noise levels in the plasma[18]. The authors do not directly comment on the effect double layers have on current collection except to mention that they occur in regions where the electron drift velocity greatly exceeds the thermal velocity. When this occurs it is very possible for the electrons to excite any one of a number of plasma instabilities. Since the authors comment that such instabilities tend to reduce the total current it can be assumed that the parameter regime in which double layers are found should be avoided.

Double layers

Since double layers play a very important role in the next model, a brief description of their history and properties is given here. Double layers are likened to shock waves in a plasma because, as in a shock wave, the parameters describing the medium (in this case, charged particle density and temperature) are very different on either side of the double layer[19]. The most pronounced difference is the change in plasma potential as the double layer is crossed. Typically, the plasma potential changes by an amount greater than several times the electron temperature over a distance small compared to the Debye length. This abrupt change in potential produces very large electric fields that are also associated with depletion of the plasma density and violation of charge neutrality.

Montgomery and Joyce[20], expanding on work done earlier by Bernstein, Greene and Kruskal[21], showed that a necessary condition for the existence of double layers is a trapped distribution of particles on either side of the layer. The positive side of the double layer contains trapped ions and the negative side contains trapped electrons. Although the necessity of trapped particles had already been realized, Montgomery and Joyce showed that a shock like solution to the Vlasov equation (or collisionless Boltzmann equation) could exit with realistic distributions of charge. Previous to their work the importance of these solutions was not realized because it was thought the shocks could exist only if the required charge distributions were negative or otherwise unrealistic[22].

Although this work shed light on the conditions needed to maintain the double layer it does not explain how the double layer forms. This topic remains an active field of research[23]. Carlqvist speculated the double layer forms because the plasma is unstable to perturbations in the plasma density[24]. He derived a relation between the plasma density and temperature that placed an upper limit on the thermal current (defined as $-env_e$) that can be supported by the plasma (a very detailed account of this theory, along with a discussion of other double layer phenomena, is given by Block[25]). When this critical current is exceeded, the plasma becomes unstable to the formation of double layers. Quon and Wong[26] did indeed observe the growth of a double layer associated with an abrupt change in the plasma potential, produced by changing the bias voltage of their plasma source, when the electron drift speed exceeded the thermal velocity.

This, however, is not the end of the story. Potential structures resembling double layers have been observed in laboratory plasma contactor experiments[27] where a high density plasma cloud, produced by a hollow cathode plasma source, expands into an ambient background plasma. Hairapetian and Stenzel have observed current free double layers[28] in a uniformly magnetized plasma. The double layers were observed as long as the neutral pressure was low enough to ensure that ionization and charge exchange collisions do not occur. The source used by the authors produced a plasma with an essentially Maxwellian electron distribution with a high energy tail population. The double layer was observed to form where the

density of these two populations becomes equal. The low energy, Maxwellian electrons are trapped on the high potential side of the double layer and the hotter, tail population is trapped on the low potential side.

Finally, double layers have been observed when no external electric field is applied across the plasma boundaries[29]. The experiments were conducted in the so called triple plasma device: two plasma sources are located in separate chambers separated by a third interaction chamber. In this case, the source chambers were separated from the interaction chamber by grounded grids. The authors observe double layers whenever the sources are biased so that ions flow into the high potential side of the double layers and electrons flow into the low potential side. No double layers are observed when the sources are biased so that no ions can enter the interaction chamber. The authors also observed that when both plasma sources are held at ground potential the direction of the double layer electric field is seen to depend strongly on the neutral pressure.

Plasma contactor operation in a magnetic field

An example of a theory which describes current collection from a magnetized plasma is the work of D. E. Hastings[30]. For a plasma cloud to collected large amounts of current, a method must be found to cause the magnetized ionospheric electrons to move across the geomagnetic field. In high density plasma clouds, this cross field motion is brought about by the heating of the cold ionospheric electrons by the hot contactor plasma[31]. Since the Larmour radius of the electrons depends on their temperature, they can travel a greater distance across the magnetic field as they heat up. This distance is often given as a limit on the current collecting radius of the plasma cloud.

The authors investigate the possibility of collecting current from regions far removed from the dense plasma contactor core, defined by the Larmour radius, by exciting turbulence in the plasma surrounding the core[32]. This plasma is composed of the essentially unmagnetized plasma contactor ions streaming

away from the source as well as the constituents of the ionospheric plasma. Electrons in this region will have a drift velocity determined by gradients in the plasma parameters

$$v_d = \frac{e}{m_e \omega_{ce}} \frac{\partial \phi}{\partial r} - \frac{1}{m_e \omega_{ce}} \frac{\partial T_e}{\partial r} - \frac{T_e}{m_e \omega_{ce} n_e} \frac{\partial n_e}{\partial r}$$

This drift velocity is perpendicular to the direction of the magnetic field and will drive a radial flux of charged particles. The force driving this flux can qualitatively be written as

$$F = f_e m_e v_d$$

where f_e represents an effective collision frequency. The drift velocity can be then be written as

$$v_r = v_d f_e / \omega_{ce}$$

so that a large effective collision frequency can cause a significant inward flow of current.

The authors assume that the total potential drop from the contactor anode to the ambient plasma is much greater than either the contactor electron temperature or the ambient ion temperature. This condition guarantees electrons will not drift away from the anode and the ambient ions will be prevented from reaching the anode and is thus equivalent to assuming the existence of trapped electron and ion populations. It is then not unreasonable to expect double layers to form. However, if double layers form they are unlikely to be spherically symmetric due to the effects of the magnetic field. Rather, double layers may form both upstream and downstream of the plasma source and extend only a few Debye lengths along the magnetic field but many meters across the magnetic field. No double layers extending meters along the magnetic field will form because these will most likely be shorted out by the collisional flow of charged particles across the field.

The radius of the double layers is calculated to be significantly greater than the radius of the dense plasma core. Electrons crossing the double layer experience a force which drives them toward the contactor anode. If this force is too weak to drive the outermost electrons directly to the anode they will shoot past the anode but eventually be reflected back by the double layer at the other end of the plasma cloud. It is this confining effect of the double layers that makes it possible for even a feeble force to drive a significant current. In this respect, the model is similar to that studied by when he considered the effects of probe geometry on current collection. In this case, though, the effects of collisions within the sheath on particle collection is considered.

The authors go on to calculate the current collection radius of the cloud as a function several important parameters

$$r_i = 1.2\phi_0^{1/16} I_i^{3/8} \mu^{3/4} \left(J_e^{\infty}\right)^{-1/4}$$

where ϕ_0 is the potential at the plasma contactor, I_i is the ion current emitted by the plasma contactor, μ is the mass ratio of contactor ions to ambient plasma ions and J is the electron current density in the undisturbed, ambient plasma. The model predicts the plasma contactor can collect up to an order of magnitude more current from the far field (the portion of the contactor cloud where the collision frequency is much smaller than the electron cyclotron frequency) than previously thought.

Experimental simulations of the electrodynamic tether

There is a body of experimental evidence that suggests plasma contactors can collect much more than the electron saturation current from an ambient plasma. Most of this work was performed by R. L.

Stenzel and J. M. Urrutia at UCLA. The authors used rapidly biased electrodes to simulate the effect a plasma contactor has on the ambient plasma. These experiments were performed in a large volume of plasma (1m diameter, 2.5m long) produced by an oxide coated cathode plasma source. A wide variety of probes were used to study the plasma and identify the mechanism driving the cross field current.

A plasma contactor moving across the geomagnetic field sends out a pulse of charged particles as it moves across the field lines. In the rest frame of the ionospheric plasma the contactor therefor represents a pulsed disturbance that has a rise and fall time dictated by the orbital velocity and size of the contactor. This model of a current collecting object as a pulsed disturbance was used by Drell, Foley and Ruderman[33] to describe the emission of Alfven waves by the Echo I satellite in the 1960's.

One of the first results of the UCLA group was the discovery that the current collected by a plasma contactor may have no steady state value[34]. When the probe was biased above the plasma potential the collected current was found to be oscillatory. The probe voltage rise time (~200 nsec) was much faster than an ion gyro period and was chosen to simulate the effects of a passing contactor in the ionosphere which would have a pulse rise time of 0.2 msec compared to the ion gyro period of 30 msec for O^+. Using probes sensitive to perturbations in the magnetic field, the authors determined the current perturbation travel into the plasma at nearly the electron drift speed. This information, along with a measurement of the average transient repetition time (which is roughly equivalent to the time it takes ions to cross the flux tube in a direction perpendicular to the magnetic field), allows an estimate of how far the transients penetrate into and disturb the ambient plasma

$$L = \frac{v_{d,e}}{v_{d,i}} r_{ft} \approx \left(\frac{kT_e m_i}{4\pi \Delta\phi m_e} \right)^{1/2} r_{ft}$$

where r_{ft} is the radius of the flux tube subtended by the current collecting electrode. This distance is much smaller than the dimensions of the plasma so that an interaction of the probe with the vacuum vessel can not be responsible for the transients.. By mapping the plasma density and temperature around the probe it was discovered the probe produces a radial electric field, caused by electron drain from the flux tube by the probe. This causes the magnetized electrons outside the flux tube to begin drifting around the flux tube. This drift is postulated to drive ion-sound turbulence (the measured drift speed greatly exceeds the ion sound speed) which produce an azimuthally directed electric field. This field then drives transport of electrons back into the flux tube.

This large current is abruptly terminated when the heavy ions are expelled from the flux tube by an unexpectedly large parallel electric field. As the ion density is depleted, the flux tube loses its ability to carry the large currents.

Another unexpected result was obtained when the probe was pulsed to voltages not exceeding the plasma potential[35]. The authors observe the perturbations in the magnetic field produced by probes biased to collect either electrons or ions. The perturbation travels away from the probe at a speed below the electron thermal speed. This transient is observed at the abrupt transitions of the collected current wave form. By plotting the field perturbation as a function of position, the authors determine that current loops are induced in the plasma by the pulsed probe[36]. The current loops are observed to travel into the plasma at the speed of a whistler wave[37]. These waves are observed even when the probe is biased to collect ions, indicating that even the ion current is carried into the plasma by electrons repelled from the positively biased probe not by ions attracted to the probe.

To verify that the probe does indeed excite whistlers, Stenzel and Urrutia pulsed the probe on and off at frequencies within the whistler wave bandwidth. The wavelength and phase of the magnetic field perturbations were observed using an interferometric technique. The observations confirmed whistlers were generated by the probe. The observed waves had the proper frequency and polarization and when the frequency of the waves was plotted as a function of wavelength, the experimental data accurately

followed the dispersion relation for whistler waves. Based on these results, Stenzel and Urrutia have predicted that a significant amount of the power generated by an electrodynamic tether will be radiated away as whistler waves[38].

Finally, in an extensive review of their own work, Stenzel and Urrutia[39] mention that their data indicate double layers may be forming in front of their probes and that these may play a role in collecting currents above the saturation current.

Possibilities for further study

There is then experimental evidence that suggests electrodes can collect far more than the classically derived electron saturation current from a plasma. However, the experimental evidence suggests that the collected current is not constant but instead exhibits fluctuations whose amplitude and frequency are determined by the ratio of the electrode diameter to the ion Larmor radius. These results were obtained in a laboratory plasma with parameters that are different from those that describe the ionosphere in at least one important respect. Hastings suggests that since the ratio of the cyclotron to the plasma frequency is uncharacteristically low for the ionosphere, the results of Stenzel and Urrutia can not be extended to the ionosphere. This leaves open the question of weather plasma instabilities will prevent the electrodynamic tether from collecting a steady current from the ionosphere. The work performed for this thesis is intends to answer this question. The plasma parameters are such that the electron flow both across and along the magnetic field is collisionless, removing Hastings objections to Stenzel's prediction of a non steady tether current and providing an opportunity to study the response of an ionospheric plasma to a pulsed electrode. The experiments build on Stenzel's work with pulsed electrodes, accepting his analysis of the tether as a

representing a transient perturbation to the ionospheric plasma, reproducing some of the work done at UCLA but in a parameter regime more characteristic of the ionosphere.

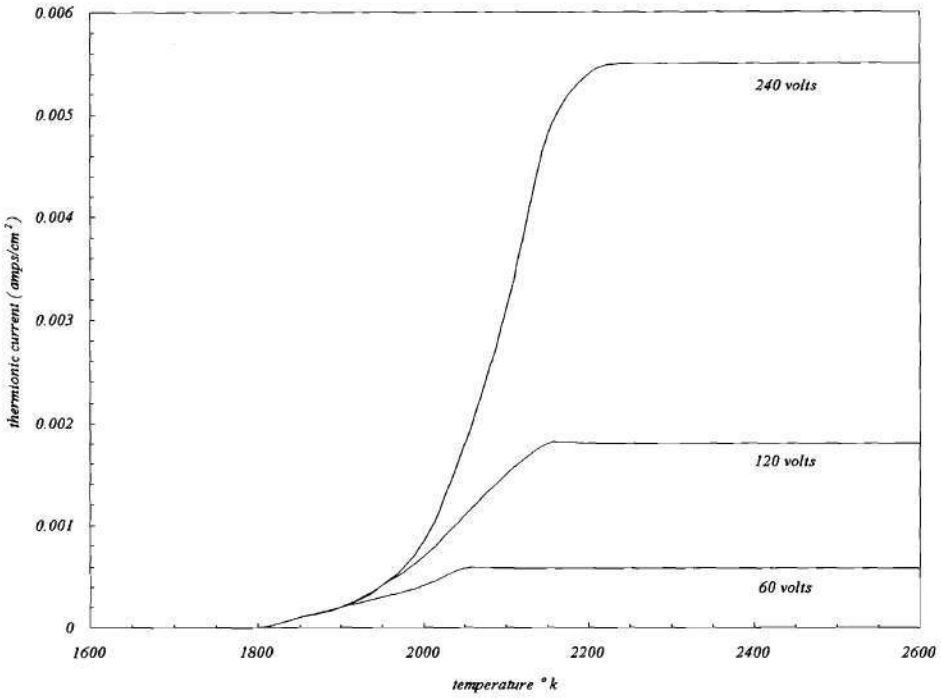

Figure 1. *Thermionic emission from a tungsten filament. This graph is from Langmuir's paper "The effect of space charge and residual gases on thermionic currents in high vacuum", Phys. Rev.,2,6,1913 and shows the dependence of the current emitted by a tungsten filament as a function of temperature and voltage. For any given probe voltage, the maximum current that can be emitted saturates at a value well below that predicted by Richardson's equation.*

CHAPTER II

Description of Experiment

The experiments are conducted in 5 inch diameter stainless steel vacuum vessel. The vessel consists of three separate sections (two "tees" and a union) which are bolted together and aligned along the local direction of the Earth's magnetic field. The alignment was supervised by Dr. Mike Hayes and was required because of the sensitivity of Dr. Hayes' experiments to the local value of the magnetic field in the plasma (an example of how the local geomagnetic field can influence plasma experiments was described by Mather and Ahluwalia[40]). Nine ports are available for introducing diagnostics or other apparatus into the vessel.

Vacuum is maintained with a hot oil diffusion pump backed up by a mechanical roughing pump. Base pressure is maintained at 50 μTorr (1 Torr = 1.3×10^{-3} Atmosphere). When experiments are performed Argon is bled into the vessel through a leak valve. Typically the system pressure increases to about a milliTorr when experiments are being performed and can be monitored either with an ion gauge tube or by a capacitance manometer. More frequently, the system pressure during an experiment is estimated from the setting on the leak valve that bleeds Argon into the vacuum vessel. Figure 2 shows the relationship between the leak valve setting and the system pressure.

Surrounding the vacuum vessel, and concentric with it, are 19 magnetic field coils. Each coil has an inner diameter of 70 cm and is connected in series to neighboring coils . The magnets are powered by a Rapid Electric S-585 DC three phase power supply located in a room adjacent to the experiment. The

power supply delivers up to 130 amps at 80 volts to the magnet coils. With this amount of power being supplied to the magnet the field on the axis of the vacuum vessel is 540 Gauss (the Gauss is the CGS unit of magnetic field strength and is equal to 10^{-4} Tesla). The coils are placed so that the axial variation of the magnetic field is less than 1% of the total field strength[41].

Plasma Production and Probe Calibration Systems

Microwave Resonant Cavity

A microwave resonant cavity is used to produce plasma[42]. The cavity consists of little more than a cylindrical aluminum can with a small magnetic loop antenna extending from the curved wall of the can. When the antenna is driven at the characteristic frequency of the cavity, determined by its diameter and its height[43], very strong, uniform electric and magnetic fields are excited in the cavity.

The resonant cavity used in these experiments 6 inches in diameter and 2 inches high, giving it a resonant frequency of 1500 MHz. A one inch diameter hole is cut into the wall of the can to allow neutral gas into the cavity and to allow plasma to escape. The interior of the cavity is painted with silver paint to increase the cavity Q, a measure of how well the cavity stores electromagnetic energy at the resonant frequency. The cavity is driven by the output of a Hughes traveling wave tube amplifier. The input to the amplifier is provided by a MiniCircuits frequency doubler which is driven by a Marconi signal generator. Power is supplied to the cavity only when the magnetic field is turned on.

With the field on, the intense electric fields in the center of the cavity ionize neutral Argon gas. The free electrons begin to spin around the magnetic field at the Larmour frequency which is about 1500 MHz when the magnetic field is 540 gauss. Thus the electric field is resonant with the free electrons and

transfers a significant amount of energy to them. These heated electrons collide with neutral Argon atoms and release more electrons. Plasma density increases in this way until the plasma frequency in the can approaches 1500 MHz. When this happens, all the energy provided by the magnetic antenna is reflected back toward the amplifier. In practice, plasma densities around $5x10^8$ cm^{-3} are easily achieved with about 10 watts of input power.

A significant advantage of this type of plasma source is the uniformity of density that is achievable across the exit aperture. Figure 3 shows some typical data indicating the radial dependence of the plasma density and the electron temperature.

Density Measuring Cavity

The plasma density was measured with Langmuir probes calibrated against the frequency shift of a microwave density measuring cavity[44] [45] located at the south end of the vacuum vessel. The change in Q of the cavity can also be used to estimate the electron-neutral collision frequency in the plasma[46] [47]. This relation is given by

$$\left(\frac{\Delta f}{f}\right) = \Delta\left(\frac{1}{Q}\right)\frac{\omega}{2\nu_c}$$

where f is the unperturbed cavity frequency, Δf is the change in the resonant frequency of the cavity and ω is $2\pi f$ (the formula is written this way to agree with the notation used in Brown, 1958).

From the difference in the measured value of the cavity Q with the plasma on and with the plasma off the estimated value of the collision frequency is 8 MHz, see figure 4.

Plasma Characteristics

Once the probes are calibrated they are also used to measure the electron temperature in the plasma. In an unmagnetized plasma, the electron temperature can be determined by the slope of the probe lnI-V characteristic between the floating and plasma potentials. This method does not always work in a magnetized plasma because of the dependence of collected current on the details of charge diffusion into the flux tube subtended by the probe. In this case, a more reliable estimate of the electron temperature can be made by taking the slope of the lnI-V characteristic for voltages below the plasma potential[48].

It is important to know if the plasma is in thermal equilibrium and this information can be obtained by analysis of the Langmuir probe data. Non-equilibrium plasma phenomena, such as electron beams coming from the negatively biased plasma source, can show up as kinks in the lnI-V plot (Hershkowitz, in Plasma Diagnostics, Vol. 1). Such nonthermal features can drive instabilities that may mask the phenomena being studied.

The two plots shown in figure 5 show the probe characteristic several microseconds before and after removing power from the plasma source. The purpose of the experiment is to verify that the plasma produced by the source is an equilibrium plasma. This is not the case in oxide coated plasma sources which emit very high energy electrons. Experiments with this type of plasma source are usually performed a short time after power has been removed from the cathode. This delay allows the plasma to thermalize so that these experiments are said to be performed in the "Maxwellian afterglow". For the reentrant cavity plasma source used in these experiments, the data indicate no change in electron temperature up to 15 microseconds after power has been removed. Since this time is much longer than either the electron-neutral or electron-electron collision time, it can be concluded that the plasma produced by the source is Maxwellian even when power is supplied to the source.

Table 2. *Comparison of characteristic plasma parameters for the three different plasmas considered in the text.*

ionosphere (500 km)

plasma density	*magnetic field*	*Debye length*	
$5x10^5$ cm^{-3}	*0.33 gauss*	*0.5 cm*	
	temperature	*thermal velocity*	*Larmor radius*
electron	*0.2 eV*	*$2.5x10^7$ cm/sec*	*3 cm*
ion	*0.1 eV*	*$1.4x10^5$ cm/sec*	*700 cm*

UCLA experiment

plasma density	*magnetic field*	*Debye length*	
$5x10^{12}$ cm^{-3}	*100 gauss*	*10^{-3} cm*	
	temperature	*thermal velocity*	*Larmor radius*
electron	*3 eV*	*$6x10^7$ cm/sec*	*.05 cm*
ion	*0.2 eV*	*2x105 cm/sec*	*2.5 cm*

Georgia Tech experiment

plasma density	*magnetic field*	*Debye length*	
$5x10^8$ cm^{-3}	*540 gauss*	*$5x10^{-3}$ cm*	
	temperature	*thermal velocity*	*Larmor radius*
electron	*4 eV*	*$8x10^7$ cm/sec*	*.01 cm*
ion	*0.1 eV*	*$2.5x10^5$ cm/sec*	*0.26 cm*

Table 2 compares some of the characteristic parameters for the three plasmas that are of central interest to this thesis. The data for the ionosphere, which is predominantly an oxygen plasma, are for the ambient plasma at an altitude of 500 km[49]. A satellite in orbit at this height would have a velocity of roughly 8 km/sec. In the frame of the satellite, the ambient plasma would have an energy (called the ram energy) of about 10 eV[50]. The UCLA and Georgia Tech plasmas are composed of Argon.

Using this information, a number of dimensionless numbers can be defined and used to compare how well the two experiments simulate the ionosphere. In fact, the work undertaken at Georgia Tech was the result of a comment made by Gerver [Gerver *et al,* 1990] that the UCLA results might not be valid in the ionosphere because electron flow in the UCLA experiment (as characterized by the ratio of the electron plasma frequency to the electron cyclotron frequency) was collisional both along and across the magnetic field while in the ionosphere electron flow will be collisionless along the magnetic field.

As pointed out by Stenzel[51], the problem of the interaction of the electrodynamic tether with the ionosphere can not be analyzed using the MHD equations. The MHD approximation is valid for low frequency plasma phenomena that satisfy the condition $\omega << \omega_{ci}$[52]. However, a plasma contactor cloud 10 meters in diameter (an adequate order of magnitude estimate) will send a disturbance down the geomagnetic field with a frequency that is roughly equal to the velocity of the cloud divided by its diameter. Taking the velocity of the contactor cloud to be equal to that of a satellite in low Earth orbit gives a rough estimate for the frequency:

$$f \sim 8000\text{m/sec} / 10\text{m} = 800\ \text{Hz}$$

this is much greater than the ion cyclotron frequency, f_{ci} = 30 Hz, and much smaller than the other frequencies characteristic of the ionosphere (f_{pe}=5 MHz, f_{pi}=30 kHz, f_{ce}=1 MHz).

For comparison, the experiments done at Georgia Tech used a probe that was pulsed above the plasma potential in 25 nsec, corresponding to a dominant frequency of 40 MHz. This frequency is greater

Table 3. *Dimensionless numbers characterizing the three plasmas*

	Alfven number A_0^2	*Magnetic Reynolds number*	*Hall parameter*
ionosphere	$4x10^5$	$2x10^5$	*5*
UCLA	*10*	*2*	*80*
Georgia Tech	$3x10^4$	$5x10^2$	*500*

To estimate the UCLA dimensionless numbers, estimates of the plasma conductivity and drift velocity were taken from Stenzel and Urrutia, 1985.

than f_{ci} (21 kHz) and f_{pi} (740 kHz) but much less than f_{ce} (1500 MHz) or f_{pe} (200 MHz). The UCLA experiments used a probe pulsed above the plasma potential in 200 nsec, corresponding to a dominant frequency of 5 MHz. This is greater than f_{ci} (30 kHz) but smaller than f_{ce} (250 MHz), f_{pi} (50 MHz) and f_{pe} (1000 MHz).

Although MHD cannot describe the instantaneous response of the plasma to the impulse associated with the tether it will undoubtedly be useful in describing the long term behavior of the ionosphere. Table 3 compares various dimensionless numbers important to the MHD equations for the ionosphere as well as the UCLA and Georgia Tech experiments. These parameters (and several others of lesser importance to the problem at hand) are encountered when the MHD equations are written in dimensionless form[53].

The Alfven number, defined by

$$A_0^2 = \frac{B_0^2}{v_0 \rho_0 \mu_0}$$

is a ratio of the magnitude of the Lorenz force on a unit mass of the plasma to the inertia of the plasma mass. V_0 is the velocity of the plasma volume and ρ_0 is its mass density. Large values of the Alfven number indicate electromagnetic forces play a major role in describing the motion of the plasma.

Table 4. *Dimensionless parameters characterizing the three plasmas.*

	ionosphere	*UCLA*	*Georgia Tech*
T_e/T_i	*7.5*	*5*	*70*
ω_{pe}/ω_{ce}	*5*	*100*	*0.2*
ω_{pi}/ω_{ce}	$6x10^{-3}$	*0.4*	$4x10^{-3}$
ω_{ci}/ω_{pe}	$7x10^{-6}$	$1x10^{-6}$	$7x10^{-5}$
vt_{he}/c_s	*115*	*100*	*269*
vt_{hi}/c_s	*0.3*	*0.2*	*0.1*

The magnetic Reynolds number

$$R_m = \mu_0 v_0 \sigma l$$

describes the rate of diffusion of a magnetic field into a plasma. The conductivity, σ, of the plasma depends on, among other things, the collective modes of the plasma. The inverse of the transverse Spitzer resistivity

$$\sigma = \frac{1}{1.03 \times 10^{-3} Z \ln \Lambda T^{-3/2}} \ \Omega^{-1} cm^{-1}$$

can be used as a general estimate of the plasma conductivity if a detailed model is not available. Z is the ionization state of the plasma ions and Λ is a number about equal to the number of electrons in a sphere with radius equal to the Debye length. The length parameter, l, is a characteristic dimension of the system. For example, it might be determined by the size of a probe or other physical object in the plasma or it may be determined by the characteristic length of a gradient in some plasma parameter. The length

parameter has no concrete definition, it depends on the experiment. Large values of R_m indicate rapid diffusion of the magnetic field into the plasma volume will occur. Since diffusion of the magnetic field is related to the collision frequency (higher collision frequencies short out the plasma currents responsible for moving the magnetic field into the plasma) the magnetic Reynolds number estimates the importance of particle interactions in the plasma.

The hall parameter is defined as the ratio of the Larmor frequency to the collision frequency

$$\Omega_\tau = \frac{e\tau B_0}{m}$$

τ is the inverse of the effective collision frequency. Large values of the Hall parameter are indicative of the plasma being "frozen" to magnetic field lines.

In addition, there are the ratios of various frequencies and velocities that can be used to judge how well the experiments simulate the ionosphere. Table 4 compares some of these.

These parameters are important because the onset of many plasma instabilities can be predicted with a knowledge of such ratios. For example, Hastings considers the effect of a current driven instability[54] on the current collected by a plasma contactor cloud and identifies a regime dependent on the electron-ion temperature ratio in which significant scattering across the magnetic field may occur. Of particular importance to this research is the observation [Gerver, 1990] that the UCLA experiments have, for the ionosphere, an uncharacteristically high value of ω_{pe}/ω_{ce}. Electrons in the experimental simulation moved collisionally both along and across the magnetic field unlike electrons in the ionosphere where electron flow along the magnetic field is collisionless. The collisional flow along the magnetic field will prevent the formation of double layers so that the effects of these objects, if they occur at all, can not be studied.

It can be seen that in many respects the Georgia Tech experiment is a good simulation of the ionosphere. The range of dimensionless parameters that describe the plasma are close to those that describe the ionosphere.

Boundary Effects

Next, the effects of the plasma boundary are considered. The plasma column in which all experiments were performed is 2.5 cm in diameter and 100 cm long. The column is terminated by the conducting wall of the vacuum vessel at the south end and by a grid located immediately in front of the source on the north end. A wire connects the grid to a BNC connector located on one of the top ports of the vessel so that the grid can be biased to any voltage with respect to the vacuum vessel.

Klozenberg, McNamara and Thonemann [KMT] studied the effect of surface currents on the propagation of plasma waves in the frequency range between the electron and ion cyclotron frequencies[55]. They considered the case of a plasma confined by surface currents and derive a relation between the magnitude of the surface current to the magnitude of the plasma wave current which must be satisfied in order for the surface currents to have negligible effect on the wave propagation. When this condition is met, the plasma can be studied as if it were an infinite medium, greatly simplifying the analysis of experiments. Although the plasma used in the experiments at Georgia Tech is confined by an external magnetic field, there is quite a bit of activity at the plasma-vacuum interface that can be attributed to surface currents. Figure 6 shows the Fourier transform of the current collected by a Langmuir probe near the plasma edge. The peak in the spectrum clearly indicates the presence of some coherent process. This peak vanishes abruptly when the probe is moved into the plasma column.

These currents may result from the gradients that exist at the plasma edge. Gradients in temperature, density and potential are known to drive the growth of drift waves on the plasma column. The currents due to these waves are a source of noise whose effect can be estimated using the KIT relations.

The first relation is satisfied if the currents are surface currents

$$\omega_{ce}/\nu_{collision} >> 1$$

the second relation is the limit on the surface current as compared to the wave current

$$\frac{\mu_0 J_0}{\kappa B_0} << \frac{\nu_{collision}}{\omega_{ce}}$$

where k is the magnitude of the wave vector along the magnetic field and J_0 is the magnitude of the surface current.

No direct measure of the surface current density was made in this experiment. In principle, such a measurement can be made by scanning a floating probe across the plasma column. However, its magnitude can be estimated by assuming it is proportional to the density gradient at the plasma edge:

$$J_0 = qnv_d$$

where the diamagnetic drift velocity, v_d, is assumed to be dependent mainly on the radial density gradient

$$v_d = \frac{T_e}{m\omega_{ce} n_e} \frac{n}{r}$$

The drift velocity is roughly 10^8 cm/sec giving a surface current density of 100 A/m^2. Using the value of the collision frequency measured with the microwave density measuring cavity (10 MHz) in the KMT relation then leads to a condition on the wave frequencies that will not be affected by the surface currents:

$$f >> 100 \text{ MHz}$$

It would appear that the characteristics of any low frequency waves observed in this experiment will be affected by the surface currents.

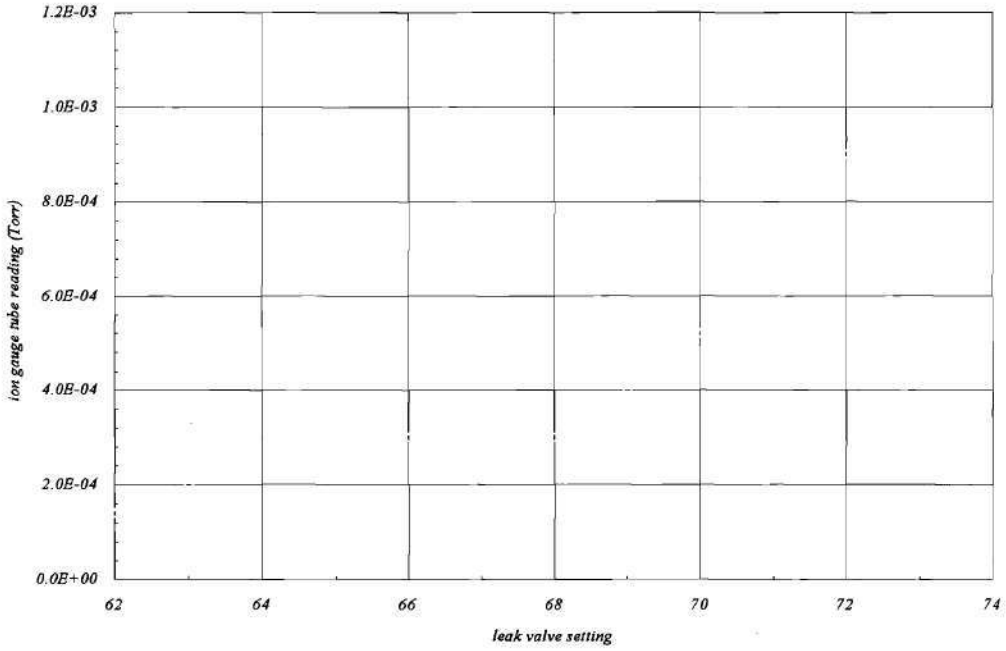

Figure 2. Neutral pressure calibration curve. Neutral pressure was controlled by a needle valve that allowed Argon into the vacuum vessel. Since the ion gauge tube can not be used when the magnets are energized, the leak valve setting was used to estimate the neutral pressure.

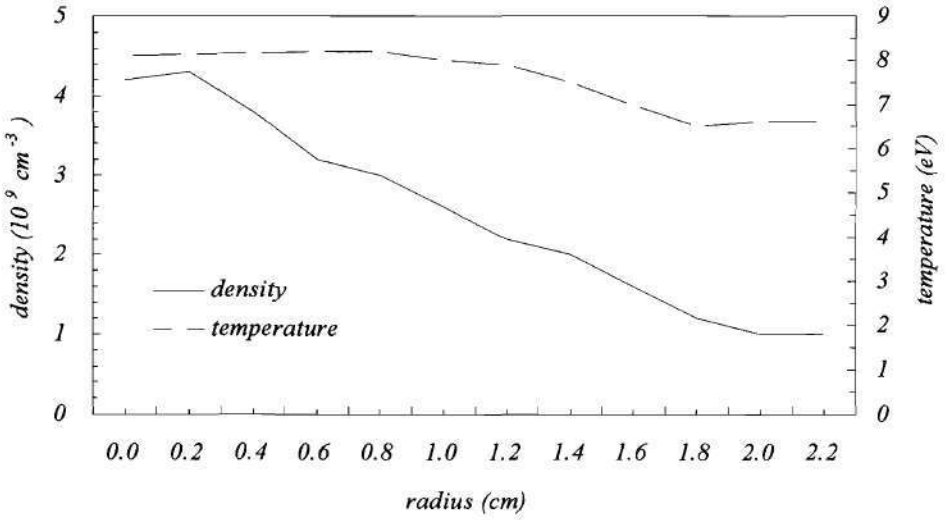

Figure 3. Measured variation in plasma density and electron temperature for the source used in these experiments. From Brown, Sheridan and Hayes, 1986.

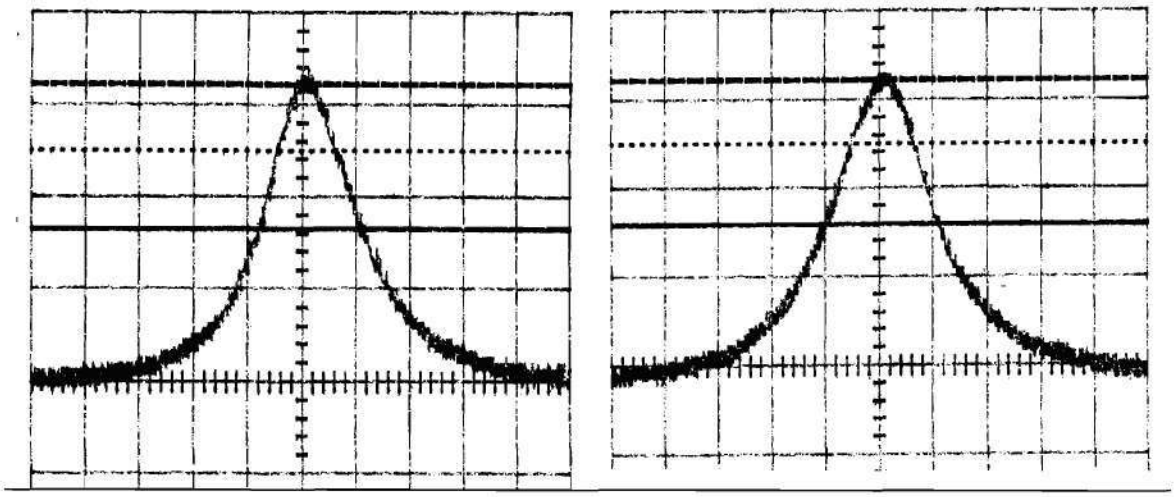

Figure 4 . Cavity response with no plasma (left) and plasma (right). The change in the full width at half maximum can be used to estimate the electron-neutral collision frequency.

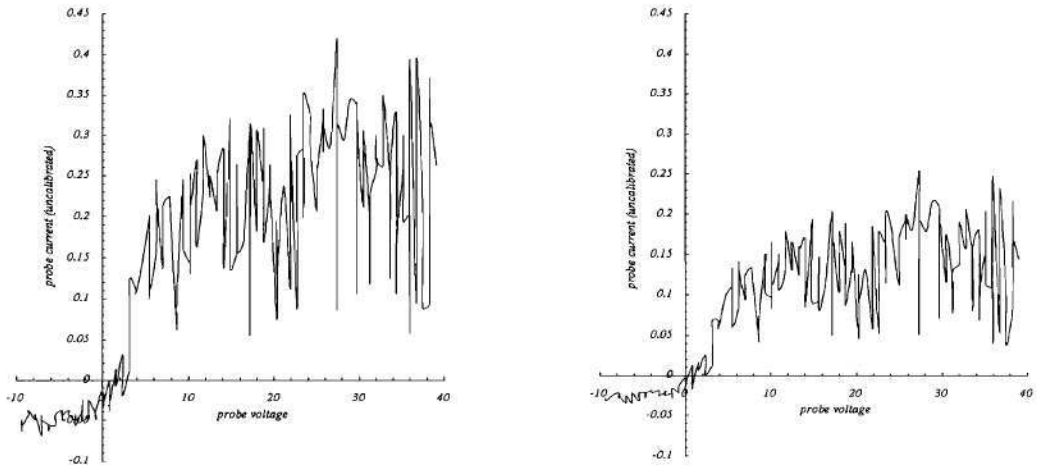

Figure 5. Electron temperature time dependence. Comparison of Langmuir probe traces during active plasma production (-5 microseconds, top trace) and 15 microseconds after power to the resonant cavity has turned off. The electron temperature estimated from the two plots is essentially time independent, suggesting that the plasma produced by the source is in thermal equilibrium.

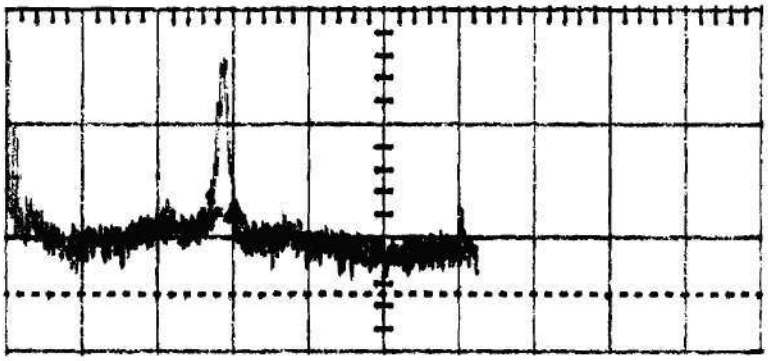

Figure 6. FFT of fluctuating voltage on a Langmuir probe at the edge of the plasma column. Frequency base is 2 kHz/ division.

CHAPTER III

Diagnostics

The simplest way to characterize a plasma is to insert a bare wire into it and record the current collected by the wire as a function of the voltage on the wire. Irving Langmuir used probes like these in his pioneering investigations of gas discharge tubes. Today, these simple probes bear his name because Langmuir was the first to derive the relationship between the wire current and voltage as a function of the parameters characterizing the plasma. These parameters are the electron density, n_e, electron temperature, T_e, and plasma potential, V_p.

Langmuir probes

A typical plot of probe current versus voltage is shown in figure 7. This data was obtained with a large (the probe radius was greater than the ion gyro radius) disc probe in a magnetized plasma. Several of the features displayed are characteristic to Langmuir probes in general while others, most notably the hysteresis, are not commonly observed. The features this trace shares with all Langmuir probes are the rapid increase in the collected current between 10 volts and 25 volts, and the relative plateau in the collected current reached for voltages between 25 volts and 30 volts. In an unmagnetized plasma this plateau would be more pronounced.

The theory that relates the plasma parameters to the features identified on the probe trace is usually developed for a maxwellian plasma and for probes with small dimensions compared to dimensions characteristic of the plasma. The assumption of a maxwellian plasma greatly simplifies the mathematics required to derive a relation between the electron temperature and the slope of the probe trace (calculated between 10 and 25 volts in the example). This assumption also simplifies the relation between the electron saturation current (the current collected by the probe above 25 volts) and the electron density. Detailed derivations, as well as an excellent discussion of Langmuir probes in general, are given by Hershkowitz[56].

In particular, the exponential dependence of the electron current collected by the probe on the inverse of the electron temperature

$$I(V) = I_{sat}\, e^{q(V-V_0)/T_e}$$

allows the electron temperature to be determined from the slope of the probe characteristic. The plasma potential, V_0, is determined by the "knee" in the probe characteristic. Referring to the example, the plasma potential is seen to be about 25 volts.

The electron saturation current is determined by the electron density and electron temperature through

$$I_{sat} = Sn_\infty e\sqrt{T_e/2m_e}$$

where S is the effective charged particle collecting area of the probe. When the probe is not in a strong magnetic field (so that the particle Larmor radius is greater than the probe dimensions) and when the plasma density is sufficiently high that the Debye length is small compared to the probe dimensions, S is

equivalent to the surface area of the probe. If the previous conditions are not satisfied, S can be considerably larger than the physical surface area of the probe.

Using the data in the example, the electron temperature is found by plotting the logarithm of the current versus the probe voltage and then calculating the slope of the resulting curve between 10 volts and 20 volts. The electron temperature is proportional to the inverse of this number. In this case, the electron temperature is found to be 4 eV. This result is then used in the formula for the saturation current in order to estimate the plasma density. It turns out that the plasma density found using this procedure, $2x10^6$ cm^{-3}, is two orders of magnitude smaller than the plasma density found using a much more reliable density diagnostic (the frequency shift of a microwave resonant cavity). This discrepancy is caused by the magnetic field and will be considered shortly.

One of the draw backs encountered when using Langmuir probes is the need to acquire complete probe traces in order to estimate the plasma parameters. This can be a serious problem when observing transient phenomena or when the probes are used in afterglow plasmas. In these cases, plasma density, potential and temperature may change considerably during the time required to obtain a complete probe characteristic. A possible solution is to sweep the probe voltage in a period shorter than that of the phenomena of interest. However, Stenzel and Urruttia have shown that rapidly biased current collecting electrodes can profoundly modify their surroundings.

The other complication encountered when using Langmuir probes is that a majority of the analysis of the probe characteristics has been done for probes in maxwellian, unmagnetized plasmas. Without a reliable theory to indicate how to extract the plasma parameters from the measured probe features, it is often necessary to calibrate the Langmuir probe against the response of a well understood probe. For example, in these experiments, the plasma density was at times monitored by observing variations in the current collected by a Langmuir probe biased at -80 volts. The response of this probe to changes in the plasma density was calibrated with the output of a microwave resonant cavity. The resonant cavity

provides a very accurate measure of the plasma density. However, this probe is not movable and has poor spatial resolution.

The effects of a magnetic field on Langmuir probes is understood in general but not in detail. The field affects the probe by 1) altering the current collection area of the probe, S and 2) greatly influencing the way in which charged particles are collected by the probe.

A magnetic field inhibits the movement of charged particles in directions perpendicular to the field lines. Consequently, a probe collecting charged particles in a magnetized plasma does not collect the particles isotropically. Instead, there is a preferential collection of particles from those magnetic field lines that intersect the surface of the probe. The set of magnetic field lines that intersect the probe surface defines the flux tube subtended by the probe. The effective collecting area of the probe is now proportional to the cross sectional area of the flux tube. This can be considerably less than the actual surface area of the probe.

The amount of current collected by a probe in a magnetic field depends to a large extent on the density of charged particles in the flux tube. The density of these particles will obviously decrease when the probe is biased to collect them. This decrease in density is manifested by a decrease in the collected current.

The charged particle drain out of the flux tube caused by the probe will be compensated to some extent by the diffusion of charged particles across the magnetic field and into the flux tube. The transport of charged particles across magnetic fields is a very active area of research and it is not yet possible to predict the diffusion coefficient, applicable to a given experiment, with certainty. However, an example of the intricacy of the problem is provided by Stenzel [Stenzel and Urrutia, 1986]. In an experimental study of pulsed electrodes, Stenzel and Urrutia observed that the diffusion of electrons into the flux tube was governed by the plasma waves generated by electrons spiraling around the outside of the flux tube. The spiraling electrons were responding to the electric field produced by the probe as it drained electrons from its flux tube, leaving behind a small amount of space charge associated with the heavier ions. The probe

was therefor responsible for destabilizing a wave in the surrounding plasma and this wave ultimately determined the amount of current the probe collected. This dependence of probe current on collective plasma modes indicates the difficulty of predicting the response of a probe in a magnetic field.

In such circumstances the ion saturation current is usually used to infer the plasma density. In this experiment, the current collected by a negatively biased probe was calibrated using a microwave resonant cavity. The resonant frequency of the cavity will shift when a dielectric medium, such as a plasma, is inserted through its axis. This frequency shift is a sensitive function of the electron density of the plasma. By correlating the ion saturation current against the frequency shift, accurate estimates of the plasma density can be obtained.

Plasma potential measurements

Low frequency changes in the plasma potential can be monitored with emissive probes[57]. The probes are similar in construction to Langmuir probes except that they use a loop of wire (typically tungsten) for the probe tip so that an externally applied current can circulate in the probe to raise its temperature. Information about the plasma potential is obtained by comparing the I-V characteristic of the probe when it is heated to the I-V characteristic of the cold probe. The plasma potential is identified as the voltage at which the two curves separate. Kemp and Sellen suggested such probes could be used to monitor small fluctuations in the plasma potential up to several megahertz. However, the probes are difficult to build and require a large number of external electronic components in order to automatically track the plasma potential[58],[59].

In order to observe high frequency fluctuations in the plasma potential an alternative to the Langmuir probe is needed. Figure 8 is an idealized schematic of the probe-plasma electrical system. The system is divided into four distinct parts:

1) the plasma impedance, represented here by the series resistor and inductor combination L_{pl} and R_{pl}. This is a vast oversimplification of the actual plasma impedance which has a much more complicated frequency dependence. The actual plasma impedance will depend on any collective modes that happen to be excited at the time of measurement.

2) The probe sheath, represented by the parallel combination R_{sh}, C_{sh}. The resistor accounts for the rapid attenuation of the probe electric field (over a distance proportional to the Debye length) of the probe electric field.

3) The probe impedance, represented by Rp and Cp. The effective of stray cable capacitance is accounted for in C_p. A simple wire probe, such as a Langmuir probe, will have a value of R that dominates the impedance of the parallel RC combination.

4) The impedance, R_m, of the device used to measure the probe characteristic. Typically, R_m should be large enough so that it does not significantly add to the probe impedance. This is accomplished by making R_m much larger than any of the components of the probe impedance.

In order to make a meaningful measurement, it is important that none of the stages of the circuit load the preceding stages. If the impedance of probe circuit, for example, is smaller than the combined impedance of the plasma and sheath circuits, the signal, V_{plasma}, will be attenuated as in any voltage divider in which the resistor to ground is smaller than the resistor that follows the voltage source.

The sheath capacitance is typically of the order of a few tenths of a picofarad. The exact value depends on the nature of the plasma but can be estimated by[60]

$$c_{sheath} \approx \frac{\ln(b/a)}{1.5 \ln\left[\left(b+\lambda_D\right)/b\right]}$$

where a and b are the radius of the probe and sheath. At low frequencies ($f_0<(1/2)\pi r_p c_{pl}$) the circuit behaves as a voltage divider with output

$$V_{out} = V_{plasma} \frac{r_p}{r_p + r_{pl}}$$

which indicates a large probe resistance (in comparison with the plasma resistance, typically a few kΩ) must be used to insure the input voltage is not significantly attenuated by the circuit. At frequencies above f_0, the circuit behaves like a low pass filter so that high frequency fluctuations can not be observed. For the probe used in these experiments, $r_p \sim 2000\ \Omega$ and $c \sim 600$ pF due to the long cable required to bring the signal to the oscilloscope so that $f_0 = 300$ kHz.

The frequency performance of the probe can be considerably improved by capacitively coupling the probe to the plasma[61] rather than having the probe in direct contact (figure 9). This works around the problem of attenuation of the input signal by unavoidable circuit capacitance by driving the circuit with a source whose impedance changes with frequency. In this way greater bandwidth is bought at the expense of a constant attenuation factor at all frequencies.

The circuit now works like a voltage divider with a transfer characteristic given by

$$\frac{V_{out}}{V_{in}} = \frac{c_1 + c_2}{c_1}$$

The bandwidth of the probe is limited primarily by the input impedance of the amplifier, which determines the low frequency cutoff (the parallel combination of the capacitance, in series with the amplifier resistance, form a high pass filter).

The circuit used (illustrated schematically in figure 10) in this experiment is based on a design developed in 1968[62]. An unavoidably long length (roughly 12 feet) of 50Ω coaxial cable was used to bring the signal from the probe to an LM310 voltage follower. The follower was connected to a wide

band width amplifier (Kalmus 102L, 25 Hz - 100 MHz, 33 dB gain) and this amplifier was connected to one of the input channels of the LeCroy DSO. The probe tip was constructed from semirigid coaxial cable with about 5 mm of the outer conductor stripped away. The dielectric core of the cable was left in place around the center conductor to prevent plasma from coming in contact with the conductor. The end of the probe was insulated using liquid tape.

The probe was calibrated using an HP240A pulse generator. Square pulses, with rise time of 25 nsec, of varying amplitude were fed to the probe via an alligator clip clamped onto the outer dielectric. The probe proved to have excellent frequency response and an attenuation factor of about 125. The response of the probe to a test square wave is shown in figure 11 and its response as a function of test pulse amplitude is shown in figure 12.

Measurement of high frequency plasma oscillations

High frequency electric field fluctuations can be measured with RF coaxial probes[63]. These probes have been used extensively to study high-frequency noise in plasmas, plasma turbulence[64] and waves in plasmas[65]. The probe is simply a length of coaxial cable with the center conductor exposed to the plasma. The other end of the cable is connected to a wide-band, low noise amplifier with 50Ω input impedance. These probes are sensitive to electric fields directed along the length of the exposed center conductor. In this series of experiments, the probes were oriented so that the center conductor lied in a plane perpendicular to the magnetic fields. The probe should therefor be most sensitive to electromagnetic waves with wave vectors pointed along the magnetic field and also to electrostatic plasma waves with wave vectors perpendicular to the direction of the magnetic field.

The expected directional characteristics of the probe were checked by inserting the probe tip between two large capacitor plates. The 10cm x 10cm aluminum plates, separated by a 2cm air gap, were differentially driven at roughly 10 MHz from the outputs of an RF pulse transformer. The primary of the transformer was connected across the output of a Tektronix signal generator. First, the probe was inserted between the plates so that the tip is perpendicular to the electric field. In this orientation, the probe detected almost no signal. Next, the probe tip was inserted through a small hole drilled through one of the plates near the center of the plate. The probe tip is then oriented along the direction of the electric field. The response of the probe is shown in figure 13.

Measuring oscillations in the electrode current

Fluctuations in the current collected by the electrode were measured using a transmission line transformer connected in series with the electrode. The transformer coupled current oscillations in the electrode circuit into a wide bandwidth instrumentation amplifier that amplified the signal before sending it to the oscilloscope. The low frequency cutoff of the transformer limited observations to frequencies greater than 4 kHz. The circuit was calibrated in two different ways using primitive current sources. Although both tests were crude, they provide independent estimates of the circuit gain that are in good agreement.

The current measuring circuit was used as part of a larger circuit that rapidly pulsed the voltage on the electrode on and off. Conceptually, the problem of pulsing the electrode and measuring the collected current is a simple and can be performed with a transistor switch. The electrode is connected in parallel with the emitter voltage supply through a resistor R_{probe}. A gate voltage applied to the transistor will switch the voltage on the electrode from the floating potential to the supply voltage when the gate signal

goes high. The time it takes to complete the transition is determined by the transistor capacitance, the transistor current and the transition time of the gate signal. High speed switching transistors require large currents to achieve minimum switching time so the value resistor collector resistor R is usually only a few ohms. R must have an adequate power rating or it will be destroyed when the transistor current flows.

The current collected by the electrode is estimated by measuring the voltage drop across a resistor in series with the electrode. The value of this resistor is kept small so that the voltage drop across it is small compared to the voltage at point A. This ensures that the voltage on the electrode is accurately known. Although the voltage difference across the resistor is small the voltage at each of the two resistor terminals will be nearly equal to the supply voltage V when the electrode is pulsed on. For the experiments conducted here the supply voltage will be above 50 to 100 volts. The differential amplifier will not tolerate these voltages at its inputs. Typically the maximum voltage that can be placed on the amplifier inputs is limited to being less than the amplifier supply voltage (about 10 volts for the instrumentation amplifier used in this experiment). Some method must be provided to couple the signal to the differential amplifier while preventing the full value of the pulsed voltage from being placed on the inputs.

One method of accomplishing this is by capacitively coupling the amplifier inputs to the resistor terminals (figure 14). However, the capacitor forms a high pass filter with the amplifier bias resistors so that only signals with a frequency greater than 1/RC will be amplified. Along with the signals, the large switching transient associated with the voltage signal rise time will passed along to the amplifier. The transient will decay away after a few RC time constants but this will clearly make it impossible to observe signal within a time RC of the pulse initiation. Choosing an RC combination that gives a faster decay time for the switching transient will also decrease the signal level at the amplifier inputs by filtering out the low frequency components. Therefor, capacitive coupling of the amplifier to the electrode circuit should be used only when the signal frequencies are well above 1/RC and no important signals are expected to occur within a time RC of applying voltage to the electrode.

An alternative to capacitive coupling is transformer coupling (figure 15). The primary windings of a transformer are connected in series with the electrode circuit. Providing the transformer has sufficient frequency response, fluctuations in the electrode current are coupled into the secondary windings and can be used to drive the inputs of a differential amplifier. This method has been used to monitor the current collected by swept Langmuir probes in fusion experiments. Transformers used for this purpose are called Pierson transformers and they typically have a bandwidth of a few kilohertz centered at a relatively high frequency (tens to hundreds of kilohertz). Unfortunately, the bandwidth is too narrow and the center frequency too low for use in this experiment. Also, these devices typically require tens to hundreds of milliamps of current to produce an output signal.

Transmission line transformers are small, high frequency transformers used for isolating high frequency circuits from one another, coupling RF power into antennas and for many other tasks. The transformers have a very wide bandwidth (hundreds of megahertz) and can operate at very small signal levels (less than a millivolt). They are constructed by winding micro coaxial cable around a ferrite core. A MiniCircuits Labs TT1-6 transmission line transformer was selected to couple the electrode signal to a INA110 (Burr-Brown) instrumentation amplifier. The transformer has a bandwidth that extends from 4 kHz to 500 MHz so that little loss of the electrode signal is expected. The bandwidth of the amplifier is about 1 MHz when the amplifier is operated at a gain of 10. Stenzel's work suggests that the duration of the current fluctuations scales as the electrode diameter divided by the ion sound speed so that a 1 MHz bandwidth should be adequate for this experiment (the electrode diameter is 0.5 cm).

The circuit was tested and calibrated by passing a current through the transformer primary and observing the amplifier output with the DSO. An accurate determination of the circuit gain (in amps/volt) required a stable source of high frequency current. This was provided by two different methods and so two independent estimates of the gain were determined. Both these estimates are in reasonable agreement.

The first method of providing high frequency current to the primary used the plasma source as a current source. A biased grid located immediately in front of the plasma source was used to modulate the flow of plasma out of the source. A positive voltage of 10 volts essentially prevented any plasma from leaving. The gate signal was provide by a Tektronix function generator and had a rise time of less than 100 nsec.

The electrode was held at a constant positive voltage during this test. The output wave form is shown in figure 16. The output wave form is a fairly good representation of the gate wave form and thus provides some encouragement that the circuit is working properly. The mean value of the output voltage when the gate signal is high is roughly 12.5 mV. In order to determine the circuit gain, an estimate of the current collected by the probe when the output voltage achieves the mean value is needed.. This estimate was provided by measuring the current collected by the probe when plasma was allowed to freely exit the plasma source. This was assumed to be equal to the current collected by the probe when the plasma source was operated in the pulsed mode. The current was measured by connecting a Keithly DMM between the electrode and the power supply. The DMM indicated the electrode collects between 16 and 20 microamps of current when operated under these conditions. Therefor, the gain of the circuit is roughly 1.6 μA/mV.

A more controlled estimate of the circuit gain can be obtained by applying a time varying current from an RF signal generator through the primary transformer winding and observing the circuit output with the DSO. The transformer therefor monitors the return current of a transmission line that is terminated in its characteristic impedance. The RMS value of the current flowing through the primary should increase as the signal frequency increases. To perform the measurement, a Marconi function generator is connected to one terminal of the primary through a 50Ω resistor and the other primary terminal is grounded. The Keithly DMM is inserted between the Marconi and the resistor and used to measure the input current. The output of the circuit is observed with the DSO. The plot of gain versus frequency illustrated in figure 17 is limited to 100 kHz by the bandwidth of the DMM. This data is not in

conflict with the conclusion that the gain of the circuit is 0.5 mV/μamp at high frequency. Finally, no variation in gain with input signal level was detected at fixed frequency.

Magnetic probe

A probe that responds to changes in the plasma magnetic field can be made from a few turns of fine gauge wire soldered to the two ends of a shielded twisted pair cable[66]. The probe can be thought of as forming the secondary winding of a transformer and the plasma currents can be thought of as flowing through the primary winding. As in a transformer, the signal at the primary is transferred to the secondary through the mutual inductance of the two windings. The small, varying magnetic field associated with time dependent plasma currents will couple to the wire loop probe and produce a voltage at the end of the twisted pair proportional to the time rate of change of the magnetic field. The probe is sensitive to the rate of change of the magnetic flux in the plane of the loop and thus can only detect current in a plane perpendicular to the loop.

Stenzel and Urrutia used a magnetic loop probe to discover current loops produced by rapidly biased electrodes in their plasma. This identification was made with only a few measurements along the axis of their device. More extensive mapping of the magnetic field allows detailed maps of the plasma current as a function of position and time to be obtained. These maps require large amounts of magnetic field data since they are produced by digitally calculating the curl of the measured magnetic field and equating this quantity to the plasma current:

$$\nabla \times \mathbf{B} = \mu_0 \left(\mathbf{J} + \partial \mathbf{D} / \partial t \right)$$

This emphasizes that the magnetic loop probe is proportional to the total plasma current (conduction current, J, and displacement current, $\mu_0 dD/dt$). In contrast, Langmuir probes only give information about the conduction current[67].

The output voltage of a magnetic probe is proportional to the number of loops used and their area[68]

$$V = nA\frac{\partial B}{\partial t}$$

where n is the number of turns in the probe coil, A is the area of each turn in m^2 and B is measured in Tesla (10^4 Gauss). Magnetic field probes of this type have a bandwidth determined by the probe inductance and the resistance connected across the probe terminals

$$\frac{1}{f_{max}} = kn^2 \frac{probe\ radius}{probe\ resistence}$$

K is a constant that depends on the probe geometry. This forces a tradeoff between wide bandwidth, which requires small values for n and radius, sensitivity, which requires a large value of n and radius, and position resolution, which requires the probe radius be as small as possible.

The probe (schematically illustrated in figure 18) was constructed from one turn of #32 heavy formvar magnet wire and had a radius of 1 millimeter. Typically, these probes are constructed from miniature coaxial cable to guarantee shielding from electrostatic fields and proper electrical balance of the probe[69]. However, Lovberg has remarked that electrostatic pickup by loop probes has been observed to be only a minor problem. In fact, a probe without a shield has been shown to have a flatter frequency response than a shielded probe [Phillips and Turner, 1965]. The probes used in this experiment were therefor constructed with materials that were simpler to work with than miniature coaxial cable. The probe terminals are connected to the input and output terminals of one winding of a pulse transformer

(MiniCircuits Labs T1-1, bandwidth 0.15 MHz - 400 MHz). The transformer is used to provide the probe with a degree of electrical balance and also to enable the essentially balanced signal from the probe to be converted to a single ended signal for transmission through the coaxial cable. The probe shaft was painted with silver paint (GC Electronics, 22-201) to further reduce electrostatic pickup.

The probe will respond to frequencies well above 1 GHz and have an output voltage of $V = 10^{-7}$ dB/dt, where B is in Gauss and t is in microseconds. A 1 μamp, 1 MHz current fluctuation originating 1 cm from the probe will produce a 0.1 nanovolt signal across the probe terminals. This is well below the thermal noise of a 50Ω resistor at room temperature (roughly 1 μvolt at a 1 MHz bandwidth[70]). In order to have any hope of seeing such a small signal, the probe was connected to two cascaded low noise amplifiers that were in turn followed by a power amplifier (Kalmus 102L power amplifier, 33 dB gain, 100 MHz bandwidth) before sending the signal to the DSO. This provides 73 dB of power gain or, roughly, a voltage gain of 45,000. In addition, the DSO can be programmed to average hundreds of received signals together, thus improving the signal to noise ratio.

The signals are brought out of the vacuum vessel using about 20 feet of 50Ω coaxial cable and connected to two low noise amplifiers (MiniCircuits LN1000, G=20 dB, 50Ω input impedance) connected in series and then sent to the DSO for storage and display (the Kalmus amplifier was not used when the probe was calibrated). To calibrate the probe, a coaxial cable, shorted at one end and driven by the Marconi signal generator, is brought into the vicinity of the probe and the probe response as a function of frequency and amplitude recorded. The applied signal has a current maximum at the end of the shorted cable and thus provides a good signal source to excite the probe. This method is not as accurate as using a Helmholtz coil[71] but it was convenient, did not require the building and testing of calibration magnets and adequate for the order of magnitude type information sought in this investigation.

Figure 19 shows the output of the probe when the loop normal is oriented $+90^{o}$ and -90^{o} with respect to the direction of the coaxial cable. The difference in amplitude is attributed to electrostatic feed through of the signal on the coaxial cable. The amplifiers provide a voltage gain of roughly 225, bringing

10 nanovolt signals into the measurable range of the DSO. The additional gain provided by the 102L (roughly a factor of 30) should make the magnetic perturbations visible to the DSO.

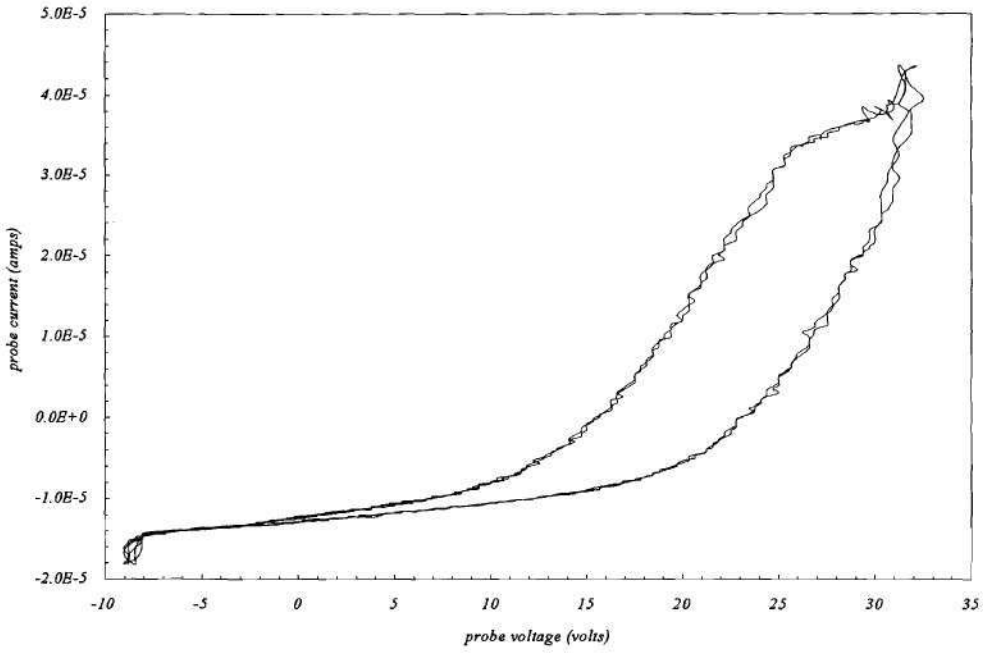

Figure 7. Current - Voltage characteristic for a swept Langmuir probe. The hysteresis in the probe trace is commonly observed with dirty probes or probes in magnetic fields.

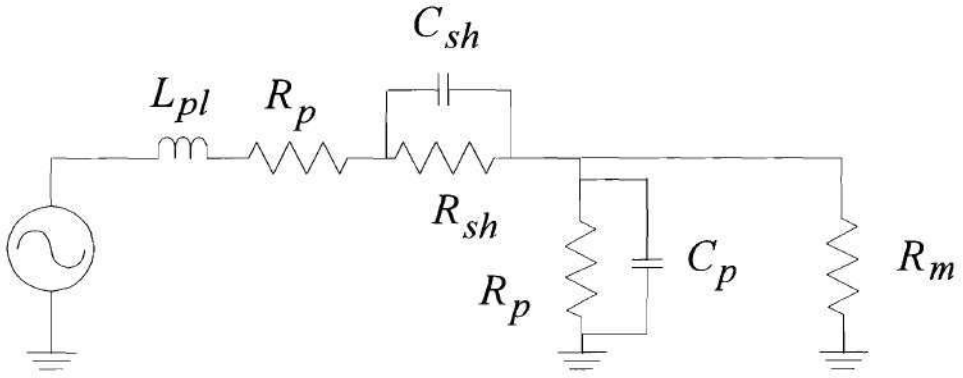

Figure 8. Equivalent circuit for a probe resistively coupled to a plasma. The plasma is modeled by a resistor in series with an inductor but this is an over simplification of the plasma impedance. The actual impedance depends on, among other things, the excited collective modes of the plasma and the frequency at which observations are made. The probe sheath is modeled by the parallel resistor and capacitor, another oversimplification.

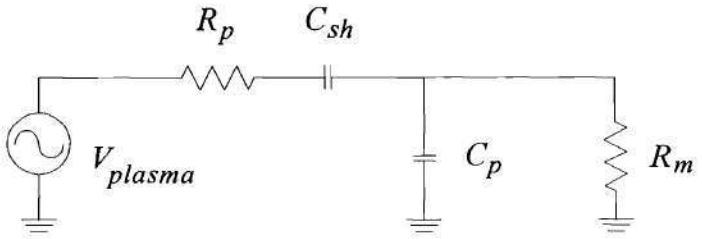

Figure 9. A simplified model of a capacitively coupled probe. The sheath impedance at high frequency is dominated by its capacitance so sheath resistance s indicated.

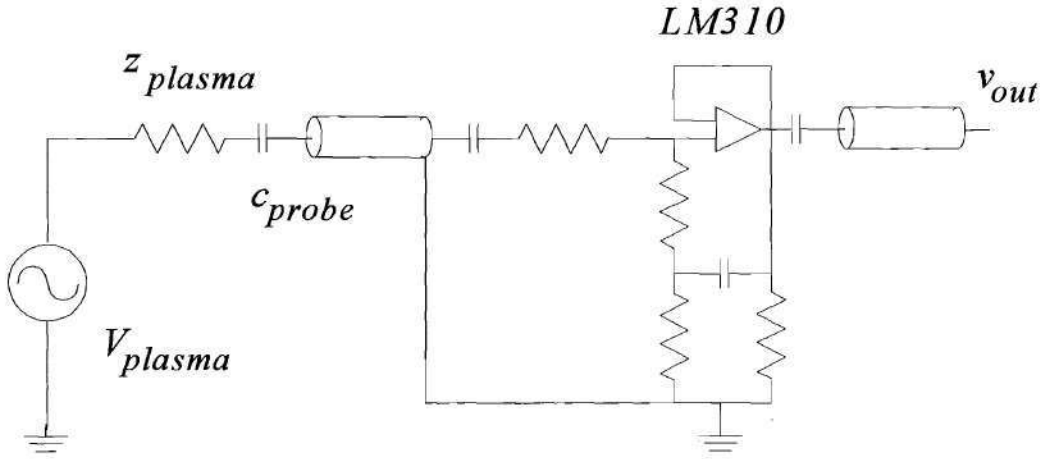

Figure 10. Capacitive probe circuit. The signal from the probe (the probe is indicated schematically by the capacitor C_{probe}) is applied to a high input impedance AC amplifier. The circuit is based on a design found in the 1988 edition of National Semiconductor's Linear Databook 1.

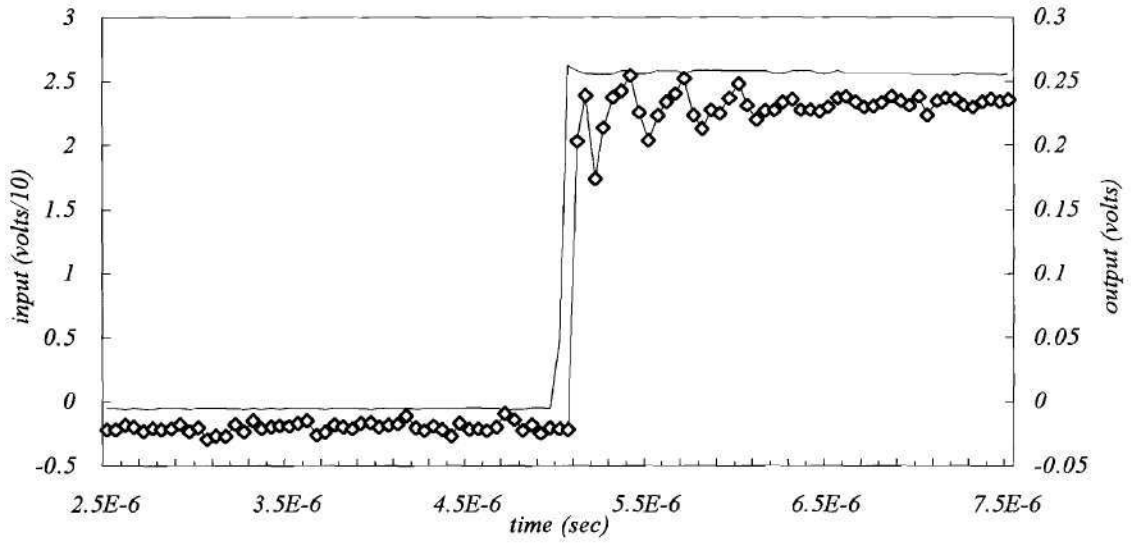

Figure 11. Response of the capacitive probe to a test square wave signal. The test signal was provided by an HP214A pulse generator that was connected to the exposed probe dielectric by an alligator clip.

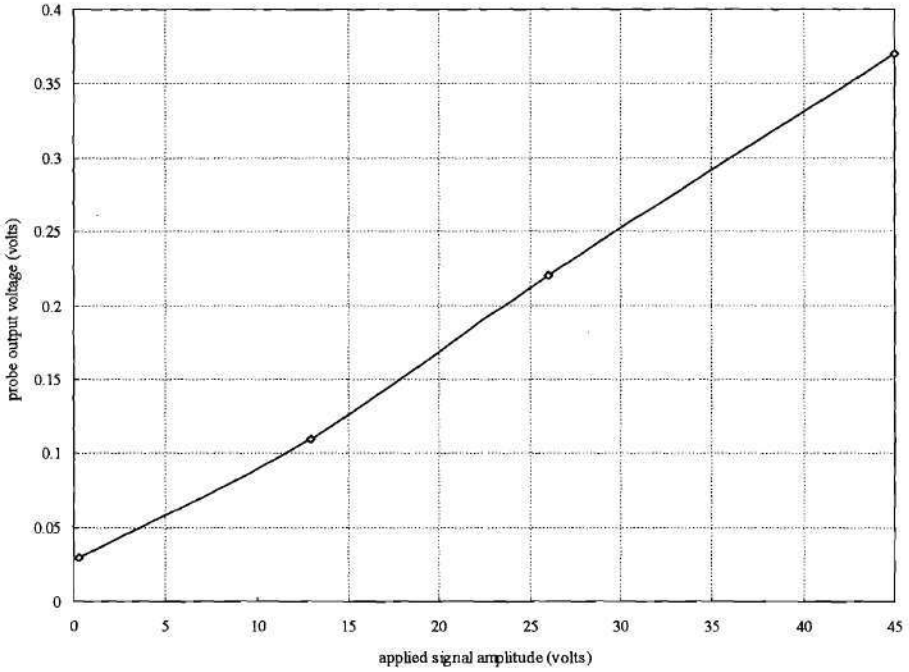

Figure 12. Capacitive probe calibration curve obtained by applying voltage pulses of varying amplitude to the alligator clip.

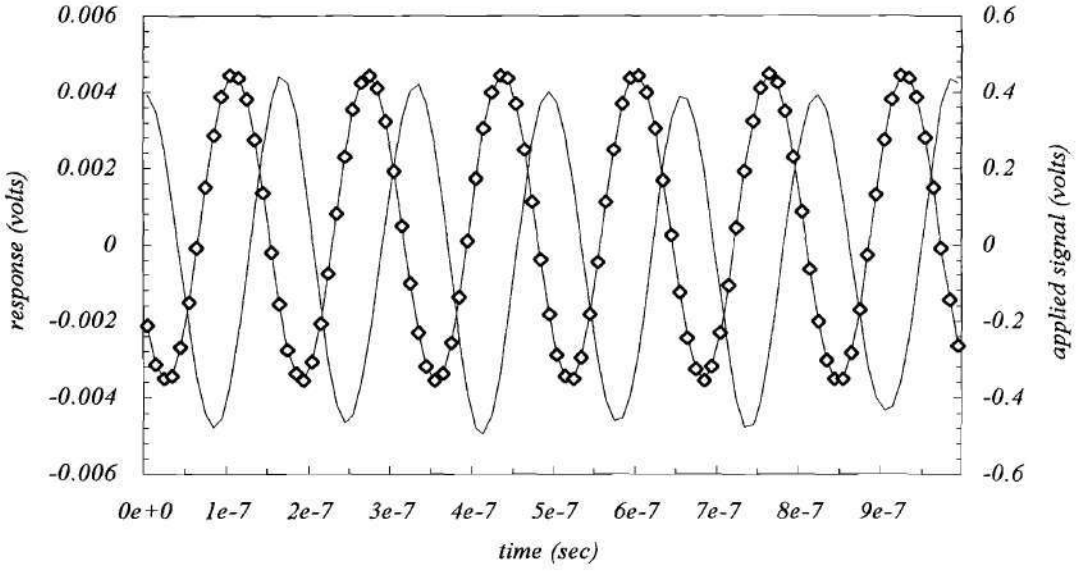

Figure 13. Response of the coaxial Langmuir probe (RF probe, indicated by the triangular symbols referenced to left most vertical scale) to a parallel plate capacitor field. The capacitor plates were symmetrically driven by coupling the input signal through a balanced transmission line transformer

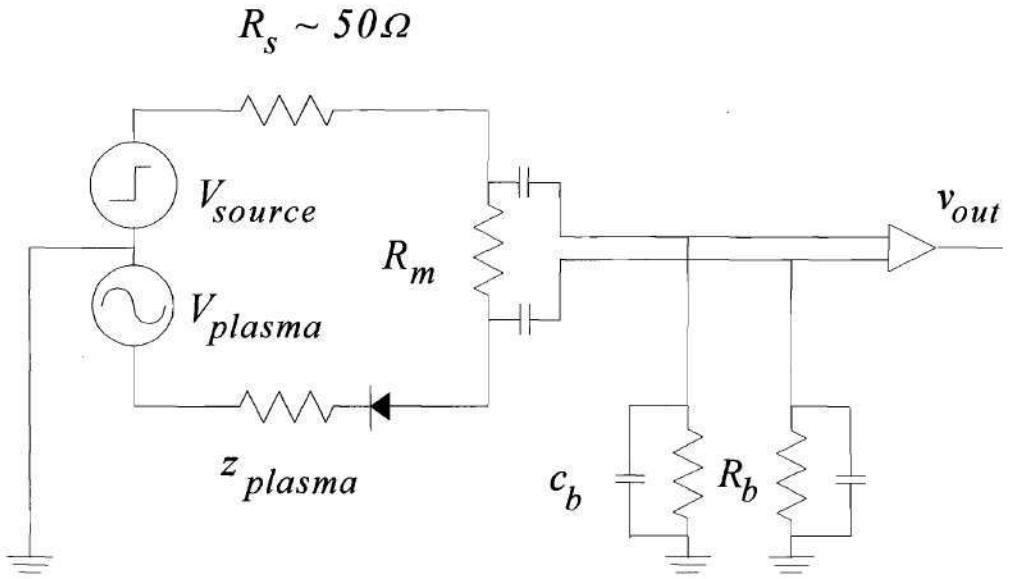

Figure 14. Model of the pulsed electrode capacitively coupled to a differential amplifier. The amplifier measures the electrode current by amplifying the voltage difference across the terminals of the small measuring resistor Rm. The diode is included in the circuit to indicate the direction of current flow when the probe is positively biased.

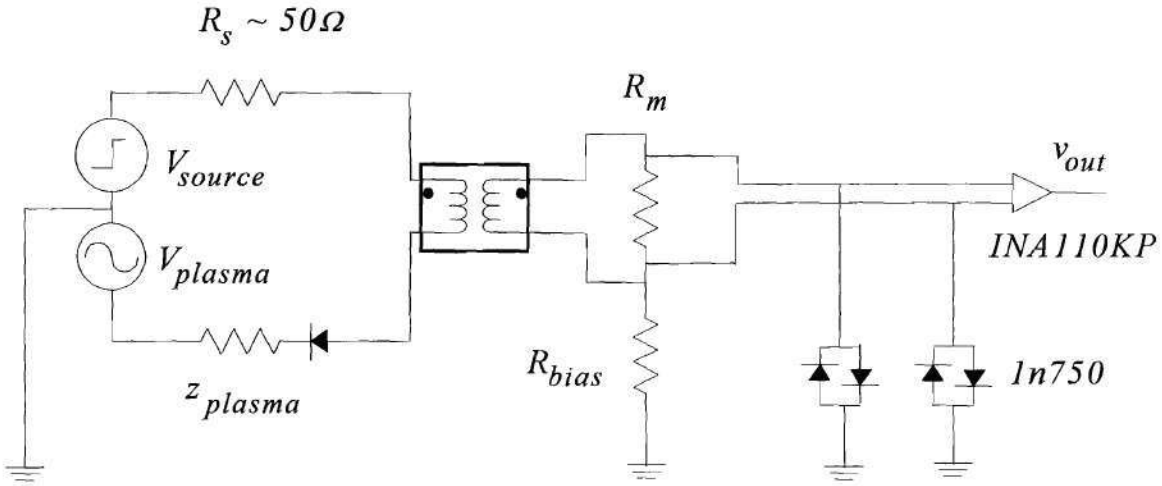

Figure 15. The circuit used to measure electrode current fluctuations in this experiment. The pulse transformer, TT1-6, couples the current fluctuations from the electrode circuit into the amplifier circuit. The resistor connected across the secondary terminals of the transformer reduces noise caused by any mismatch between the transformer and the 50Ω transmission lines that connect the electrode to the pulser.

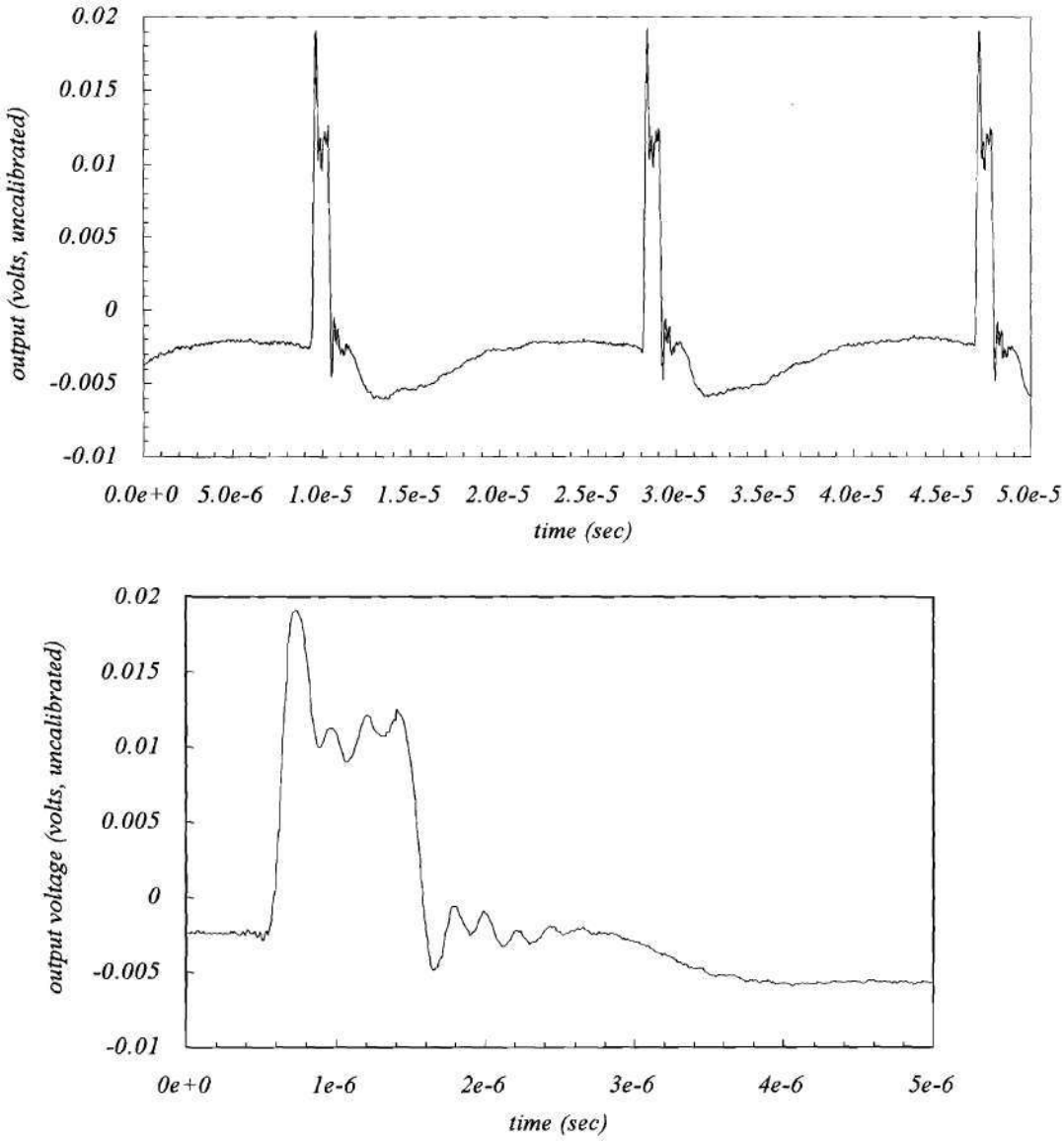

Figure 16. Response of the current measuring circuit to a time varying current supplied by the plasma source. A square wave voltage applied to a grid immediately in front of the plasma source acted as a valve for turning the current on and off.

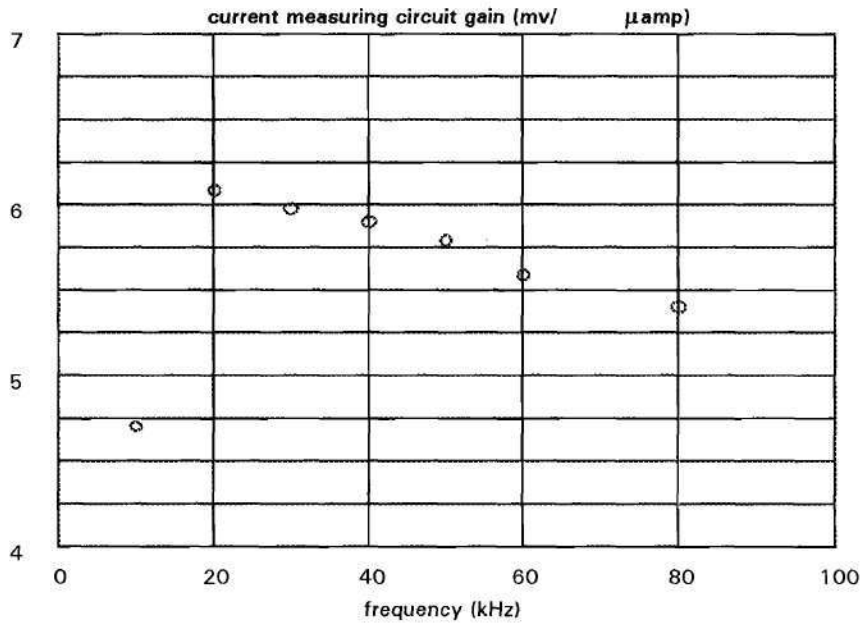

Figure 17. Results of calibrating the current measuring circuit using an RF signal generator. The data is in relatively good agreement with the gain determined by using the pulsed plasma source.

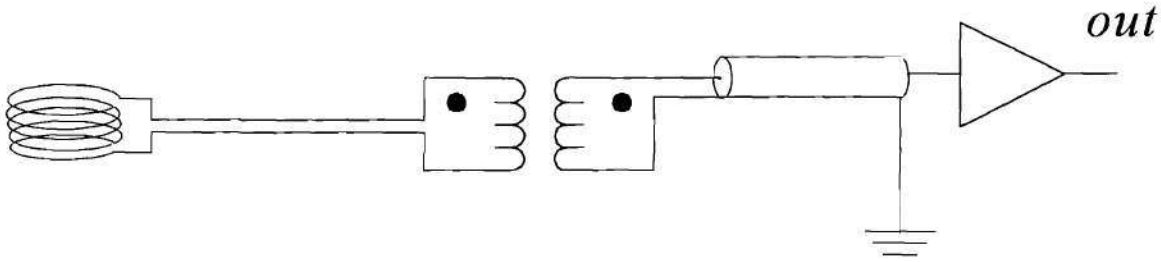

Figure 18. Schematic of magnetic probe circuit. The transmission line transformer is used to maintain the electrical balance of the probe and reject electrostatic pickup. The probe shaft (about 1 cm in length) was insulated with silver paint. Two LN-1000 amplifiers and a Kalmus 102L power amplifier were used to amplify the signal.

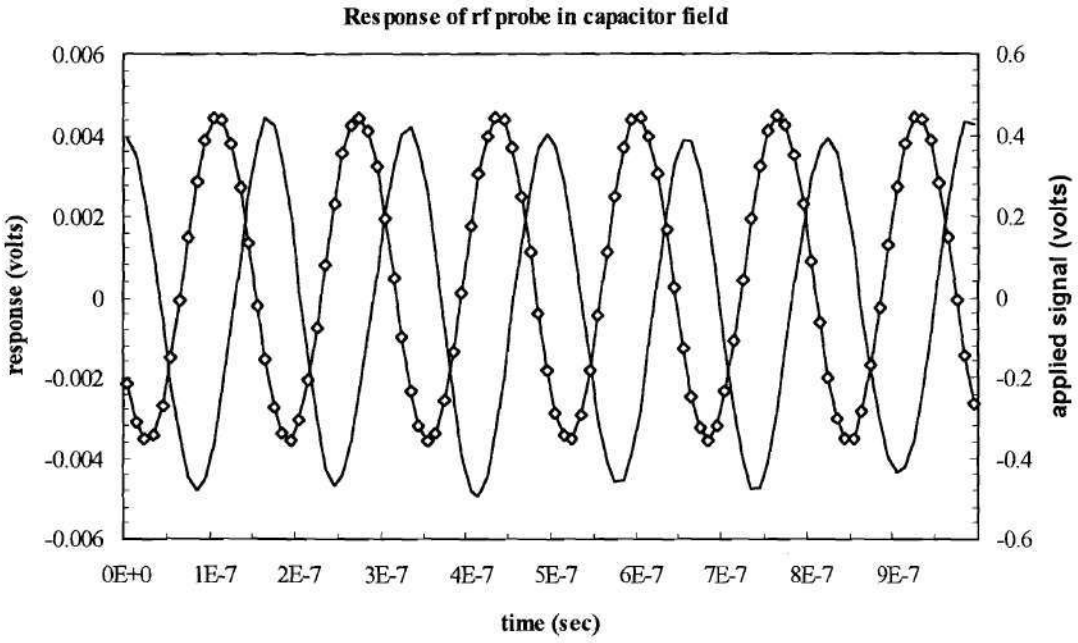

Figure 19. Response of the magnetic probe to a time varying current. The two traces show the probe response with the probe normal oriented at +90° and -90° to the direction of current flow. The magnetic field driving the probe is provided by current flowing in a terminated transmission line.

CHAPTER IV

Fluctuations in the Electrode Current

A typical example of the data collected is shown in figure 20. Fluctuations in the plasma potential (top trace) appear to be correlated with fluctuations in the current collected by the electrode (bottom trace). A more precise description of the correlation between various measurements will be given at the end of this section. These and subsequent observations are used to compare and contrast the operation of the electrode with the models of current collection proposed by Hastings and observed by Stenzel in an unmagnetized plasma.

The current oscillations observed here bear some similarity to those observed by Stenzel and Urrutia. The electrode used in this experiment was roughly 1.5 ion Larmor radii in diameter, much larger than the maximum electrode size used by Stenzel and Urrutia in their investigations. However, the data does bear some resemblance to that collected by Stenzel [Stenzel and Urrutia, 1990, figure 209] using an electrode that was roughly 0.1 ion gyro radii in diameter. The authors found that as the diameter of their current collecting electrode increased, the magnitude of the current oscillations increased while the time between current maxima decreased. For the smallest electrodes used in their experiments (1 mm or 0.004 r_{ci}) no current oscillations were observed, the electrode collected a small amount of current in agreement with the predictions of classical probe theory. When the electrode size was increased to 0.05 r_{ci}, the current collected by the pulsed electrode became sporadic with a repetition rate determined by the probe diameter. When probes of very large diameter (0.1 r_{ci}) were used, the electrode collected a dc current that was only a small fraction of the observed amplitude of the sporadic current pulses (~10%). Thus it might be

expected that increasing the electrode size further would increase the dc current level. This has in fact been observed in the present experiment. The UCLA and Georgia Tech data therefor share the following features:

1. quasi periodic fluctuations in the collected current.
2. a non zero value for the dc current collected by the electrode.

However, unlike the data obtained by Stenzel and Urrutia, in this case there are no large excursions of the current above the saturation current. The amplitude of the current fluctuations is relatively minor compared to the dc current collected by the pulsed electrode. These measurements are described next.

Estimation of the Absolute Magnitude of the Current Oscillations

Because the transmission line transformer used to couple the time varying current from the electrode circuit into the amplifying circuit has a low frequency cutoff at 4 kHz, it is not possible to measure the low frequency components of the probe current, as was done by Stenzel and Urrutia in their experiments. This introduces the following problem in interpreting the signals from the current measuring circuit: are the observed current oscillations riding on a much lower frequency current signal, with a magnitude much greater than that of the oscillations, or are they a true representation of the current collected by the electrode? For this experiment, it was assumed that the maximum amplitude of the current fluctuations can be no more than the electron saturation current drawn by the electrode. This is what Stenzel and Urrutia observed. The electron saturation current drawn by the electrode was measured by placing a dc bias on the electrode equal in magnitude to the amplitude of the pulsed voltage that is applied to the electrode during an experiment. This current is measured with a Keithley digital multimeter in series with the electrode and the bias supply. The amplitude of the current oscillations observed during the course of an experiment are calibrated using the data in figure 207 which indicates the circuit has a gain

of 1.6 μA/mV. The electrode current oscillations are then indirectly compared with the electrode saturation current. The difference between these two values is taken as an estimate of the magnitude of the dc current drawn by the electrode. This procedure indicates the magnitude of the current fluctuations is about 30% of the magnitude of the electron saturation current.

Stenzel and Urrutia do not comment on the dependence of the mean electrode current on the size of the electrode. However, referring to their figure 209, it is not unreasonable to assume the mean current increases in proportion to the electrode diameter. Therefor, the ratio of the current oscillation amplitude to the mean current must decrease as the electrode size increases. Using the data for their 25 mm electrode (~0.1 r_{ci}), the peak to mean ratio is about 10 and should decrease to about 1 when the electrode diameter is equal to the ion cyclotron radius. A further increase in probe size should then drive the ratio below 1 (indicating the current oscillations become negligible in comparison to the saturation current). It is therefor somewhat surprising to find that the peak to mean ratio for this experiment is 1/0.7 = 1.4. Therefor, an ionospheric type plasma seems to be more susceptible to the instability identified by Stenzel than the plasma that he and Urrutia studied.

Regarding Hastings model of current collection in the ionosphere, there is no evidence to support the idea that a current collecting electrode in an ionospheric plasma can collect current in excess of the electron saturation current. Hastings model requires the establishment of double layers downstream from the electrode to increase the collected current. Data concerning the potential structure around the electrode will be presented shortly but considering the current data by itself, the dc value of the saturation current collected by the electrode (~50 μamp at +50 volts) is consistent with the maximum expected saturation current

$$I_{sat,\,max} = J_{sat} A_{probe}$$

$$= (5x10^{8}\ cm^{-3})\ (1.6x10^{-19}\ C)\ (5x10^{7}\ cm/sec)\ \pi\,(0.25\ cm)^{2}$$

$$= 800\ \mu amps$$

The factor of 20 difference between the measured saturation current and the calculated value can be attributed to the effects of the magnetic field and the uncertainty in the measured value of the electron thermal velocity. In any case, the observed current fluctuations certainly do not exceed this value. Additional evidence that the anisotropic contactor theory does not describe the phenomena observed in this experiment comes from measuring the current-voltage characteristic of the electrode when the electrode voltage is varied relatively slowly in time (100 Hz). The collected current can be monitored in the traditional way by placing a resistor in series with the bias supply and measuring the voltage difference across this resistor. No dramatic increase in the collected current was observed.

Perturbations Caused by the Pulsed Electrode

It is important to note that these fluctuations are only observed when the voltage on the electrode is rapidly changed using the HP pulse generator. The fluctuations are not observed when the electrode voltage is supplied by a dc power supply. Figure 21 compares the fluctuation level when the electrode is pulsed (top) and when a dc bias is applied to the electrode (bottom). This important figure illustrates the fact that the oscillations are not due to fluctuations in any of the parameters that describe the ambient plasma. Such fluctuations can occur due to variations in the rate neutral gas enters the vacuum vessel or may be due to a variation in the power supplied to the reentrant cavity plasma source. Under normal operating conditions, these variations are very small and the plasma produced by the source is uniform in both space and time. When the plasma source has been operating for a long period of time, though, rapid variations in the plasma density are often observed. These variations are usually accompanied by noticeable variations in the light output of the plasma column. If such variations were responsible for the observed fluctuations in the collected current, the fluctuations should be observed whether the voltage on

the electrode is provided by a voltage pulse or by an applied dc voltage. This is not the case. Significant fluctuations occur only when the voltage is pulsed and these persist for long periods of time (compared to the pulse rise time). It appears the pulsed electrode is responsible for a major modification of the ambient plasma. Similar observations were made by Stenzel and Urrutia at UCLA.

Comparison with Previous Work

Stenzel and Urrutia concluded that the fluctuations they observed were produced by a density gradient driven ion acoustic type instability. In the experiments reported here, the electrode is large (0.5 cm) compared to the ion Larmor radius (0.3 cm) and is located in the center of the plasma, about 4 ion Larmor radii from the plasma edge. At this position, the gradients in density and temperature are small (n/(grad n) ~ 4 cm) and the electron temperature distribution is nearly flat across the aperture of the plasma source (see Brown et al., 1986) so there is little free energy available for driving drift type instabilities. The density gradients observed by Stenzel and Urrutia were produced by expulsion of ions from the flux tube subtended by their electrode ($\Delta n/n \sim 80\%$, Stenzel and Urrutia, 1990). Since the diameter of their electrode was much smaller than the ion Larmor radius, ions could quite easily leave the region of plasma dominated by the action of the electrode. This effect is unlikely to play a significant role in the experiments reported here because the electrode is almost twice the size of the ion Larmor radius. This implies that ions located in the central portion of the electrode flux tube, greater than a Larmor radius from the edge of the flux tube, can not be expelled. The maximum expected density depletion can then be no more than 40% and, assuming the flux tube remains quasi neutral when the electrode draws current, thus the collected current should have variations of about this magnitude. This is estimate is in good

agreement with the observations, suggesting that the current spikes are due to expulsion of the outer ions from the flux tube.

Measurement of plasma density variations with a floating Langmuir probe indicate that at low neutral pressure (and thus low plasma density) do indicate a substantial decrease of the plasma density in the flux tube. However, at high neural density, plasma density increases when current is drawn by the electrode. This can be explained by ionization of the neutral background gas by electrons accelerated toward the pulsed electrode. The increases in plasma density was measured at a position hundreds of Debye lengths from the electrode so that this phenomenon is not confined to the vacinity of the pulsed electrode but rather effects the whole flux tube.

Consequently, two mechanisms are identified that lead to fluctuations in the collected. The first mechanism, that identified by Stenzel and Urrutia, will occur whenever current collecting electrodes with a diameter more than a few tenths of an ion Larmour radius are used in a magnetized plasma. The other mechanism, ionization of neutral gas in the flux tube, can be suppressed by completely ionizing the gas used in generating the plasma clouds used by plasma contactors.

Observation of a High Frequency Instability Associated with the Pulsed Electrode

The next set of data (figure 22) documents an instability observed when the electrode is pulsed above 50 volts. The instability was initially observed using a glass insulated coaxial Langmuir probe. This probe can be inserted through an Ultra-Torr vacuum fitting in one of the top ports of the vacuum system. The probe was typically located about 5 cm in front of the pulsed electrode and was used to look for any radial dependence of the frequency, growth rate and duration of the instability. The probe shaft was insulated with glass to prevent interference of the probe signal by currents in the stainless steel vacuum

vessel. This later proved not to be necessary since the instability is readily detected using the high frequency coaxial Langmuir probes. No changes in the properties of the instability were noted when the switch from the glass insulated to the coaxial probes was made. An additional coaxial Langmuir probe was mounted on one of the movable probe shafts and used to observe the instability at different axial positions.

First, the instability does not occur promptly with application of the voltage pulse to the electrode but rather occurs after a time delay that may be as long as 5 μsec. In figure 22, the narrow positive going spike in the data is a result of pick up of the probe voltage pulse by the RF probe, it is present even when no plasma is being produced. Since the spike occurs promptly upon application of the voltage to the electrode, it is used to estimated the time delay between the voltage pulse and initiation of the instability. This time delay is highly variable and can last as long as 5 μsec or be so short as to be unobservable on the time scale used in the figure. No relationship between the time delay and the peak electrode voltage, plasma density or neutral pressure was determined during the course of these experiments.

Second, the figure shows the instability is active as long as the 50 volt bias is applied to the electrode. During this time period, the instability grows, saturates, decays and grows again on a time scale of about 20 microseconds (see figure 22). This time scale is much shorter than that associated with the current fluctuations so it is unlikely that the instability plays a direct role in perturbing the current collected by the electrode. Subsequent measurements (to be presented) show that the instability can be detected when no significant fluctuations exist in the collected current.

The data can be expanded (lower trace) and the growth rate of the instability estimated by noting the time it takes for the amplitude of the instability to increase by a factor of 2. From the figure, this happens, for instance, between $t = 3.3 \times 10^{-5}$ sec and $t = 3.7 \times 10^{-5}$ sec. The growth rate is then given by

$$f_i = ln2/(4\ \mu sec)$$

so that $f_i \sim 200$ kHz. This frequency is much greater than the ion cyclotron frequency (20 kHz) and somewhat smaller than the ion plasma frequency (400 kHz).

The amplitude and duration of the signal was observed to be a function of the repetition rate of the pulser driving the electrode. When the repetition rate of the pulser is increased above a few kilohertz and if the peak voltage is above 50 volts a noticeable sheath forms close to the tantalum electrode. The sheath thickness, estimated by visual inspection, is no more than a few millimeters. The light emitted from the sheath is very bright and can exceed the brightness of the plasma column. The correlation of the signal intensity with the formation of the sheath suggests the signal originates somewhere within the sheath.

Fourier analysis of the oscillations (figure 23, using the DSO's FFT option) indicates the frequency of the oscillations is centered near 6 MHz. This is roughly equal to the lower hybrid frequency of the plasma ($f_{lh} = (f_{ce}f_{ci})^{1/2} \sim 6$ MHz). The frequency of the signal decreases as the neutral pressure is increased.

This frequency is much greater than that of the fluctuations in the current collected by the electrode and no correlation is seen between the two phenomena.

Using the movable probe, the dependence of the oscillations on axial position is observed. This data was obtained by squaring the signal from the probe (i.e., using the DSO to square the data used to produce figure 24, for instance) and then averaging this conditioned signal over 100 shots. This provides an estimate of the mean square amplitude of the fluctuations at a given position.

Figure 25 compares two such signals obtained with an 8 cm probe separation. The upper trace was obtained closest to the pulsed electrode, about 8 cm in front of it. This data can be used to infer the axial propagation properties of the instability. In particular, if the instability is an excited normal mode of the plasma with a large axial wavelength, it should travel along the plasma column with minimal attenuation. The signals received at different axial probe positions should look approximately the same. However, the data show this is not the case.

The signal level rises rapidly near the electrode and the amplitude of the disturbance is nearly uniform over a 100 μsec time interval. At the farther probe position, the signal achieves nearly the same amplitude of the first signal but this is maintained for only a short time and the rise time of the signal has increased (it is about a factor of 3 longer). The change in rise time of the signal is indicative of significant attenuation of the disturbance along the plasma column, particularly of the high frequency content of the signal.

The more intense probe signal is observed just inside the potential structure confining electrons to the vicinity of the collecting electrode. This suggests the instability originates near the pulsed electrode. Since the RF probe is primarily sensitive to radial electron density fluctuations, the data indicates the electrode is responsible for initiating a cross field electron density perturbation that travels down the plasma column at a speed that can be calculated from the data in figure 25. By finding the point at which the (roughly) linear rise of the signal meets the line of (roughly) constant signal amplitude for each set of data, a difference in arrival times of 1 μsec is found. This gives a signal propagation speed of 8×10^6 cm/sec. This is well below the electron thermal speed in the plasma (8×10^7 cm/sec) and well above the ion thermal speed (2.5×10^5 cm/sec). The propagation speed is comparable to the measured value of the axial plasma drift velocity ($\sim 3 \times 10^6$ cm/sec, measured with a pulsed plasma source and a Langmuir probe). Since the signal propagates in a direction opposite that of the plasma drift velocity, the signal propagation velocity in the plasma rest frame may approach a significant percentage of the electron thermal velocity (perhaps as much as 20% $V_{th,e}$). The high frequency of the instability suggests that variations in the electron density are involved in its development and growth and the relative large value of its propagation velocity in the plasma rest frame suggest a two stream type instability (involving plasma electrons streaming out of the plasma source and electrons repelled by the electric fields generated by the electrode) may be responsible for the observed signals. This possibility will be analyzed shortly.

Sources of Error

It is possible that the instability is not associated with some plasma phenomenon initiated by the electrode but is instead a signal produced by a sheath-plasma resonance induced in the probe sheath. To investigate this possibility, a positive bias was applied to the probe. This has the effect of reducing the physical size of the sheath surrounding the probe and therefor will alter the frequency of the resonance, if it in fact exists (see Stenzel, 1989). The amplitude and frequency of the disturbance did not change as the dc bias was varied between 0 and 20 volts. This supports the assertion that the RF probe is actually detecting a disturbance in the plasma. Also, when the probe is moved out of the plasma, the signal disappears. This further supports the conclusion that the signals are coming from somewhere in the plasma.

Analysis

The signal from the RF probe is produced by changes in the plasma density. The high frequency of the signal (6 MHz) suggests that it is produced by changes in the electron density rather than the ion density. Since the probe is most sensitive to electric fields oriented along the length of its tip, the observed signals must be caused by radial oscillations in the electron density. Stenzel has observed similar density perturbations and concludes they are due to a two stream instability excited when the electron drift exceeded the thermal speed [Stenzel and Urrutia, May, 1990]. The growth rate of the two stream (or weak beam) instability [Melrose, pg. 34]

$$|\gamma_{\max}| = \sqrt{3}\left(\frac{n_1}{2n_0}\right)^{1/3} \omega_{p0}$$

where n_1 is the electron beam density, n_0 is the ambient plasma density and ω_{p0} is the unperturbed electron plasma frequency, would require an unrealistically low value for the beam density (tens of electrons per cubic centimeter) to be consistent with the observed growth rate of 200 kHz. In addition, the weak beam instability should produce density perturbations along the magnetic field and thus produce electric fields normal to the probe rather than the observed radial electric fields.

The data does not support the idea that the electrode current will excite oblique ion acoustic and scatter electrons toward the flux tube [Hastings, 1987, 1990] since this instability has a real frequency that is close to the ion plasma frequency (400 kHz in this case). To be fair, the wavelength of the observed instability is probably large compared to the plasma radius. If this were not the case, the oscillating radial electric fields would average themselves out over the length of the probe (5 mm) and no signal would be detected. Therefor, there is a possibility that the plasma boundary plays some role in determining the nature of the observed density fluctuations. This is probably unlikely, since the signal dies away quickly when the probe is moved away from the flux tube.

The data can not be described by an ion cyclotron instability driven by a deflected ion beam[72]. The ion beam would be provided by ions streaming out of the source. The beam would be deflected by the electric field near the electrode. However, the growth rate for this instability is much slower than the observed growth rate and the real frequency of the instability, which scales directly with the perpendicular wave number, requires that ions be expelled across the magnetic field at about 10 times the ion sound speed in order for the perpendicular wave length to be 0.5 cm. The plasma density information is not inconsistent with plasma being expelled from the flux tube at this speed ($>10^6$ cm/sec) but, again, the growth rate at this value of the perpendicular wave number is an order of magnitude too low to account for the observations.

Mikhailovskii discusses a high frequency instability in plasmas with a non-maxwellian ion velocity distribution that does fit the observed growth rate and frequency[73]. The instability arises out of an interaction between electron plasma oscillations and a beam of ions moving perpendicular to an applied magnetic field. The instability has both a real frequency and growth rate that are much greater than the ion cyclotron frequency, characteristic of the instability observed in these experiments. The necessary conditions for the instability are that the plasma density be high enough to satisfy $\omega_{pi} >> \omega_{Bi}$ (400 kHz >> 20 kHz in this case) and that the ions have a perpendicular velocity V_o such that $T_e << m_i V_0^2/2$. The ions do attain a high perpendicular velocity due to the ExB drift associated with the observed radial electric fields ($V_{ExB} \sim 4x10^6$ cm/sec >10 C_s). This provides the ions with a perpendicular energy of about 250 eV so that the previous inequality is easily satisfied (T_e = 4 eV).

The growth rate for the instability is

$$\gamma = \left(\frac{m_e}{m_i \cos^2 \theta} \right)^{2/5} \frac{\omega_{pe} \cos\theta}{\left(1 + \omega_{pe}^2 / \omega_{Be}^2 \right)^{1/2}}$$

This can be solved for the direction of propagation, θ, by setting the right hand side equal to the observed growth rate $\omega_i = 2\pi$ (200 kHz). The value obtained is very close to 90^o ($\cos\theta = 1.4x10^{-4}$) which agrees with the observation that the principle component of the electrostatic instability is directed along the plasma column radius.

Once θ is determined, it can be used in the dispersion relation to see if the predicted value of the wave number is in reasonable agreement with the observations. The dispersion relation for the instability is given by

$$1 + \frac{\omega_{pe}^2}{\omega_{Be}^2} - \left(\frac{\omega_{pe} \cos\theta}{\omega} \right)^2 - \frac{\omega\, \omega_{pi}^2}{\left(\omega^2 - k^2 V_0^2 \right)^{3/2}} = 0$$

Note that this relation has a dependence on the plasma density that is similar to the observed density dependence (see figure 23). The value of V_0 is determined by the ExB drift velocity obtained by the ions due to the strong perpendicular electric fields generated by the electrode. For this analysis, this value is assumed to be equal to the value consistent with the strength of the measured electric field (10^6 cm/sec). The observed value of the frequency (6 MHz) is also used. These numbers predict the wave number k of the instability to be around 5.5 cm^{-1} and thus the wavelength of the instability is roughly 1 cm. The plasma column is just wide enough to accommodate the wave.

The effects of the plasma vacuum interface have been ignored. However, for this instability, the boundary is not likely to play a crucial role. This high frequency instability is possible as long as the plasma density and magnetic field satisfy the requirement

$$\omega_{Bi} > \omega_{Pi}$$

This implies the instability can no longer propagate, in this experiment, when the plasma density falls below $4x10^5$ $cm\text{-}^3$. The measured plasma density is fairly flat across the plasma column but falls off drastically outside the column. If the density is assumed to fall exponentially with distance and if the plasma density is assumed to be $3x10^8$ cm^{-3} at the plasma edge, then the conditions for instability are not satisfied at a distance of 6 to 7 cm from the plasma axis. Therefor, the effective plasma edge is many wavelengths away from the region where the instability originates.

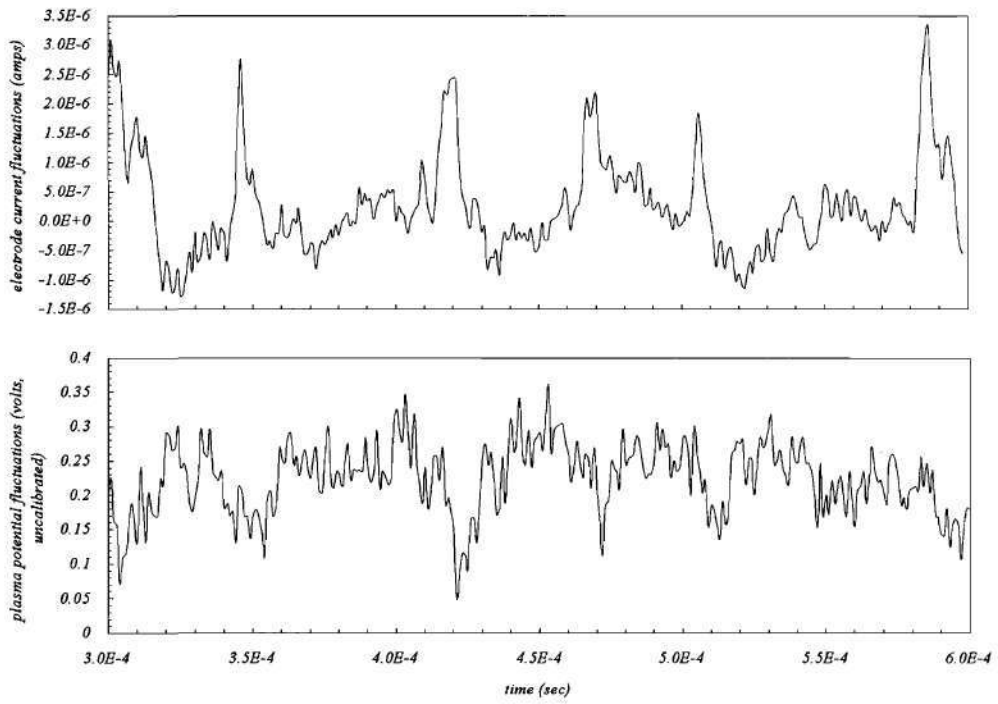

Figure 20. This data is representative of the data collected and used to investigate the effect of a pulsed electrode on the ambient plasma. Signals collected by a movable probe (plasma potential in this case) are correlated with fluctuations in the current collected by a biased electrode.

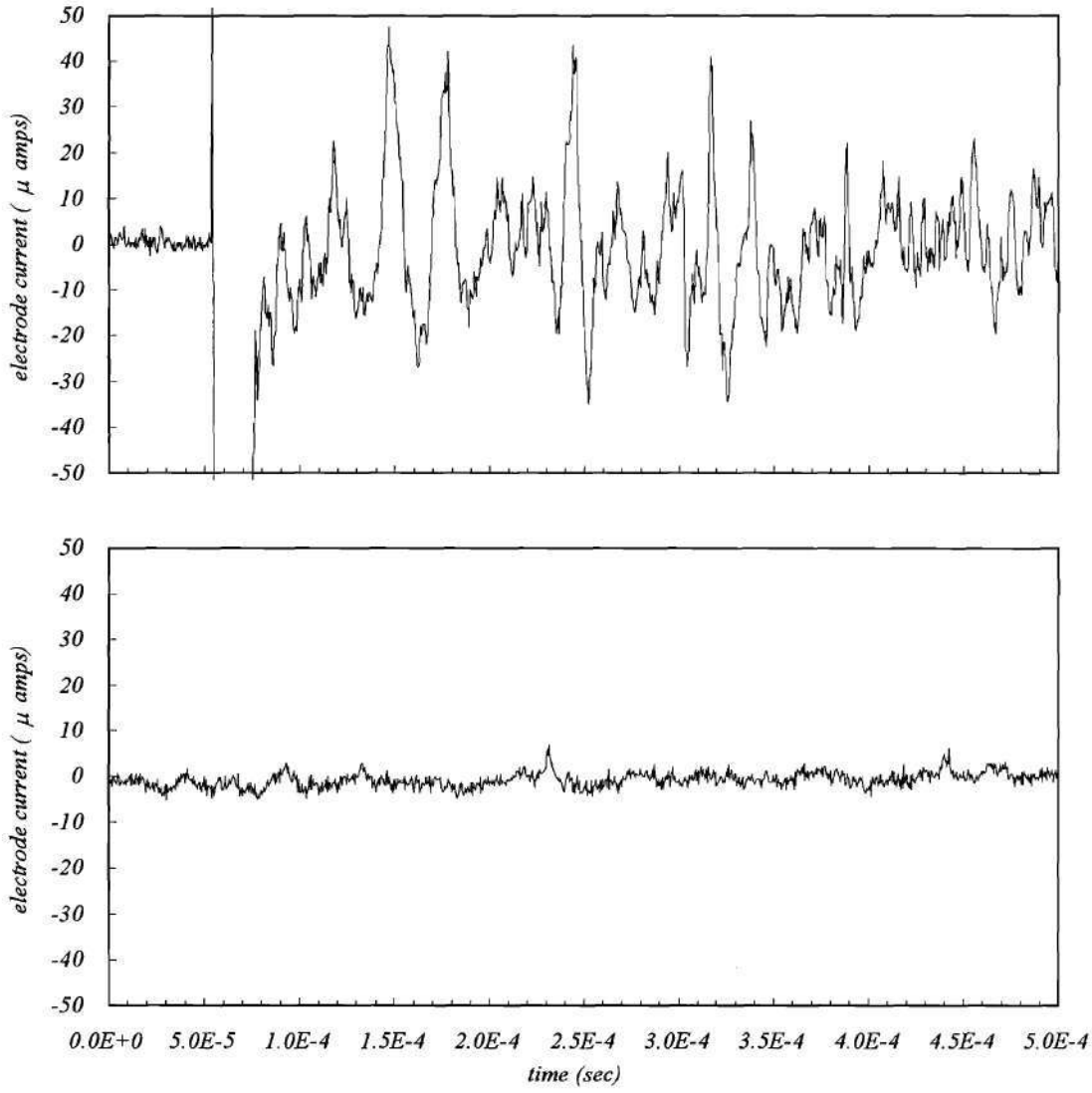

Figure 21. Electrode current oscillations. The upper figure shows the transient current spikes in the current collected by a pulsed electrode. The lower figure shows the fluctuations when a dc bias is applied to the same electrode. The vertical scale is in amps.

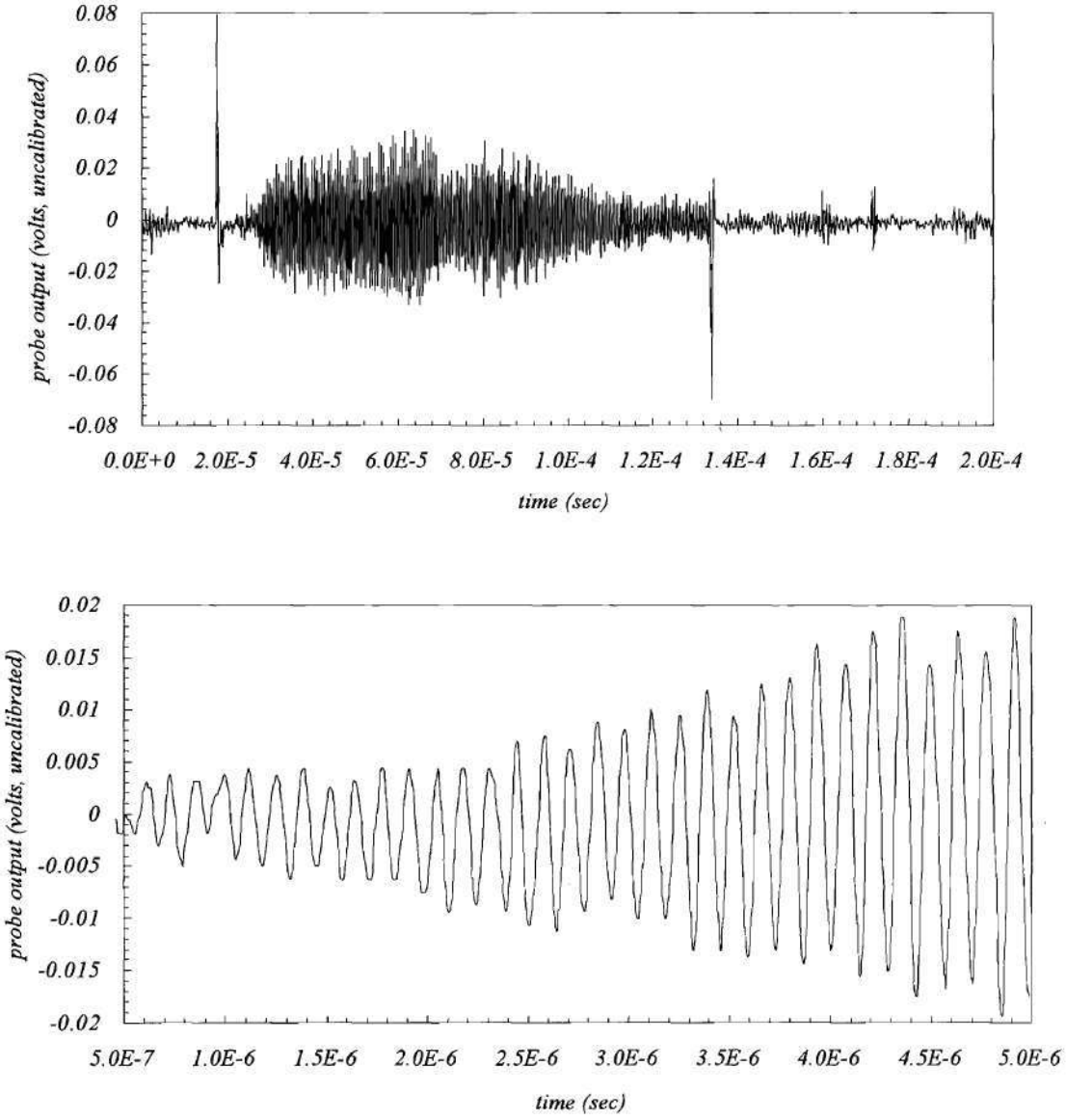

Figure 22. Electrostatic fluctuations observed with a coaxial probe. The lower figure is an expanded view of the upper trace and shows the growth rate of the instability and its well defined frequency.

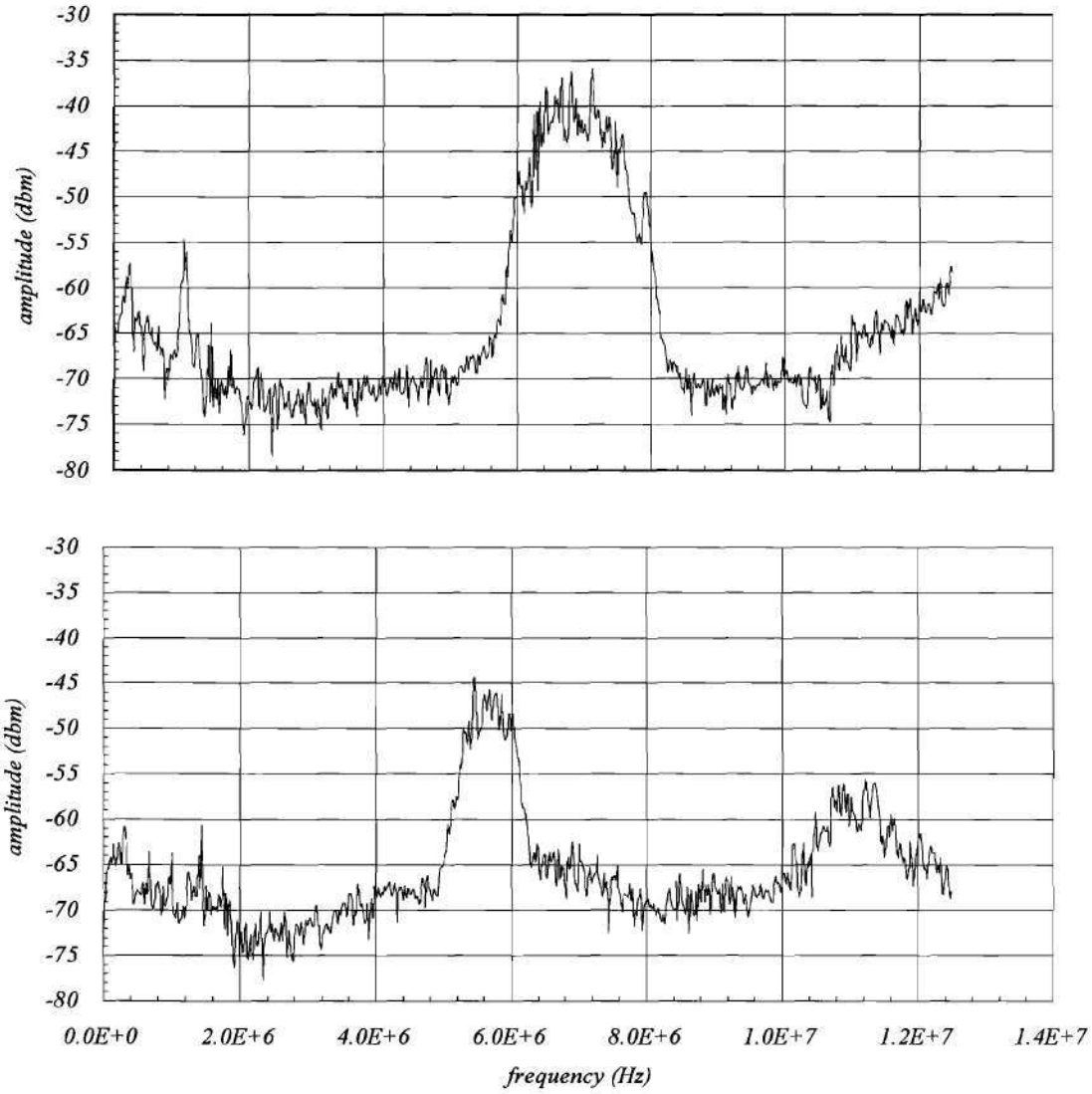

Figure 23. Frequency spectrum of plasma instability excited by a rapidly biased electrode, detected by an RF probe in the plasma. The probe signal was coupled via a transmission line transformer to two low noise amplifiers. Upper trace taken at $8x10^{-4}$ Torr, lower trace taken at $3x10^{-4}$ Torr.

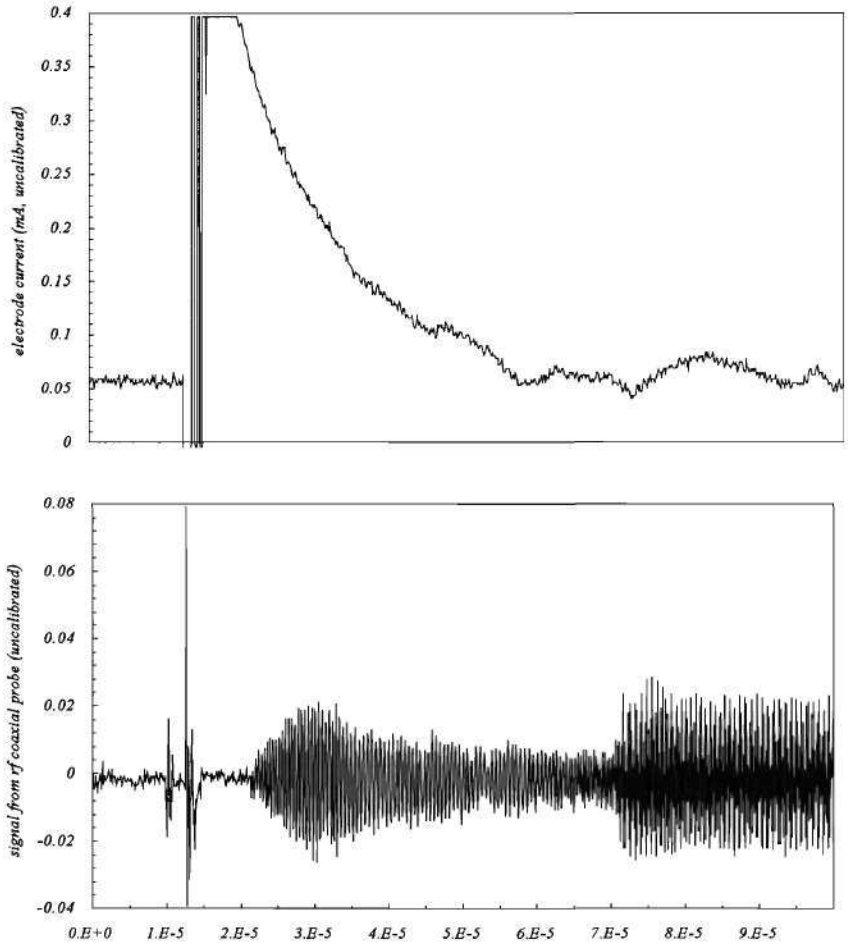

Figure 24. Electrostatic fluctuations do not always correlate with fluctuations in the current drawn by the pulsed electrode. These observations were made at a neutral pressure of 3 x 10^{-4} Torr.

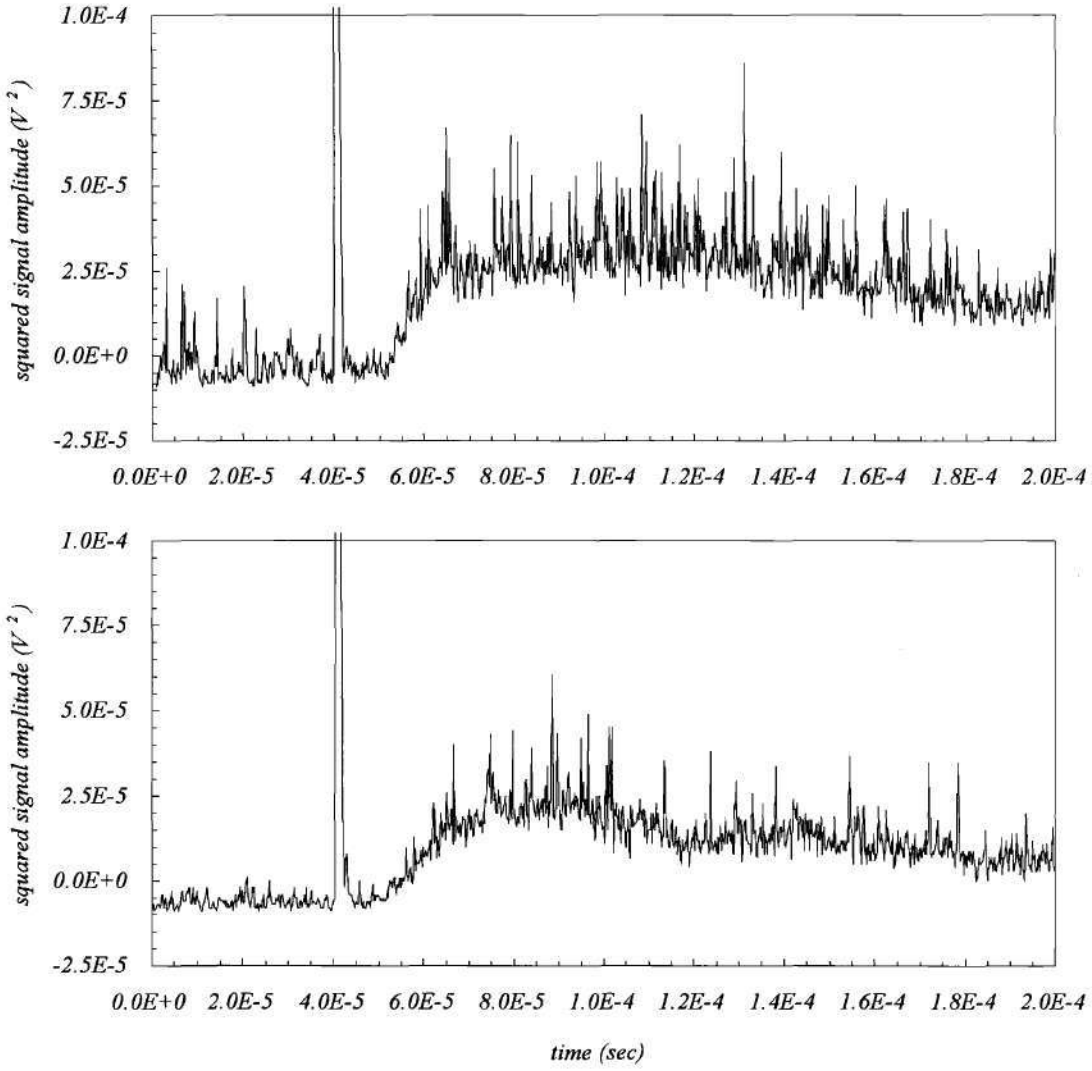

Figure 25. This data was acquired by squaring the signal from the RF probe and averaging the result over 100 shots. The upper trace was obtained 10 cm in front of the electrode. The lower trace was taken 18 cm in front of the electrode. Wave intensity is greatest near the electrode where large radial electric fields exist.

CHAPTER V

Plasma Potential Measurements

Axial measurements were made to identify double layers. Hastings theory conjectures that a current collecting electrode in a magnetized plasma will create a double layer downstream of the electrode that will extend radially in a plane perpendicular to the magnetic field lines. Collisional flow of charged particles across the magnetic field will prevent the formation of double layers in the plane of the magnetic field.

Mapping the plasma potential along the axis of the vacuum system provides a way of searching for double layers by looking for the characteristic potential drop that is associated with them. Ideally, such a search would reveal a dramatic drop in the plasma potential from a value determined by the voltage applied to the electrode (50 to 100 volts) to a value determined by the potential of the plasma source (which is typically grounded to the walls of the vacuum tank) over a distance of not much more than one centimeter (since the Debye length is roughly $5x10^{-3}$ cm). The position at which the transition takes place is a function of the current collected by the electrode. As the electrode current increases, the double layer must move further away from the electrode, giving the trapped electrons more time to diffuse to the place of current collection. Therefor, and again ideally, the double layer transition will occur far enough away from the electrode so that the spatial resolution of the capacitive probes should not limit the observations.

If an object such as a double layer is produced by the pulsed electrode, there is the possibility it will not remain near the position of its initial formation but will instead travel down the magnetic field (as may be

required in order to satisfy the Langmuir condition in its reference frame, see Carlqvist, 1972). In this case, its presence can be detected in a plot of the average plasma potential in the vacuum vessel at various times after the voltage pulse is applied, see figure 26.

The three pictures at the top of the figure indicate the instantaneous value of the plasma potential (V) at three times after the voltage pulse is applied to the electrode. A double layer formed by the rapid voltage pulse travels away from the electrode (from left to right in the figure). A capacitive probe at the position labeled X' records the plasma potential at position X' continuously from time t=1 to time t=3. The output voltage of the capacitive probe, viewed with an oscilloscope, would look like the picture at the bottom of the figure. A collection of such pictures at various probe positions X' can be used to study the evolution of the plasma potential throughout the plasma column, provided the plasma parameters are constant from shot to shot. This will be discussed shortly.

These methods provide a crude way of identifying double layers. A more sophisticated approach would use energy analyzing probes to identify the trapped particle distributions that are necessary for the formation of the double layer[74]. An energy analyzer was not used in this experiment because the small diameter of the plasma column (2.5 cm) places severe restrictions on the probe size. Swept Langmuir probes[75] [76] have been used to study the evolution of plasma properties on time scales that are long compared to the sweep rate but this technique was not used because of the uncertainties introduced by the magnetic field in the interpretation of the probe trace. Never the less, double layers are always associated with a potential drop greater than the electron thermal energy and are seldom more than several Debye lengths thick[77]. Identification of such a structure in the data would provide strong evidence for the anisotropic contactor model.

Experimental Procedure

The average plasma potential at a given position was measured using a capacitive probe and averaging the signal (using the built in functions of the DSO) over 100 shots, see figure 27. The probe was moved in 1 cm increments along the vessel starting at about 2 cm in front of the pulsed electrode. The probe head was positioned so that it was always just inside of the outer edge of the flux tube subtended by the electrode. This was done to minimize any perturbations that might be caused by the presence of the relatively large capacitive probe. A typical example of the measured potential is shown in figure 28.

To obtain a plot of the plasma potential along the axis of the vacuum chamber as a function of time, the average potential at various axial positions was measured using the DSO and the resulting data stored on a Macintosh II computer. Each measurement is initiated by a trigger signal from the HP pulser so that data acquisition is accurately timed to coincide with the voltage pulse applied to the electrode.

The resulting data consists of pairs of numbers (time and voltage) representing the digitized signal from the DSO. The data is written to files that are readable by a spread sheet program (KaleidaGraph by Abelbeck Software). Each file therefor contains information about the average plasma potential at a specific location. The files are loaded into the spreadsheet program and arranged so that the data contained in individual files is stored in separate columns of the spread sheet. The rows of the spreadsheet therefor represent unique moments in time after the trigger. It is then a simple matter to select a row from the data set, transpose it and then graph it. This provides a plot of the "instantaneous" average plasma potential along the axis at any time relative to the trigger signal.

Data Obtained with the Capacitive Probe

When analyzed in this way, the data indicate the pulsed electrode is responsible for the creation of a complicated axial potential. The overall plasma potential increases by approximately 10 volts within 1 μsec of pulse initiation, see figure 29. For comparison, the data at 162 μsec indicate the state of the ambient potential fluctuations before application of the pulse. Relatively large potential structures (~ 8-10 volt amplitude) form in front of the pulsed electrode (at position 4000) and the plasma source (a few centimeters to the left of position 800). The amplitude of these structure is greater than the electron energy (4 eV) and have relatively steep potential gradients: $dv/dx = 8v/3$ cm for the left hand structure.

Analysis of Capacitive Probe Data

Such a potential structure has the possibility of trapping the low energy ions, coming from the plasma source, in the central portion of the vessel (between positions 1900 and 3600). Provided a trapped electron population exists in the high potential structure, this can be considered evidence of double layer formation by the pulsed electrode. It is likely that electrons are trapped in the potential structure but such a statement can only be confirmed by measuring the electron distribution function, either with an energy analyzer or by careful analysis of Langmuir probe characteristics, within the potential structure. As mentioned previously, the energy analyzer was not constructed because the small size of the plasma column necessitates the use of a very compact instrument. Analysis of Langmuir probe characteristics was not performed because of the very great uncertainty that the magnetic field introduces into the interpretation of the probe characteristic.

Some of the features in figure 29 and figure 30 are due to unavoidable variations in the raw data. For instance, the apparent potential trough located between positions 1600 and 2000 in the 162 μsec and 163

μsec curves is due to a slight decrease in the amplitude of the signal received by the capacitive probe at position 1800. Similarly, the trough at position 3200 in the 550 μsec and 530 μsec data is again most likely to due a change in the capacitive probe signal intensity associated with a slight change in the plasma parameters. However, the trough that begins to develop on the right hand side of the 163 μsec data set, as well as the peaks in the data at positions 1200 and 3600, appear to be real structures that form in response to the pulsed electrode. This assertion is based on the observation that these structures are composed of several data points and therefor appear to represent a real trend in the data.

The peak closest to the pulsed electrode forms in less than a microsecond after application of the electrode voltage and appears to travel about 4 cm into the plasma in about 40 μsec. The potential gradient associated with this structure will retard the flow of low energy electrons to the electrode. However, due to the potential structure near the plasma source, the population of low energy electrons in the plasma column is likely to be very low. The column must consist primarily of cold ions trapped between the potential structures and hot electrons streaming in from the plasma source. This situation is maintained as long as the voltage is maintained on the electrode (see the 250 μsec and 525 μsec data, figure 30, which shows the behavior of the potential structures as the bias is removed from the electrode) although the amplitude of the potential structure in front of the source does increase over time.

Radial Plasma Potential

Experimental Procedure

The radial plasma potential was measured in an attempt to observe the strong radial electric fields observed by Stenzel and Urrutia. These authors determined that their pulsed electrode produced electric

fields that extended far into the plasma, well beyond the limits of the classical electrode sheath. This field played a large part in determining the repetition rate of the instability they observed.

In this experiment, the radial field created by the electrode can be indirectly measured using the capacitive probe. The difference in the probe signal between two radial positions divided by the average radial separation of the two positions is roughly equal to the value of the electric field. Figure 31 illustrates the relationship between the probe radial position and the electrode for several different probe orientations.

Radial Electric Field Data

The data in figure 32 was taken at a neutral pressure of about 3 x 10^{-4} Torr. The electric field was measured by subtracting the plasma potential measurement at 5^{0} from the measurement taken at 0^{0} and then dividing by the radial separation between these positions (about 5 mm). Since the electric field in the plasma is given by

$$E = -\nabla\phi - \nabla(nkT_e)/ne$$

this method ignores the contributions of any gradients in density or temperature to the electric field. In particular, the density gradient is ignored and there is some evidence (to be presented) that the electrode produces a large depletion of the plasma density in its flux tube when the neutral pressure is above $3x10^{-3}$ Torr. For the following analysis, this contribution is ignored.

The data indicate that a weak radial electric field, directed toward the center of the plasma column, exists in the vacinity of the pulsed electrode (position 3681). The field has a sharp rise time (5 μsec) and decays within 200 μsec of initiation of the voltage pulse. A residual field, directed outward, may remain.

As the capacitive probe is moved away from the electrode (position 3072) and toward the plasma source, a strong outwardly directed electric field develops (the plasma potential at 0^o is greater than that a 5^o, the electric field points in the direction of decreasing potential: $E=-\text{grad}(\Phi)$). This will cause electrons and ions to drift in a clock wise direction around the plasma column with a maximum speed of

$$v_{drift} = cE/B = (3x10^{10}\ cm/sec) \times (8/300\ statvolts)/(0.5\ cm \times 540\ gauss)$$
$$= 4x10^{6}\ cm/sec$$

This speed is much less than the electron thermal speed ($8x10^7$ cm/sec) but much greater than the ion sound speed (3×10^5 cm/sec). Therefor, the possibility exists for the drifting plasma to excite instabilities.

Note that initially the radial electric field at all positions is positive. This is most likely due to electrons being drained from the flux tube by the electrode. This leaves the slowly moving ions alone in the flux tube and these produce the observed electric field. This explanation is in qualitative agreement with plasma density observations made with a floating coaxial probe. This initial field configuration is rapidly replaced by one in which the radial field is negative and thus points away from the plasma axis.

When the capacitive probe is located near the ends of the plasma column (near the source or the electrode) the initially positive electric field decays within 200 μsec to a value that is indistinguishable from the thermal noise received by the probe in an undisturbed plasma. Thus, these regions do not support radial electric fields. Interestingly, these are the regions where the axial electric field is greatest.

In the center of the plasma column, the initially positive electric field is replaced by a substantially larger negative electric field. Fields of comparable magnitude have been observed by Stenzel [Urrutia and Stenzel, 1986] but these reportedly did not exist for as long as those observed in the present experiment (several microseconds compared to several milliseconds). In addition, the UCLA group found strong radial electric fields existed near the pulsed electrode, unlike the fields observed here. Stenzel postulated that the radial electric fields caused electrons to ExB drift around the electrode flux tube and caused the

essentially unmagnetized ions to be expelled from the flux tube. The relative drift of the electrons with respect to the ions was thought to generate ion sound turbulence, resulting in cross field transport of electrons into the flux tube. Clearly, this can not be the case in the experiments reported here since the ion motion must be considered magnetized when compared to the diameter of the flux tube. However, it is interesting to note the occurrence of radial electric fields in a magnetized plasma.

Referring to figure 29, the strong radial field exists in a region where the axial electric field is relatively weak (midway between the source and the electrode). The data is not incompatible with the existence of weak, outward directed, radial fields in the region where the axial electric field is greatest (near the source and the electrode). The combined effect of both field components acts to reduce the flow of low energy electrons to the electrode. The axial field retards the motion of electrons produced by the source and the radial field acts to decrease the local value of the magnetic field through the diamagnetic drift of electrons. The electron Larmor radius increases as the magnetic field decreases and thus electrons can have larger excursions away from the electrode flux tube, possibly causing fluctuations in the current collected by the electrode.

Sources of Error

1. long term drift in plasma parameters

The method used here to study the plasma potential is susceptible to long term drifts in the plasma parameters that could lead to subtle changes in the potential profile (at a given position) over time. For example, long term drift in the plasma density has been observed to occur as the magnets heat up during the course of an experiment. This most likely changes the resistance of the magnets and therefor changes the current flowing in them, affecting the magnetic field and thus the electron cyclotron frequency. The efficiency of the plasma source is greatly dependent on resonantly heating the electrons thus a change in

the magnetic field leads to decreased plasma density. To verify this effect was not influencing the plasma potential measurements, plasma potential was measured in front of the pulsed electrode at the beginning and end of each run. If the two measurements were not sufficiently similar (as determined by eye) the data were discarded and another set taken. Such unprofitable data taking was minimized by allowing the magnets to warm up for roughly 30 minutes before beginning each experiment.

2. transient nature of the signals

An additional limitation of this procedure is due to the transient nature of the phenomenon being studied. Plasma potential information obtained at different times will be of limited utility in explaining the observed fluctuations at any specific time. It would be preferable to measure the plasma potential throughout the vacuum vessel nearly instantaneously with respect to the repetition period of the current fluctuations. This is, of course, not possible due to the small time scale of the current fluctuations and the very long time required to position probes using the existing system.

This problem becomes even more severe when comparing instantaneous values of the plasma potential or electric fields and the chaotic fluctuations in the current collected by the electrode (to be discussed). Figure 34 shows the relationship between the instantaneous plasma potential, current fluctuations and the average plasma potential at position 3681. The instantaneous plasma potential is a combination of the effects of the pulsed electrode and the thermal fluctuations that are always present in the plasma.

The magnitude of the thermal fluctuations can be estimated by considering the plasma to have a resistance determined by the slope of a Langmuir probe I-V characteristic near the knee in the characteristic (which is a measure of the plasma potential). Using the data pictured in figure 32, this resistance is found to be about 200 kΩ. This number can then be used in the formula for the thermal noise in a resistor

$$V_{noise\ (rms)} = (4\ kT\ R\ B)^{1/2}$$

where T is the plasma temperature, R is the resistance of the plasma and B is the bandwidth of the LM310 voltage follower used in the capacitive probe circuit (20 MHz). The value arrived at for the thermal plasma noise (~50 mV) is consistent with the fluctuations observed in the capacitive probe data after accounting for the gain of the 102L amplifier (33 dB).

Some of the features of the averaged potential can be seen in the unaveraged data but no features in the averaged data correspond to the observed current fluctuations. Some correlation is seen between the current spikes and the plasma potential peaks in the unaveraged data. Thus, although the average potential exhibits some interesting properties, it can not be used to explain the current oscillations.

3. strong dependence of signals on neutral pressure

During the coarse of acquiring this data, a strong dependence of the output of a coaxial floating on neutral pressure was observed. An example of this dependence is given in figure 33. In each trace the probe is responding to a 50 volt pulse on the electrode. At the lower pressure, corresponding to a leak valve setting of 66, the probe responds as one would expect: the probe potential increases above its ambient value. At the higher pressure, corresponding to a leak valve setting of 67.5, the probe signal becomes negative after application of a positive voltage pulse. In fact, the low pressure signal is nearly a mirror image of the high pressure signal.

Since the output of the floating probe is sensitive to the plasma density, this data indicates the pulsed electrode depletes the plasma density in the flux tube when the neutral pressure is low (this has been

observed by Stenzel) and increases the plasma density in the flux tube when the neutral pressure is high. This is consistent with ionization of neutral gas in the flux tube. This sensitive dependence of behavior of the plasma potential with neutral pressure makes it difficult to construct maps of the plasma potential that can be compared between different experiments, because of the large variability in neutral pressure at a given leak valve setting. To avoid problems associated with the effects of the neutral pressure, the neutral pressure was measured before each experiment using an ion gauge tube. This provides a gross estimate of the pressure and can not be used when the magnetic field is on.

Comparison with Previous Work

The measured electric fields are in major agreement with those observed by Stenzel. The electrode produces significant parallel and perpendicular fields that exceed those allowed by classical theories and these fields penetrate far into the plasma, well beyond the distance of a classical probe sheath. However, differences in the data do exist. There is no large perpendicular field near the electrode, as observed by Stenzel and Uruttia, but there is a large perpendicular field in the center of the plasma column.

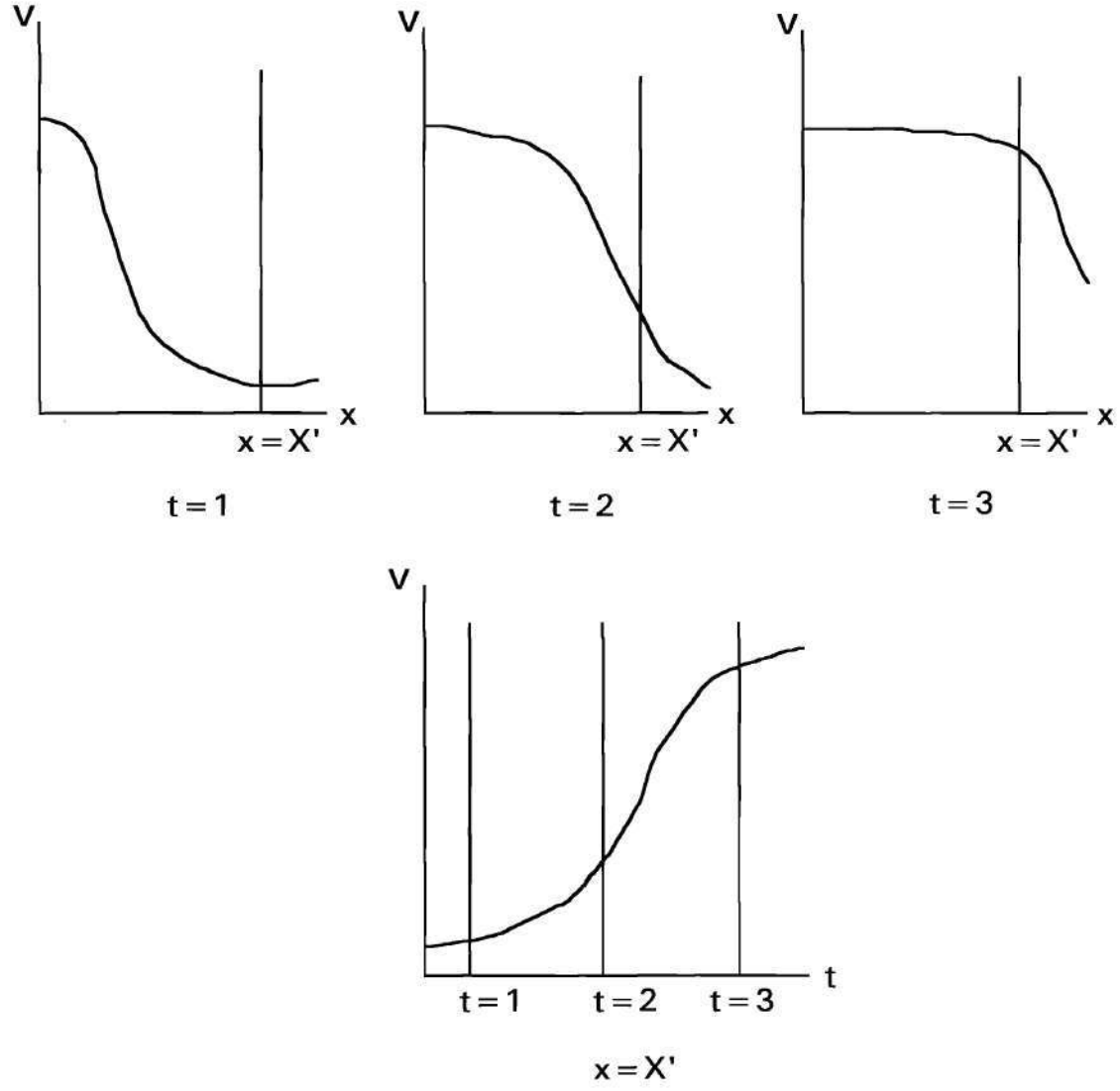

Figure 26. A moving double layer, top row, can be detected by analyzing the output of a capacitive probe, bottom row.

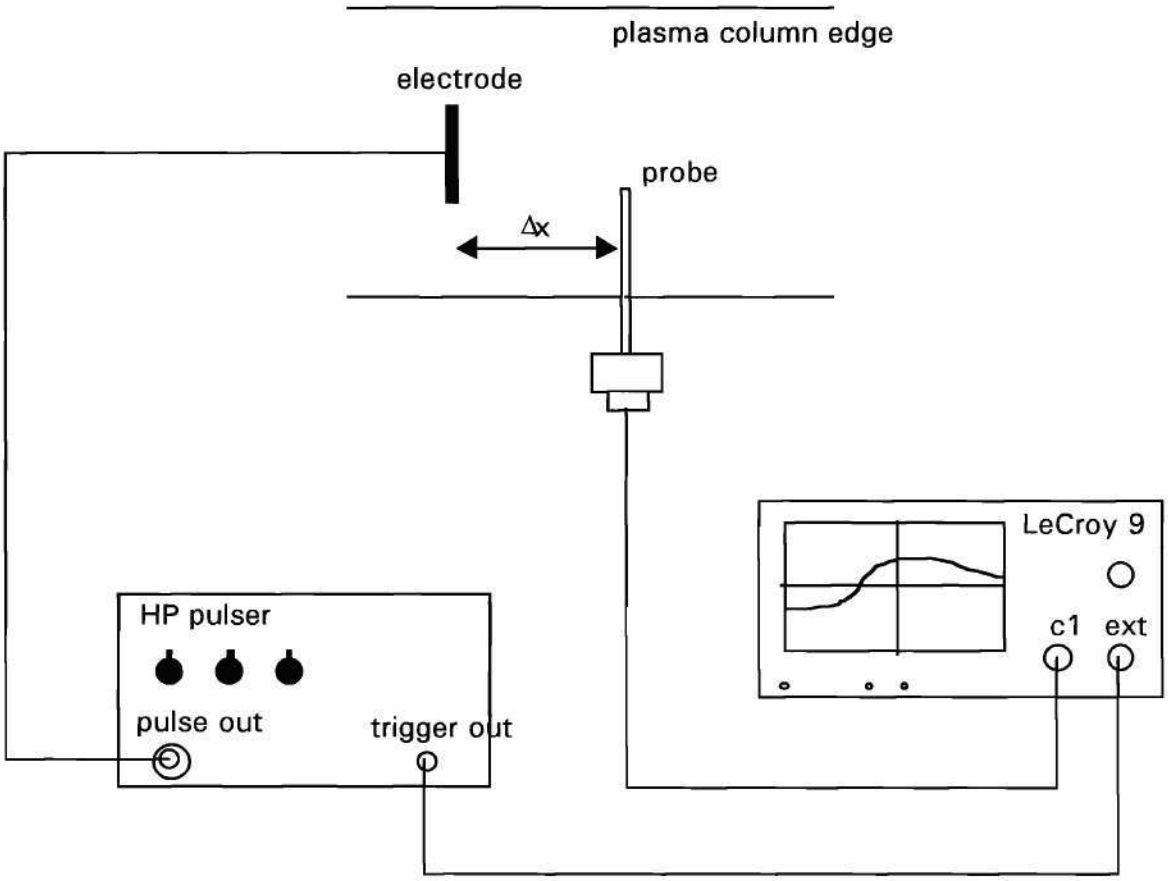

Figure 27. Schematic diagram of data acquisition system used to observe fluctuations in the plasma potential.

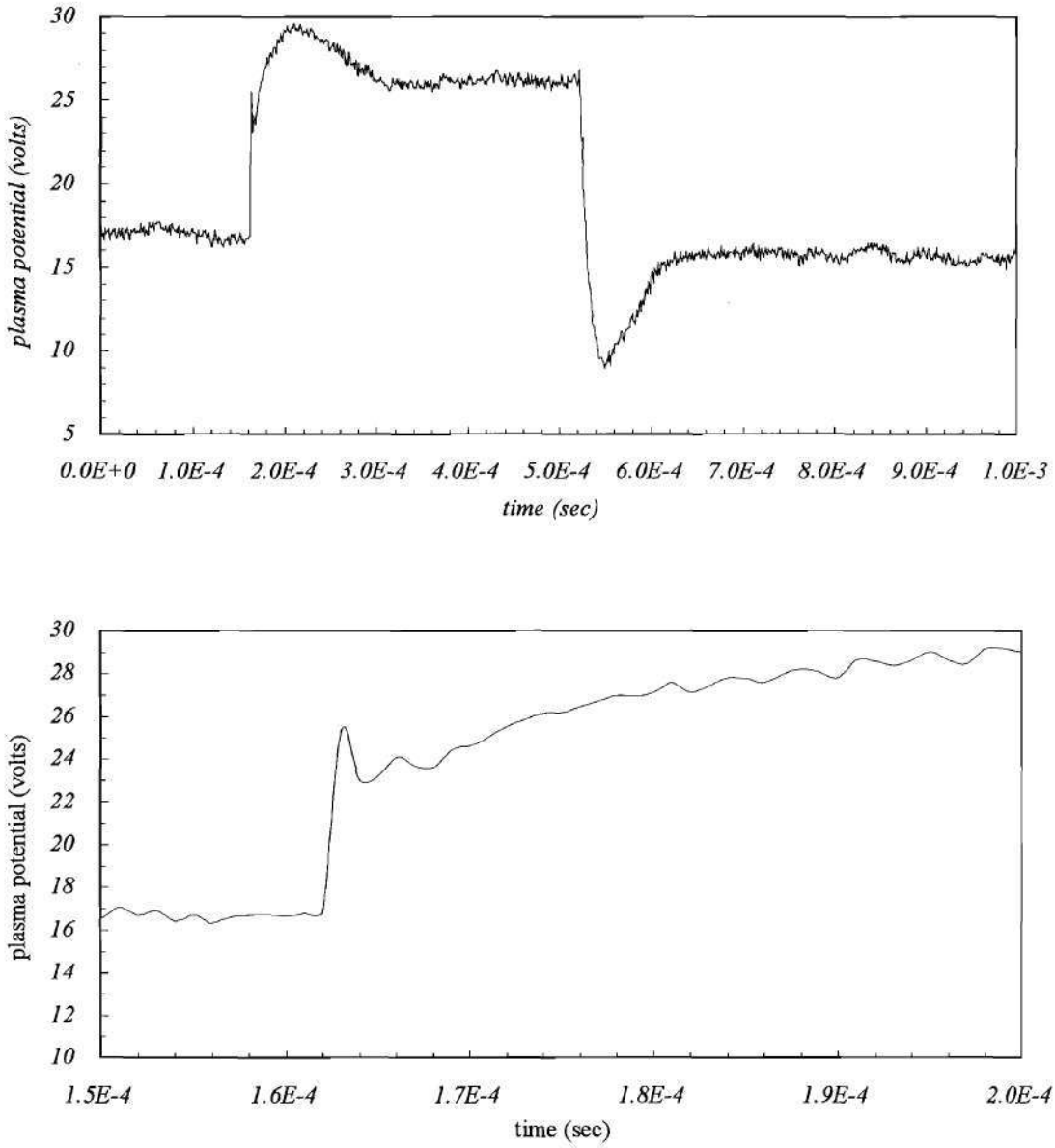

Figure 28. Signal from the capacitive probe when the neutral pressure in the system is relatively high. The rapid rise of the signal and its slow decay suggest a double layer has moved past the probe.

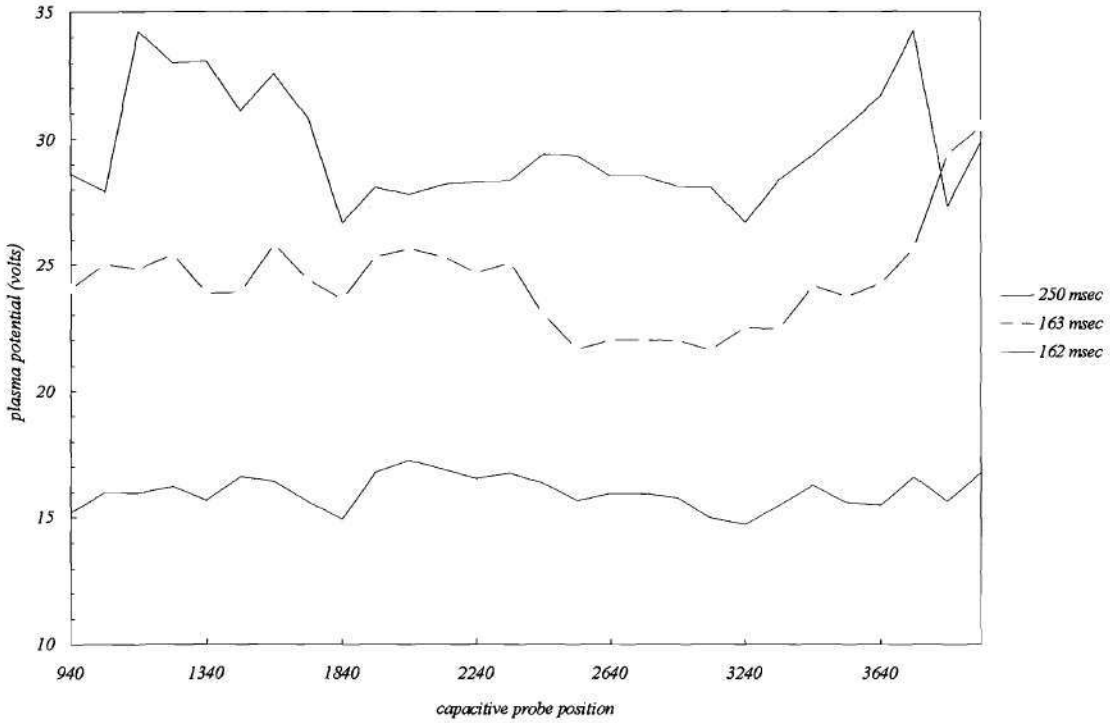

Figure 29. "Instantaneous" map of the plasma potential at various positions along the axis of the vacuum system. The electrode pulse is applied at roughly 163 μsec. The plasma source is located near position 500 and the electrode is near position 4000.

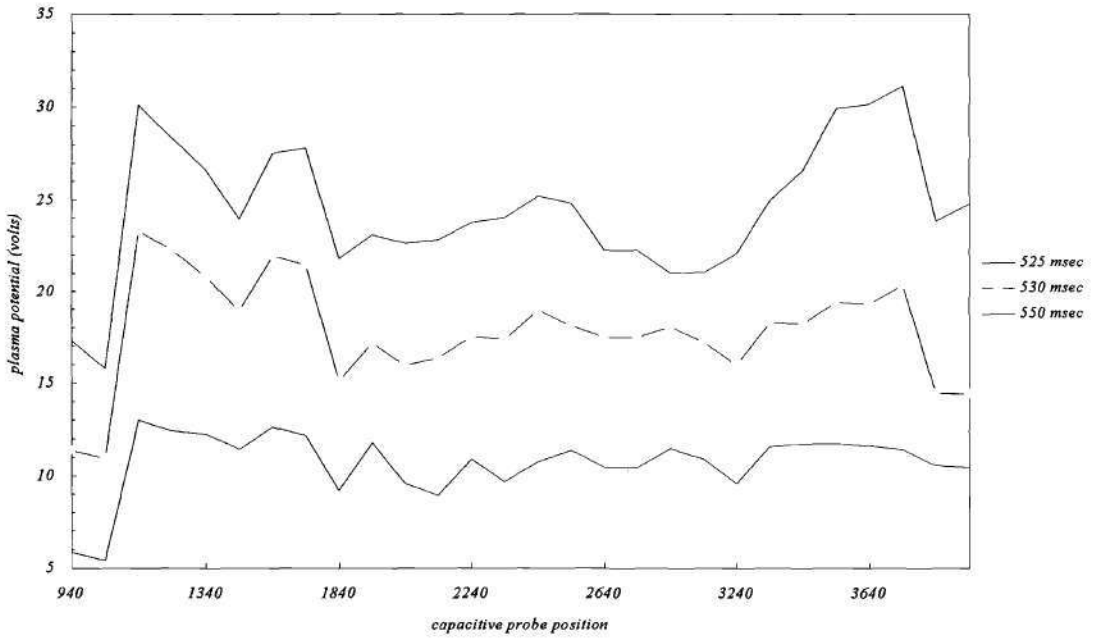

Figure 30. Response of the plasma potential to removal of the electrode voltage. Unlike the case at turn on, the plasma potential decreases relatively slowly and no fast transients are detected in the vacinity of the electrode. The probe bias is removed between 525 and 530 μsec.

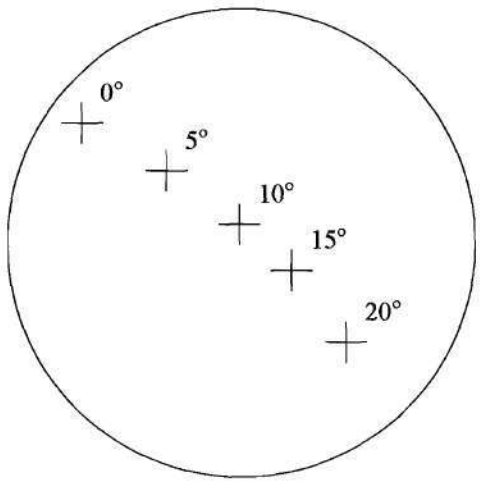

Figure 31. Diagram indicating position of capacitive probe (crosses, with goniometer settings indicated) with respect to the pulsed electrode (small circle) and the plasma boundary (large circle).

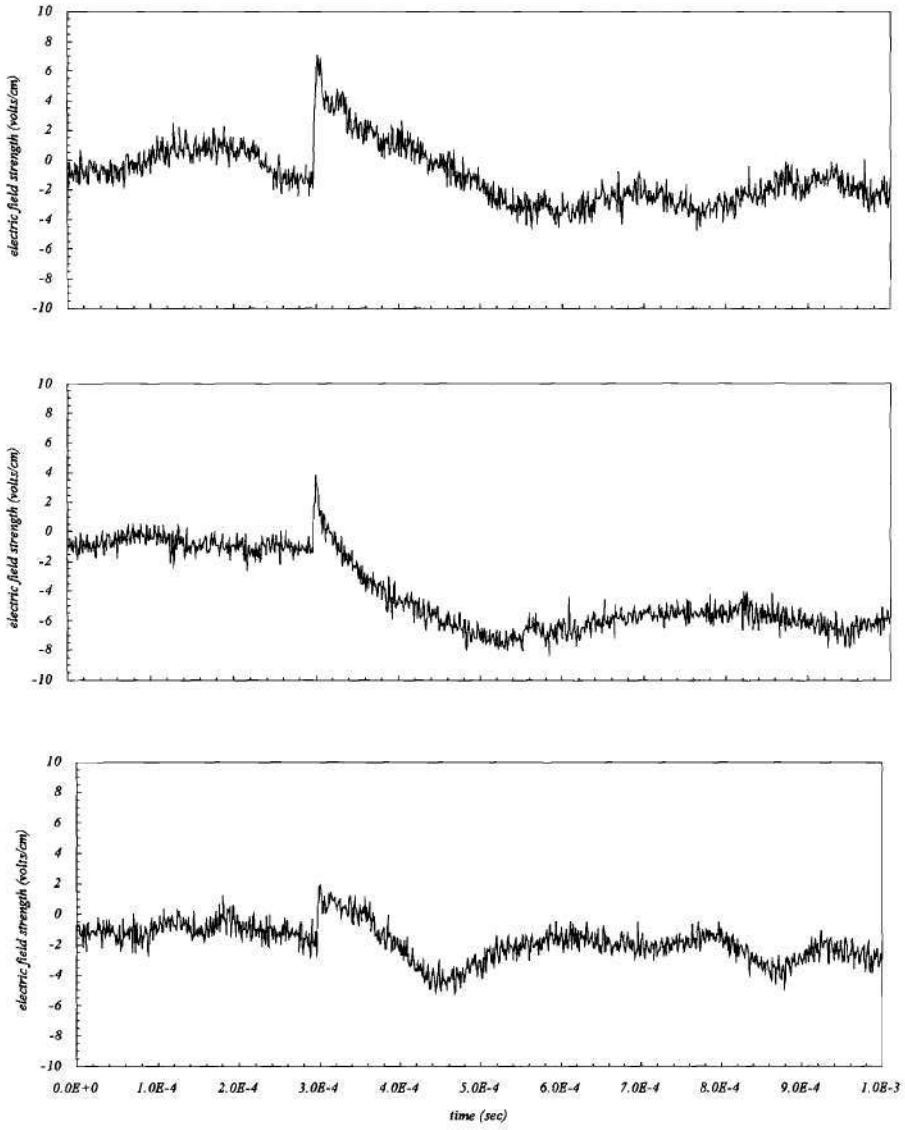

Figure 32. Radial electric field measured with a capacitive probe.

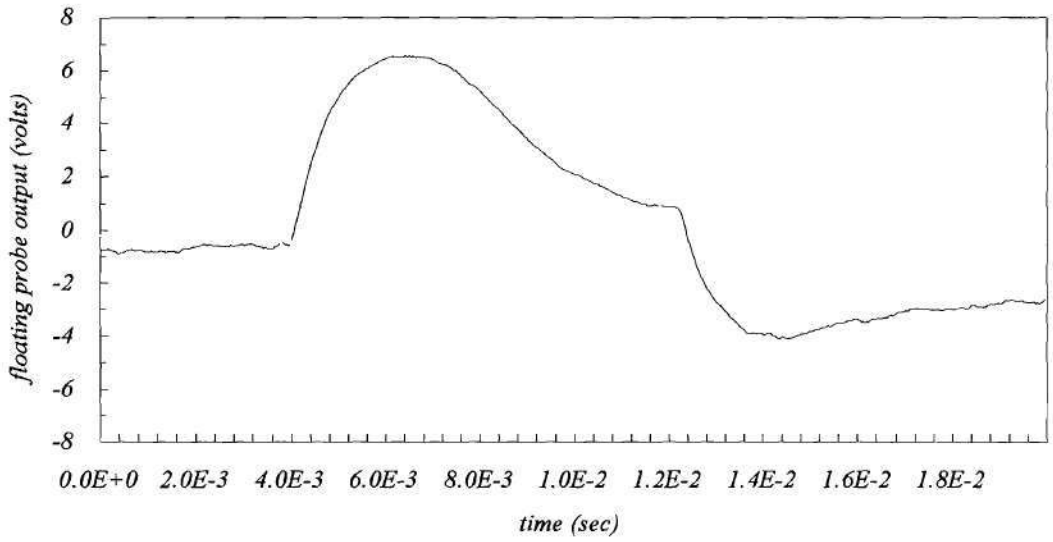

Figure 33. Pressure dependence of the response of a coaxial floating probe to a 50 volt pulse. The source is biased to 40 volts and the probe is located 5 cm in front of the pulsed electrode. The heavy line is data obtained at a neutral pressure of $3x10^{-4}$ Torr. The lighter line is data obtained at a neutral pressure of $0.5x10^{-4}$ Torr.

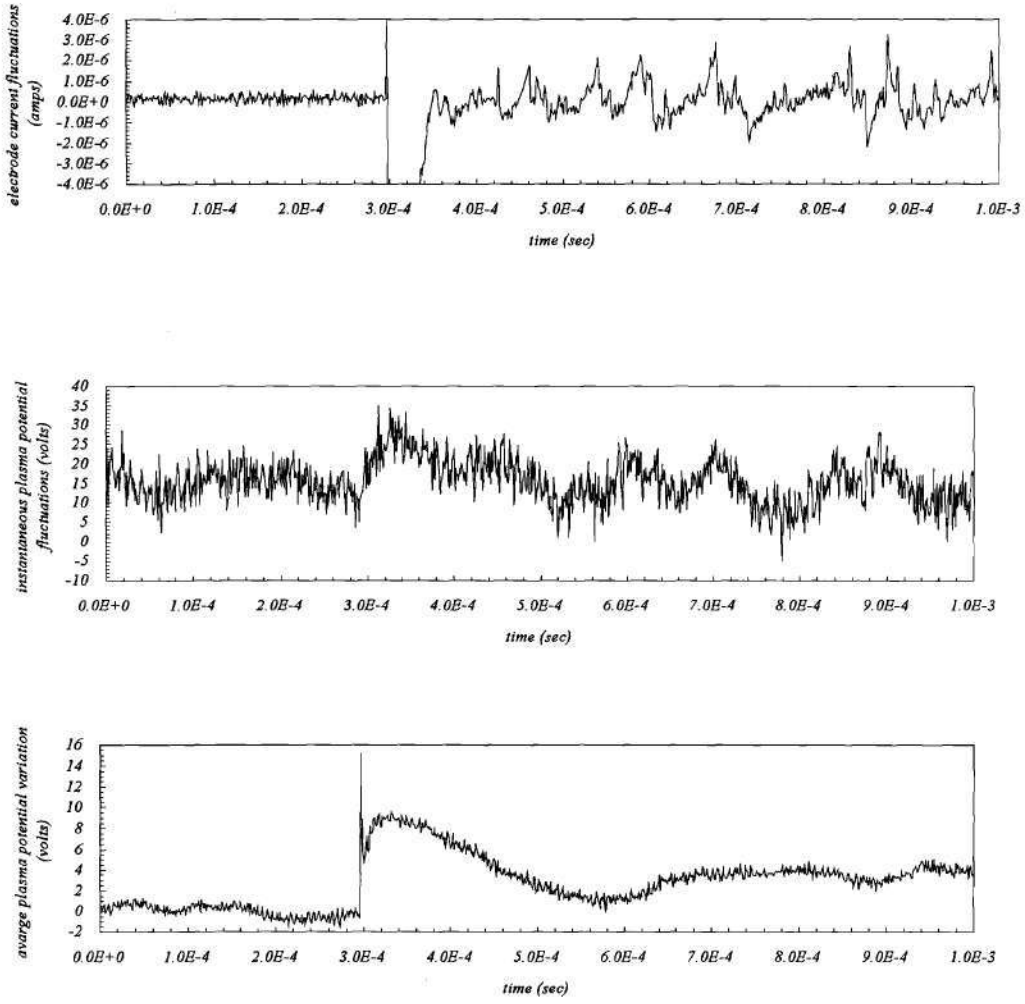

Figure 34. Simultaneously measured density and plasma potential fluctuations. The average plasma potential at the probe position is displayed in the bottom panel.

CHAPTER VI

Magnetic Probe Signals

Magnetic loop probes were used to search for perturbations in the magnetic field caused by plasma currents induced by the pulsed electrode. Stenzel and Urrutia used similar probes to study the propagation of current into an ambient plasma. These observations identified current loops in the plasma and indicated that, contrary to the classical picture of a current collecting electrode, the probe current was carried into the plasma by whistler waves and not by the random motion of the collected particles. Based on these results, Stenzel and Urrutia conjectured that up to 50% of the power developed by an electrodynamic tether would be uselessly radiated away as whistler waves. The present measurements were made to look for similar radiation from an electrode in a simulated ionospheric plasma.

Experimental Procedure

The probe loop normal was oriented perpendicular to the direction of the magnetic field so that the probe would be sensitive to current flowing primarily along the field. The probe was mounted on a movable shaft that can be moved axially down the vacuum chamber. The shaft can also be rotated so that the probe loop rotates in a plane perpendicular to the magnetic field. This allows some measurement of the radial dependence of the signals at the expense of introducing an error signal due to any components of the plasma current in the plane perpendicular to the magnetic field. Figure 35 shows the relationship between the probe radial position and the electrode.

The probe was moved along the magnetic field starting at an axial position near the electrode. At each axial position the probe was rotated into different radial positions and the resulting signal recorded on the DSO. Timing of the data acquisition was similar to that used for the capacitive probe. A trigger signal from the HP pulse generator was used to trigger the DSO and data was read from the DSO using a Macintosh computer.

The signal from the loop probe proved to be much noisier than expected. The high frequency probe signals were superimposed on a much lower frequency background signal that was present at all times and was not associated with the electrode pulse or with plasma production. It was not possible to eliminate the effects of the background by using data averaging because the combined effects of the small signal to noise amplitude, the 8 bit resolution of the oscilloscope and jitter in the signal all combined to effectively wash out the signal. Therefor, unaveraged data was collected and stored for later analysis.

Magnetic Probe Data

Figure 36 is an example of the signal received from the probe. The upper trace is the signal received by the magnetic probe when no plasma is being produced. The high frequency fluctuations between t = 0.6 μsec and t = 1 μsec are pickup by the magnetic probe of the rapid voltage ramp being applied to the electrode:

$$\Delta x B = \mu_0 \varepsilon_0 \, \delta E / \delta t$$

$$B \sim c^{-2} (50 \text{ volts} / 25 \times 10^{-9} \text{ sec})$$

$$B \sim 2 \times 10^{-4} \text{ gauss}$$

Using this value of the magnetic field in the probe response function gives an output voltage in reasonable agreement with the observed value (~ 2 volts). This pickup is to be expected since the probe tip is not completely shielded and also because the return current path for the electrode voltage pulse includes the steel vacuum vessel. This is in direct contact with the transmission line that brings the probe signal out to the amplifiers. It is therefor possible that currents induced on the transmission line shield produce some signal at the amplifier input. This pickup is also evident in the lower trace which was taken when plasma was being produced. However, there is also substantial activity that extends past t = 1 μsec. The increased level of activity is evidence of magnetic perturbations produced in the plasma by the pulsed electrode. By comparing the two traces, it is clear that the signal is associated with the voltage pulse being applied to the electrode and that the activity can not all be attributed to a simple, uninteresting, coupling of the probe to the electrode.

The data obtained at different positions and orientations exhibit a surprising degree of consistency. At first, it was thought that single probe measurements would be of limited value because possible jitter in the oscilloscope trigger and electrode voltage pulse would make it difficult to compare data taken at different times. Such an effect was not so much of a concern in the plasma potential measurements because the repetition rate of those signals was much slower than any (possible) nanosecond drift in the triggering. In addition, there was a concern that noise in the measuring circuit would also make it difficult to make meaningful measurements.

These concerns proved to be unjustified. The time relationship of the peaks and troughs of the oscillations, in relation to the oscilloscope trigger, is very consistent. For example, the signals shown in figure 35 were obtained at different times and places but when the data is analyzed in detail general features, occurring at nearly the same time after the trigger, can be identified in each shot. If the magnetic probe were detecting truly random events, such a correlation would not be expected. Therefor, although the amplitude and duration of the events varies from shot to shot, gross relations between the phase of the phenomenon at different points in space can be compared and used to infer the presence of an oscillating current in the plane of the magnetic field.

Data Analysis

From figure 4 the radial propagation speed of the signal can be estimated. The sloped line in the figure indicates this speed to be roughly 10^7 cm/sec. In addition, the wavelength of the signal can be estimated by drawing a vertical line through the data (at $t=1.3\times10^{-6}$ sec, for example) and noting the apparent oscillatory nature of the signal at this time (this sort of basic analysis was used by Stenzel and Urrutia to identify current loops using their magnetic field data, [Urrutia and Stenzel, 1989]).

Since the separation between the 10^o and 20^o data is about 1 cm, this gives an estimate of the perpendicular wavelength of the disturbance. The values of the propagation speed and the perpendicular wave length do not change appreciably when data from other probe positions or orientations is used. In a similar manner, the axial propagation speed and wave length can be estimated from figure 39. The axial propagation speed is about 10^8 cm/sec and the axial wavelength is about 36 cm.

The frequency of the magnetic probe signals is roughly 50 MHz and the signal amplitude is about 2 volts in general. Using the response function of the magnetic probe, this suggest that the pulsed electrode produces axial magnetic field perturbations on the order of

$$v_{out} = G_{amplifiers} \times 10^{-7}\ \Delta B/\Delta t$$
$$2\ volts = 4.5\times10^{4} \times 10^{-7}\ \Delta B_\theta(gauss)/(5\times10^{-8}\ sec)$$
$$\Delta B_\theta = 2\times10^{-5}\ gauss$$

This is at best an order of magnitude estimate for the field perturbation since the response of the magnetic probe at high frequency is extrapolated from the rather crude low frequency calibration data. The axial symmetry of the system can be exploited to simplify the expression for the axial current density

$$\mu_0 j_z = 1/r\ \delta(rB_\theta)/\delta r$$

where j is measured in amps/M^2 and B is measured in Tesla. Using the data in figure 38, at the 20^o and 25^o radial positions, the axial current density at the outer edge of the plasma column is found to be about

$$\mu_0 j_z = 1/(1\ cm)\ [\ 1\ cm\ (2x2x10^{-9}\ Tesla)/(0.1\ cm)\ ]$$
$$j_z = 1\ \mu A/cm^2$$

Integrating this current across the plasma column yields a value (5 μA) that is much smaller than the peak current collected by the electrode (~ 50 μA). The oscillating currents, within the bandwidth of the current sensing probe and the DSO, can therefor account for no more than 10% of the current collected by the electrode when voltage is initially supplied to the electrode. Since the geometry of the plasma is unfavorable for the generation and detection of whistler waves (the small diameter of the plasma column puts severe restrictions on the wavelength of the waves since they are radiated in a cone with an 11° opening angle) it is not possible to say such waves will not play a role in the operation of plasma contactors in the ionosphere. However, the experiments do suggest that a fraction of the collected current (possibly as much as 10%, in this case) is accompanied by the emission of magnetic waves from the electrode. Generation of these waves represents a power loss mechanism associated with the movement of the tether across the geomagnetic field and therefor reduces the efficiency of any plasma contactor.

Discussion of Results

It is possible that the electrode in this experiment emits waves in a band where the magnetic probe has low sensitivity. Very low frequency waves would be difficult to detect because the probe response decreases with signal frequency. A probe with a larger cross sectional area would needed to look for such waves but a larger probe is

more likely to disturb the plasma and compromise the measurement. Therefor, these measurements can not conclusively rule out the existence of a plasma instability that will limit current collection by inducing cross field currents in the ambient plasma. However, they do suggest that a fraction of the electrode current couples to a plasma wave. This further supports Stenzels conjecture that the electrodynamic tether will not draw a steady current from the ionosphere and calls into question the importance of collisionless electron flow along the geomagnetic field, a condition required for the anisotropic contactor model.

While these signals are interesting, they can not be used to explain the observed current oscillations. These occur on a time scale that is dozens of times slower than the time scale of these signals. However, it is interesting to note that the magnetic probe signals occur within the short span of time between the application of the voltage pulse to the electrode and initiation of the instability detected with the coaxial Langmuir probes suggesting that the instability modifies the plasma in such a way as to quench the magnetic oscillations.

Finally, the penetration distance into the plasma of the currents responsible for the waves can be estimated using Stenzel's relation

$$L = \frac{v_{d,e}}{v_{d,i}} r_{ft} \approx \left(\frac{kT_e m_i}{4\pi \Delta\phi m_e} \right)^{1/2} r_{ft}$$

and using the measured value for the radial potential difference, $\Delta\phi \sim 4$ volts. This gives a value of about 40 cm for the penetration distance. Since the electrode is located (axially, in the direction of wave propagation) almost 100 cm from the nearest conducting surface, it is unlikely the currents responsible for the waves are effected by the boundaries of the vacuum system.

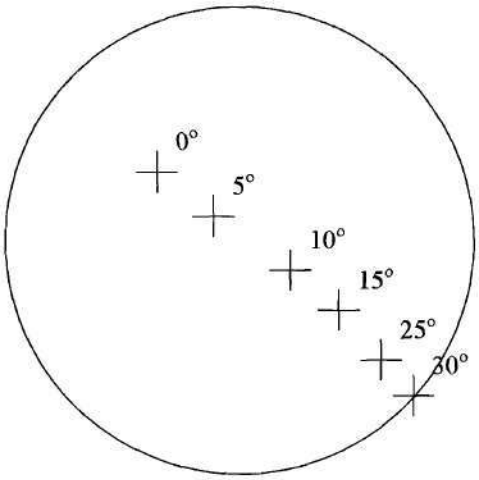

Figure 35. Diagram indicating position of the magnetic probe (crosses, with goniometer readings indicated) with respect to the pulsed electrode (small circle) and the plasma boundary (large circle).

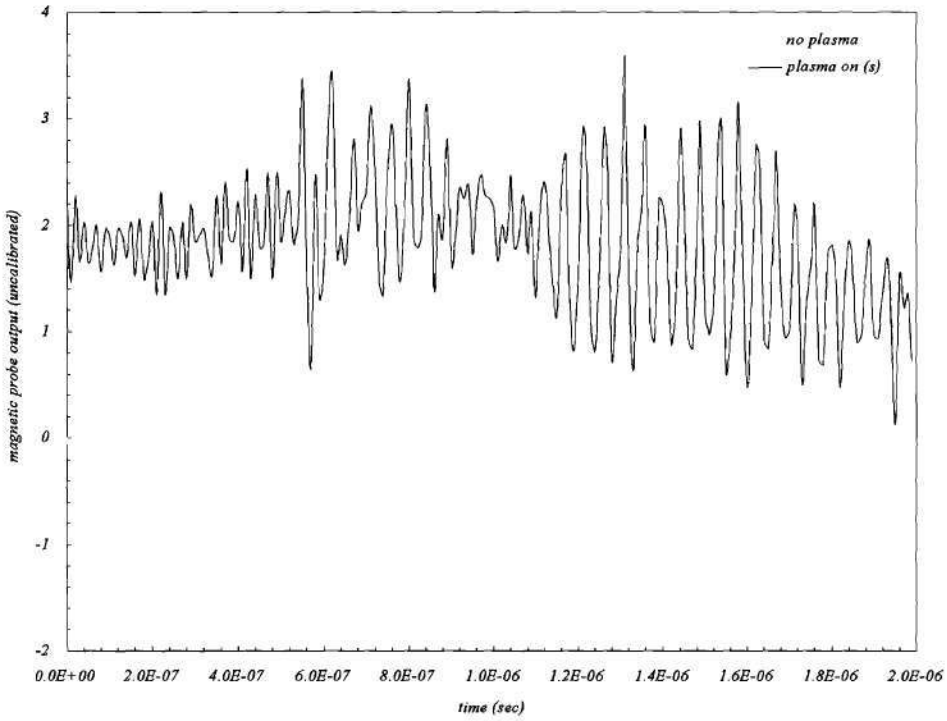

Figure 36. The upper figure is the vacuum response of the magnetic probe to the pulsed electrode. The oscillations that occur before t=1μsec are therefor not associated with any plasma phenomenon. The lower trace shows the response of the probe when it is surrounded by plasma. The duration of the signal, as well as its instantaneous amplitude is highly variable.

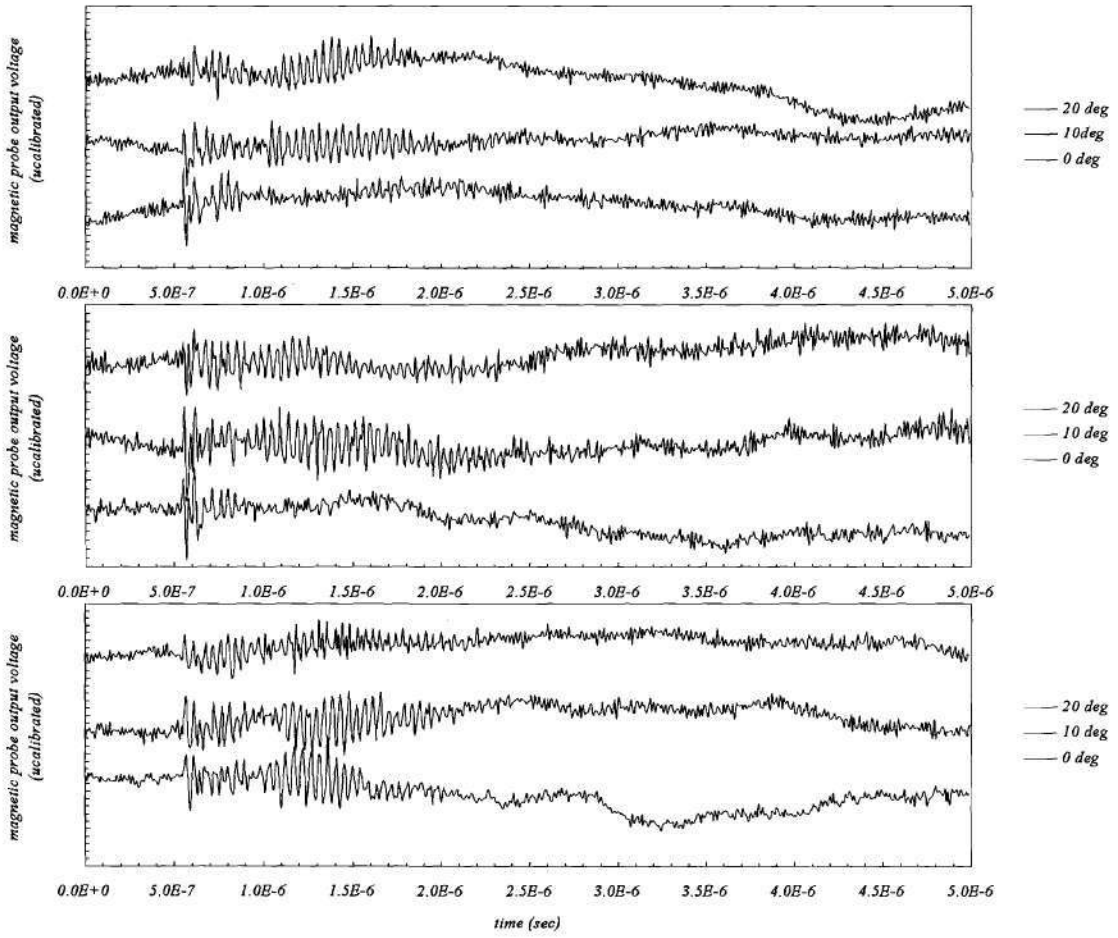

Figure 37. Signals received by a magnetic loop probe at three different axial locations. The upper panel was obtained at position 3846, the central panel was obtained at position 3700 and the lower panel was obtained at position 2100. The 10 and 0 degree data has been offset for purposes of comparison.

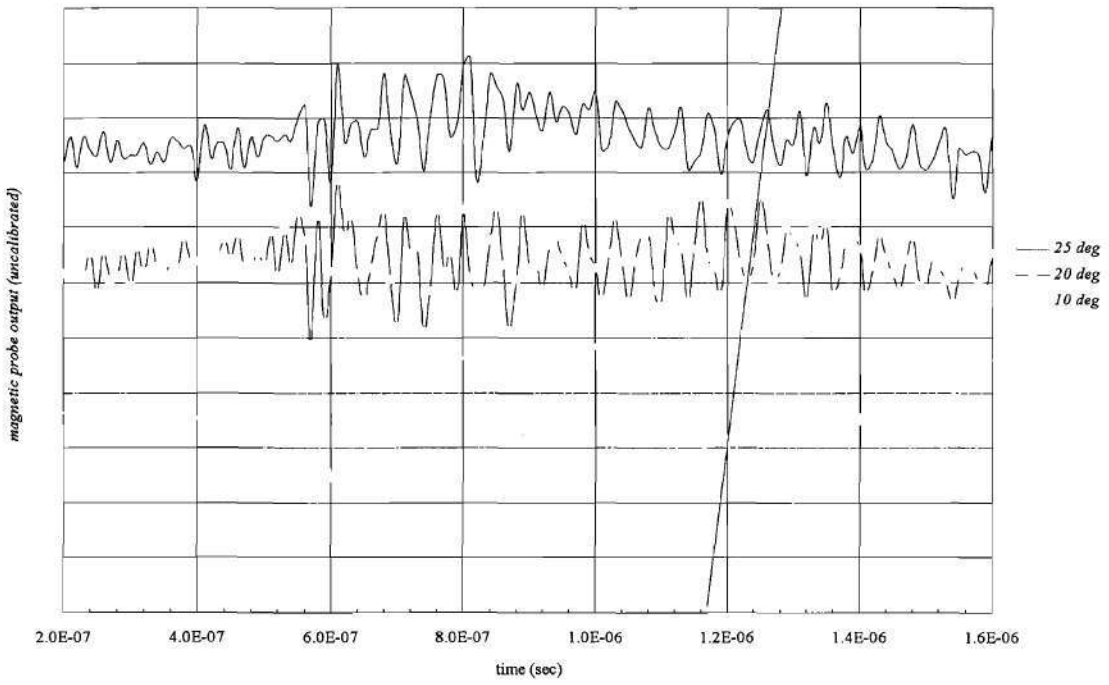

Figure 38. Magnetic probe signals recorded at position 3700. The consistent phase relationships of the radial magnetic probe signal allows the radial propagation speed and the perpendicular wavelength of the signal to be estimated.

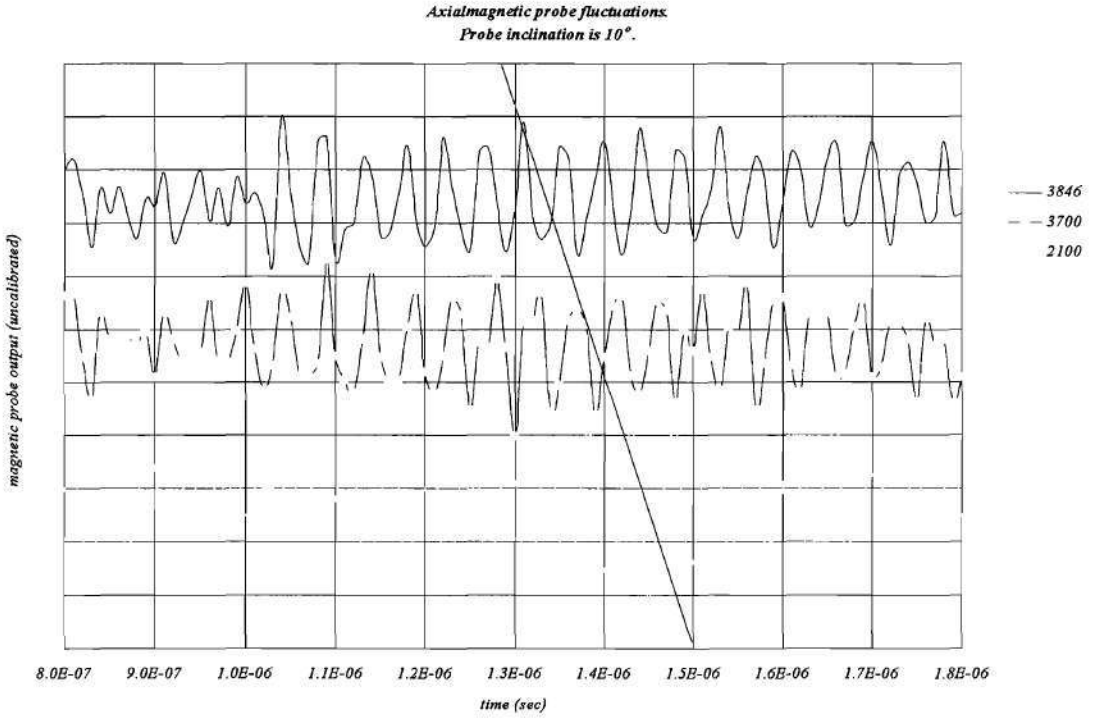

Figure 39. Measurement of the axial propagation speed and wavelength of the magnetic probe signals.

CHAPTER VII

Correlations

In order to quantify the degree of correlation between different sets of data, a computer program was written to calculate the auto and cross correlation functions for various data sets. The autocorrelation function $R_X(\tau)$ for a series of data points x(t) is defined as

$$R_x(\tau) = \lim_{T\to\infty} \frac{1}{T} \int_0^T x(t)\, x(t+\tau)\, dt$$

and measures the dependence of the function at time $t+\tau$ on its value at time t. The principle use of the autocorrelation function is in detecting deterministic data in a background of random fluctuations[78]. A related function, useful for measuring the dependence of one set of data on another, is the cross-correlation function defined by

$$R_x(\tau) = \lim_{T\to\infty} \frac{1}{T} \int_0^T x(t) y(t+\tau)\, dt$$

Both functions can be easily implemented on a computer using the function

$$\hat{R}_{xy}(rh) = \frac{1}{N-r} \sum_{n=1}^{N-r} x_n y_{n+r}$$

where N is the total number of data points, r is called the lag value and is equal to the number of time units, h, the x data is displaced relative to the y data. This function will produce a single output value for each of the lag values r. The resulting set of values (r, R) can be plotted and the resulting graph used to decide if the two sets of data (x, y) are related.

A program was written that implemented this equation on a Macintosh computer. The program requires two input files, for the X and Y data sets, containing an equal number, N, of data points. The time separation of the data points, h, in file X must be the same as the time separation of the data in file Y. The output of the program is a file containing the value of the function R_{xy} calculated at (0.75)*N lag values r.

Testing the program with simulated data

The program was tested with sample data files and the output compared with autocorrelation and crosscorrelation functions listed in Bendat and Piersol. The four sample data files used to test the code consisted of 100 values of the functions $\cos(\omega t)$, $\cos(\omega t)+R$, $\cos(\omega t+37^{o})$, $\cos(\omega t+37^{o})+R$, where t runs from 0 to 99, $\omega = 10$ and R is a random number between +3 and -3. The addition of R to the sample data set is used to simulate the effects of uncorrelated noise on the data. The output of the code is shown in figure 40 and figure 41.

Figure 40 shows both the autocorrelation of cos(wt) and the crosscorrelation of cos(wt) and $\cos(wt+37^{o})$. The functions agree to a large extent with the expected results but the autocorrelation function (solid line) displays an unanticipatedly large amount of noise (indicated by the spikes in the auto-correlation curve). Also notice that in each case, the amplitude of the oscillations in R_{xy} seems to gradually increase with increasing lag values. This is an artifact of the finite size of the data set. The

value of R_{xy} is computed from fewer data points as the lag value increases and thus represents a less accurate estimation of the correlation function.

Figure 40 also shows how the cross-correlation function can be used to estimate time or phase delays between two sample data sets. While the autocorrelation function achieves a maximum value at zero lag time, the crosscorrelation function peaks at a lag value near 30, indicating the two data sets are out of phase and that the second data set ($\cos(\omega t+37^{o})$) leads the first data set ($\cos(\omega t)$).

The program was next tested to see if the correlation functions can be used to detect a periodic signal masked by a randomly generated background. The test files were generated by adding a randomly generated signal to the previous data files. The random signal was generated using the built in random number generator in KaliedaGraph and multiplying the result by 3. Thus, the random signal has a maximum amplitude 3 times greater than the signal (the data $\cos(\omega t)$). The data in one of the input files provided to the program is pictured in figure 42. The signal is very well hidden by the noise.

The program output is pictured in figure 43, and can be directly compared to the previous output shown in the upper panel of figure 40. Once again, the correlation function achieves its maximum value at a lag value of about 30. Therefor, the program accurately implements an estimation of the sample correlation function and can confidently be used to look for deterministic trends in the data recorded by the oscilloscope, even when the data contains a significant amount of noise.

Auto correlation functions computed from the data

Figure 44 shows the autocorrelation functions for the raw data displayed in figure 22. Since the data recorded before $t=2x10^{-4}$ sec is greatly influenced by feed through of the electrode voltage pulse, the data was truncated to about 800 data points between $t=2x10^{-4}$ sec and $t=9x10^{-4}$ sec before being used with the correlation program. The output of the program is normalized, after the program has run, by dividing the

output at each lag value by the value of the autocorrelation function at zero lag value. The lag values on the horizontal axis of the figure correspond to time offsets in 1 μsec intervals.

The oscillations in the autocorrelation function indicate the presence of similar oscillations in the data. This was obvious for the current fluctuation data (figure 20) but was not so obvious for the associated plasma potential fluctuations. Note that the current autocorrelation function has been displaced relative to the potential autocorrelation function by an additive constant (0.5) so that the two functions can be easily analyzed on the same plot. The autocorrelation functions for the two data sets are remarkably similar, particularly for lag values greater than 275. Therefor, it can be inferred that oscillations are present in both the current and potential data and that the period of these oscillations are very similar. In particular, using the data between lag values of 300 and 400, the period of the oscillation is estimated to be around 100/2.5 = 40 lag values or 40 μsec. This suggests the current and potential oscillations are related and are not due solely to random fluctuations in the collected data. In order to investigate this relationship further, the cross correlation function was constructed, figure 44.

Cross correlation of electrode current fluctuations and plasma potential fluctuations

Once again, the raw data was corrected for any linear trend by subtracting the mean value of each data series from the individual data points in that series before the data was used to form the cross-correlation function. The function obtained using the corrected data was then normalized by finding the maximum positive value of the function and dividing all the data by this value. The cross-correlation function, figure 44, confirms the presence of an oscillatory relationship between the current and potential data and suggests that the oscillations are at most weakly damped in the plasma. The period of the oscillations in the cross-correlation function is almost identical to that found in the individual auto-correlation functions, confirming the presence of a 25 kHz oscillation in the data. Furthermore, the cross-

correlation function shows that this oscillation is present for all lag values, not just those for which rh > 275. The lack of any apparent decay envelope in the amplitude of the oscillations suggests the pulsed electrode has excited a normal mode of the plasma as observed by Stenzel and Urrutia in their experiments.

A similar analysis can be performed on the data shown in figure 45. Once again, the cross-correlation function, figure 46, indicates a definite relationship between the current and potential fluctuations. As before, the raw data has been transformed by subtraction of mean values and the resulting cross-correlation function scaled by dividing through by the maximum positive value of the function. Each increment of the lag value corresponds to 5 μsec. The oscillations shown in the figure therefor have a period of about 250 μsec, much longer than the data in figure 44. Notice that once again, there is no evidence that the oscillation amplitude decays at large lag values, suggesting that a normal mode has been excited.

Cross-correlation of electrode current fluctuations and fluctuations received by the RF probe

Figure 48 shows the cross-correlation function obtained using the data pictured in figure 47. Before computing the correlation function, the data was truncated so that only data received after $t=3.5\times10^{-4}$ seconds was used in the computation. This eliminates the effects of feed through of the electrode voltage pulse apparent as the sharp transients in figure 45. The correlation lag values correspond to 1 μsec intervals. This function indicates that the fluctuations received by the RF probe (as pictured in figure 47 and in more detail in figure 22) are associated with the fluctuating electrode current. The excessive noise present in the unsmoothed function was removed using a 15 point smoothing algorithm provided with KaleidaGraph.

As with the current-potential fluctuations, the structure of the cross-correlation function indicates there is a definite association of the electrode current fluctuations with the fluctuations received by the RF probe. Part of the reason for the poor quality of the correlation function is due to the high frequency oscillations (~6 MHz) in the RF probe data. These oscillations tend to hide the relationship between the low frequency envelope of the RF fluctuations and the electrode current fluctuations that is being tested by constructing the cross-correlation function. The KaleidaGraph smoothing function was used to eliminate the effects of the high frequency RF data so that any relationship between the oscillation envelope and the electrode current could be more easily seen. The smoothed function clearly indicates there is a relationship between the two phenomena. Evidently, the electrode current oscillations are accompanied by radial oscillations in the electron density near the electrode. The relatively constant amplitude of the peaks in the cross-correlation function indicate that the ratio of the current oscillations to the peak amplitude of the RF oscillations is constant. That is, larger current perturbations are associated with larger RF oscillations and therefor larger radial density variations.

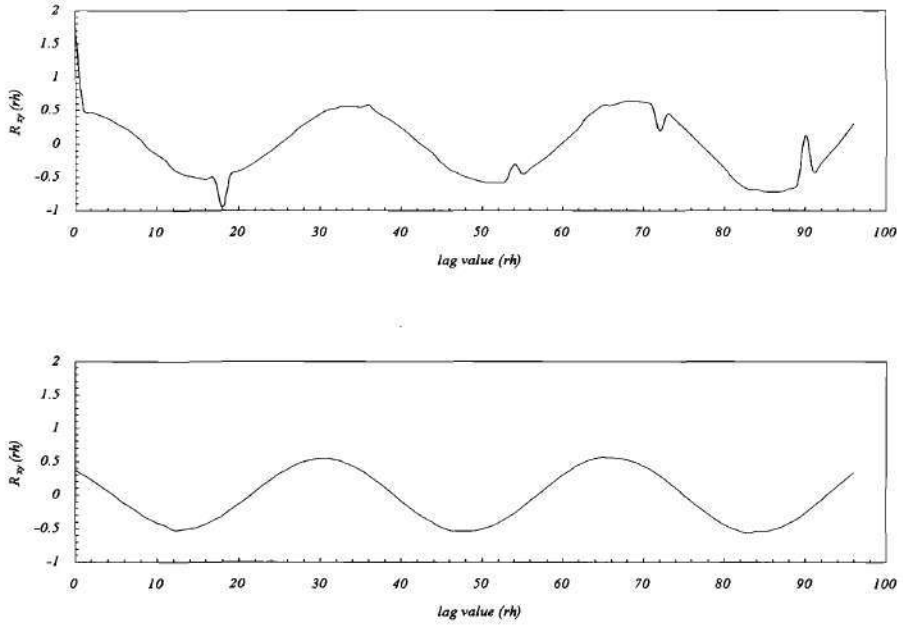

Figure 40. Output of correlation program with simple harmonic functions used as input. Upper trace is the cross correlation function computed from the test data, the lower trace is the auto correlation function.

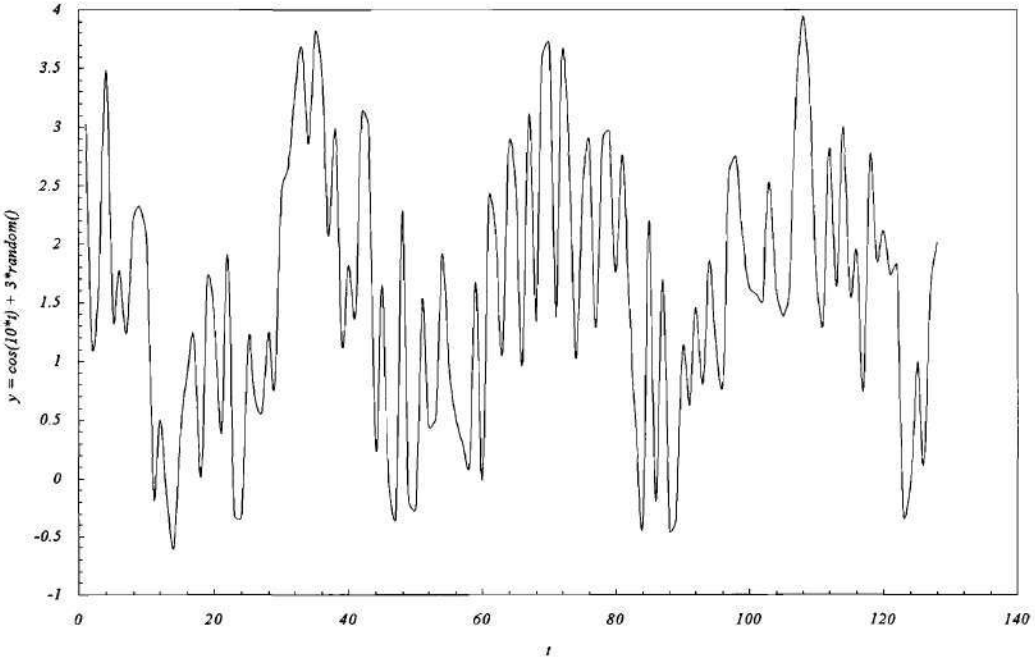

Figure 41. Noisy harmonic function used to test correlation program.

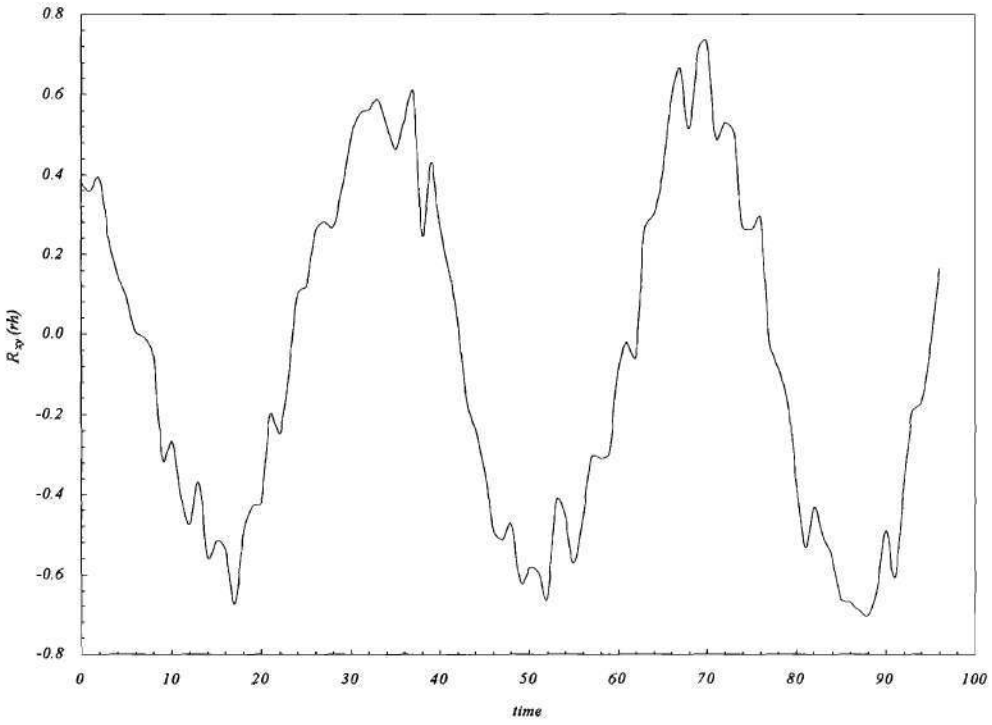

Figure 42. Output of the correlation program with noisy data applied as input.

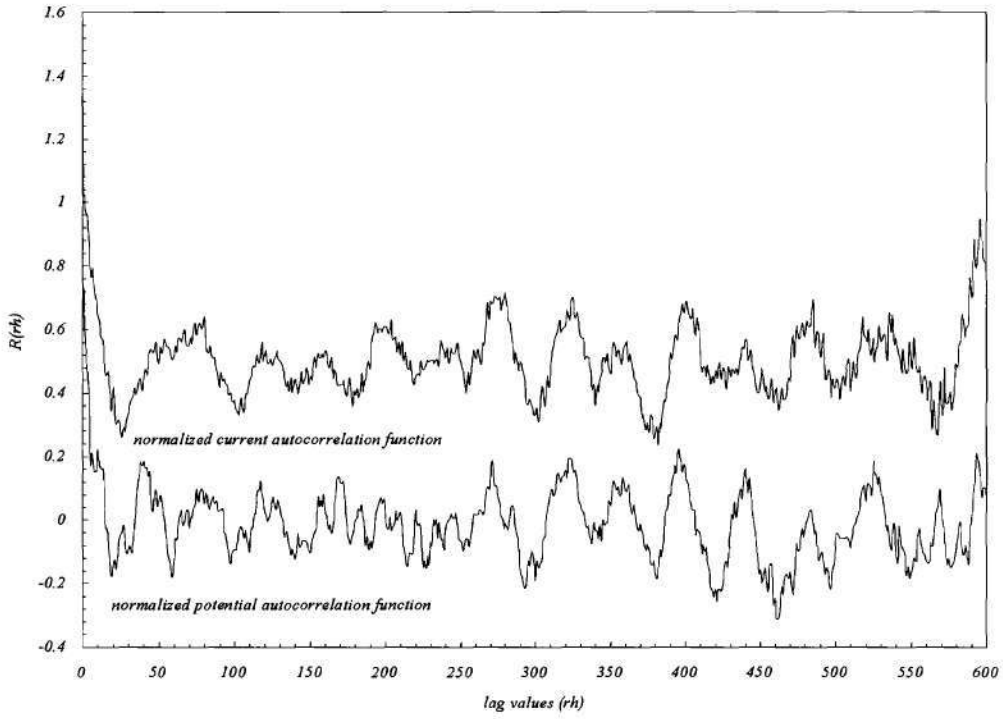

Figure 43. Correlation functions computed from experimental data.

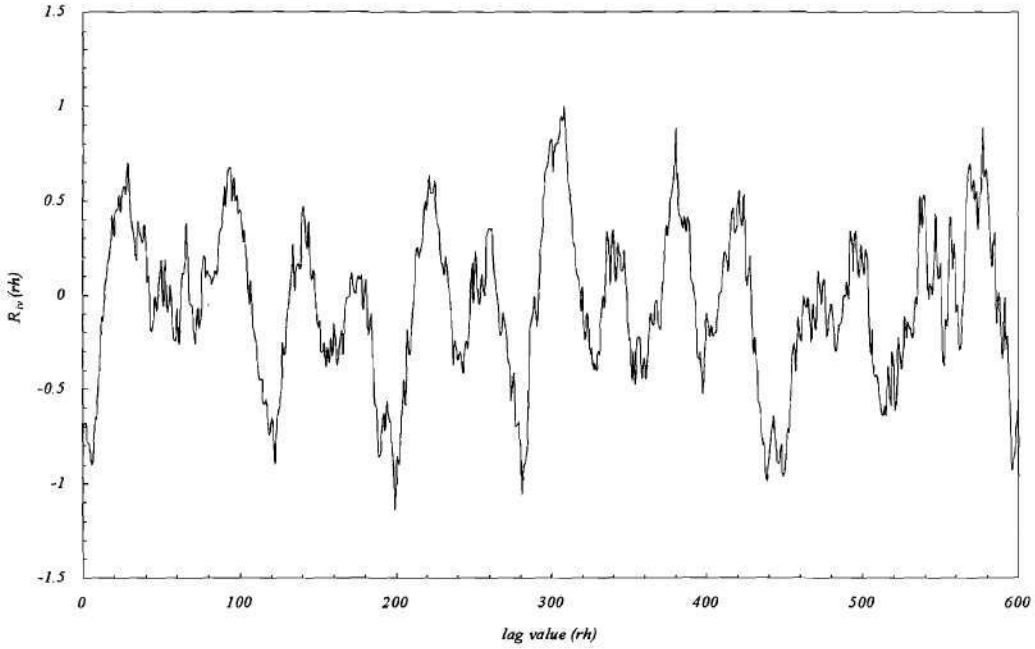

Figure 44. Cross-correlation function calculated from current and potential fluctuation data

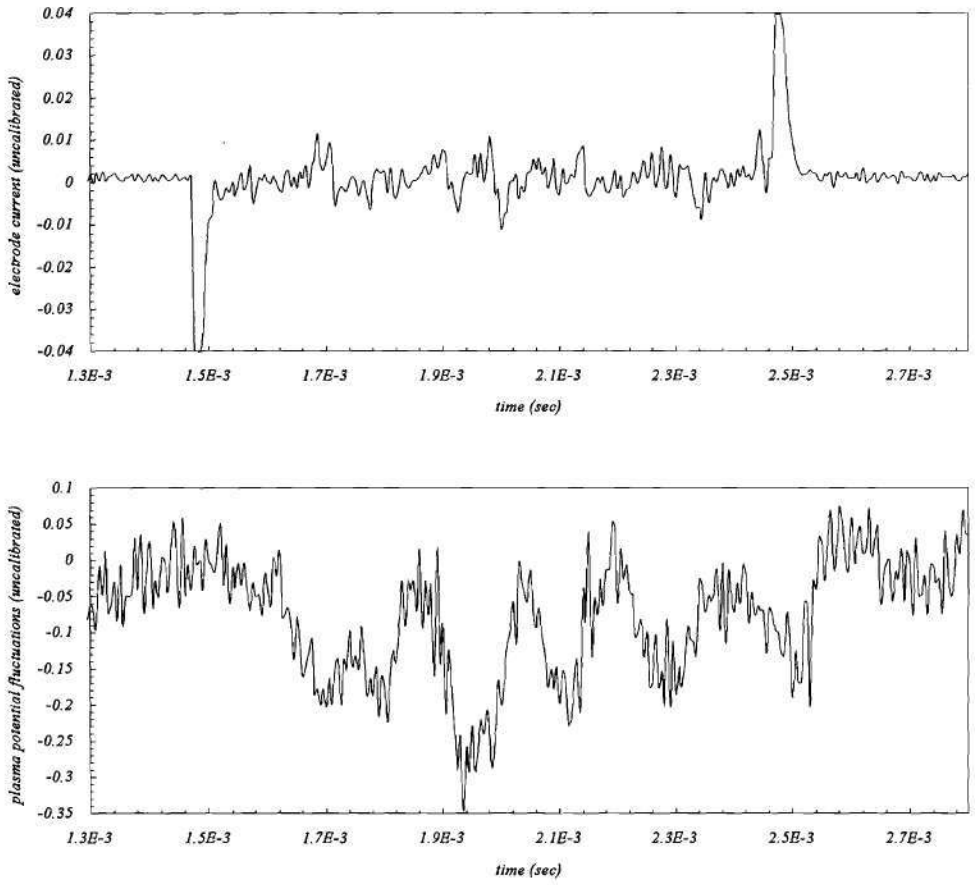

Figure 45. Simultaneously measured fluctuations in the electrode current and the plasma potential.

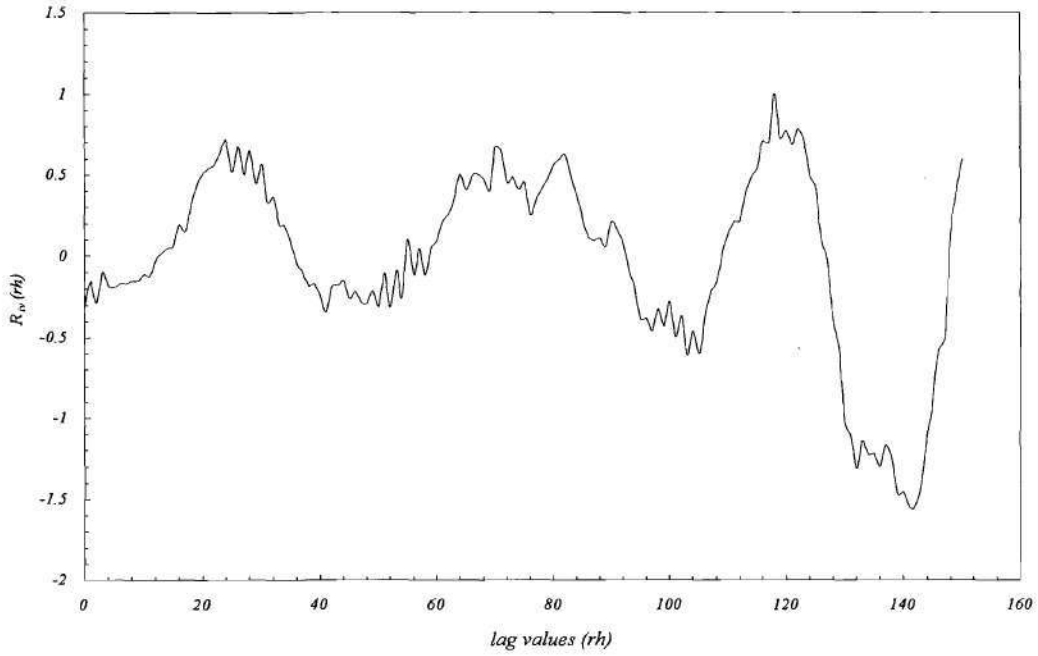

Figure 46. Cross correlation function calculated from current and potential fluctuation data pictured in Figure .

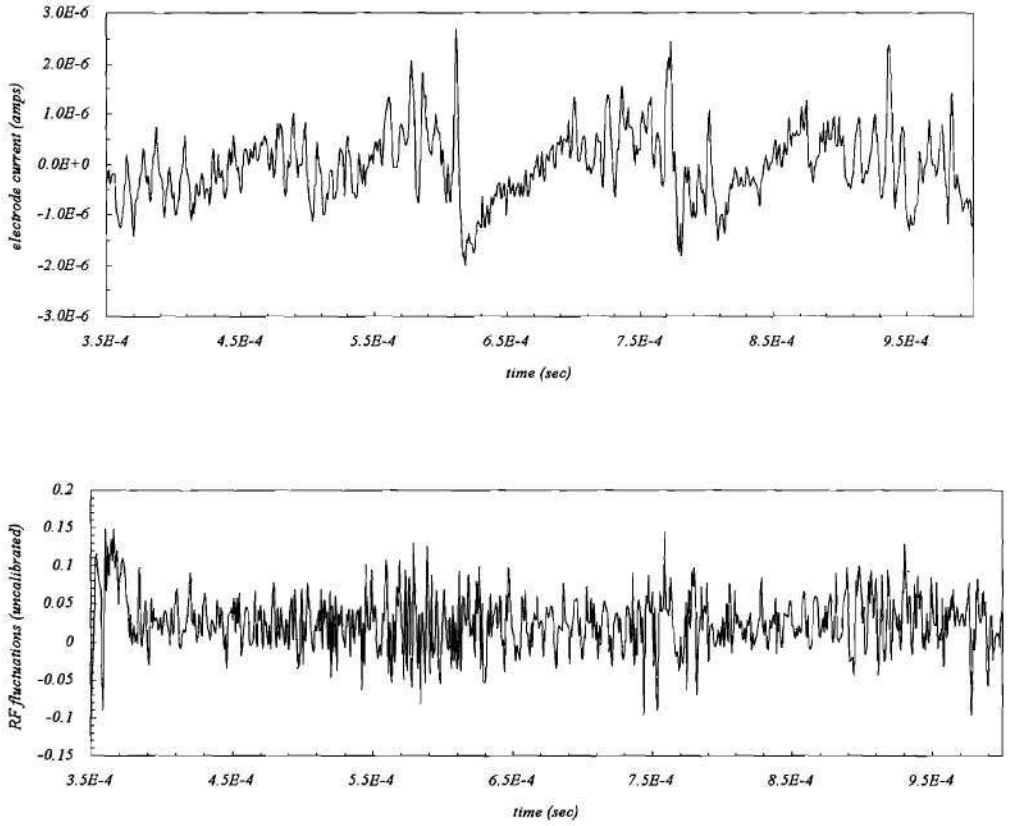

Figure 47. Simultaneously measured fluctuations in the electrode current and fluctuations received by the RF probe.

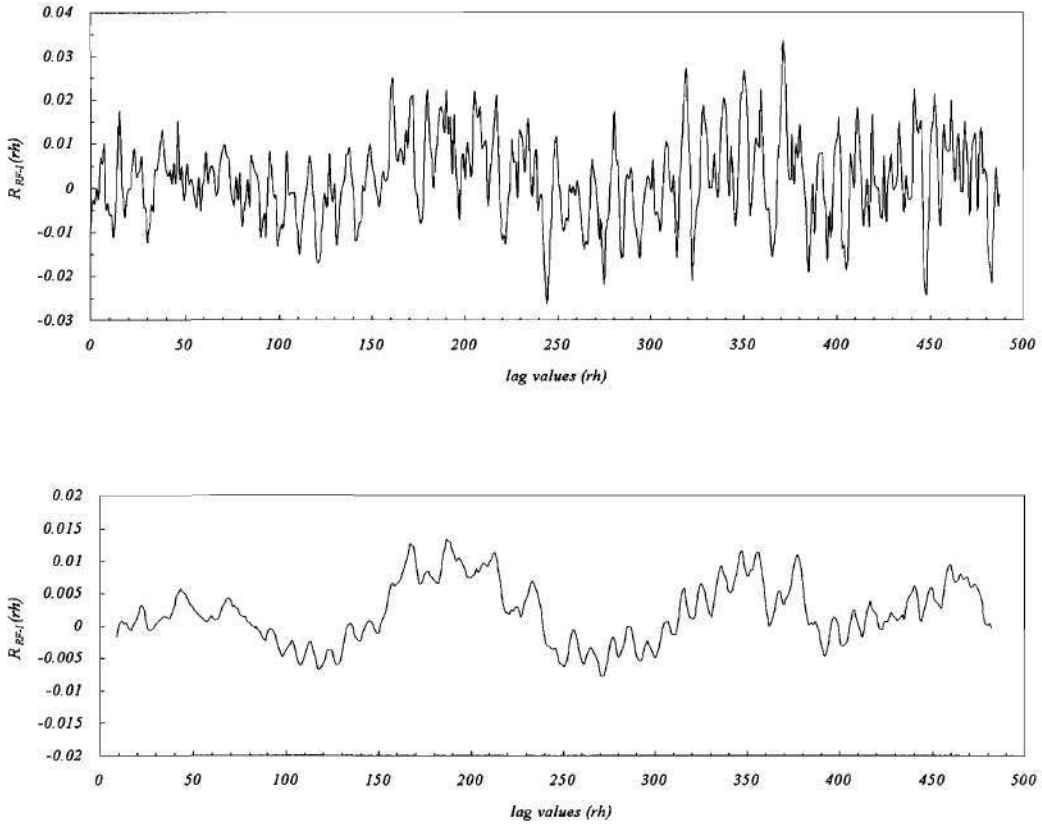

Figure 48. Cross-correlation function computed from the data in Figure

Chapter VIII

Conclusions

These experiments were motivated by the work of D. E. Hastings and R. L. Stenzel on plasma contractor interactions with the ionosphere. Hastings' model of current collection by plasma clouds in the ionosphere suggested that the current collecting clouds would induce electrostatic double layers to form across the geomagnetic field. The double layers increase the current collected by the cloud by preventing ionospheric electrons from leaving the cloud. Stenzel's model of the interaction is based on the extensive experimental work he an J. M. Urrutia performed at UCLA using a large laboratory plasma. This work suggests that plasma contractor clouds with a radius more than a few tenths the size of the ion Larmor radius will not collect a steady state current and that the electrodynamic tether will radiate a way a substantial amount of its power in the form of whistler waves. Hastings suggested, though, that these results may not be applicable to the tether because the experiments were performed using a plasma with characteristic substantially different from those that describe the ionosphere (UCLA: $T_e = 5$ eV, $n_e < 10^{12}$ cm^{-3}, $B \sim 5$ G, Argon plasma; Ionosphere: $T_e = 0.2$ eV, $n_e < 10^6$ cm^{-3}, $B \sim 0.3$ G, Oxygen plasma). The experiments performed for this thesis represent an attempt to test the validity of Hastings objection by using a laboratory plasma with characteristics closer to those of the ionosphere ($T_e = 4$ eV, $n_e < 10^9$ cm^{-3}, $B \sim 540$ G, Argon plasma).

The results of this work suggest the model proposed by Stenzel is the appropriate one to use in the ionosphere. A rapidly biased, current collecting electrode exhibits large oscillations in the collected current. These oscillations are not observe when a dc biased is applied to the electrode. A large density

depletion in the electrode flux tube suggests the mechanism responsible for the current fluctuations appears to be ion expulsion from the flux tube subtended by the electrode.

Capacitive probes indicate the formation of weak potential structures ($< 2T_e$) in front of both the pulsed electrode and the plasma source. These structures may act to trap electrons streaming from the plasma source in the center of the plasma column, preventing them from reaching the electrode. The two structures are roughly 40 centimeters long and extend along the magnetic field. The relatively gradual change in potential with distance and the small amplitude of the structures suggest they are not double layers. Conclusive measurements of the electron distribution function could not be made because of the small diameter of the plasma column.

Associated with the application of voltage to the electrode is a high frequency (~ 6 MHz) instability whose frequency depends on the plasma density. The instability is observed whenever the electrode is pulsed and does not appear to be associated with the current fluctuations. There is a qualitative correlation of the repetition rate of the instability with the brightness of the sheath surrounding the pulsed electrode, suggesting that the instability may originate somewhere in the sheath. However, the instability can be detected with RF probes located tens of centimeters from the electrode and appears to travel away from the electrode at roughly the ion thermal velocity. This, along with the density dependence of the frequency and the measured value of the growth rate, suggest the instability is caused by cross field propagating ions (the cross field transport is initiated by the radial electric fields observed near the electrode flux tube) interacting with electron plasma oscillations. The properties of this instability are discussed in the Mikhailovskii reference and fit the observed properties rather well. Thus, Plasma contactors will not only be plagued by current fluctuations but also by electrostatic noise generated by their operation.

Finally, magnetic perturbations associated with the application of a bias voltage to the electrode have been observed. Unlike the perturbations observed by Stenzel, these are more likely Alfven waves than whistler waves and they appear to carry only a small fraction of the total current collected by the electrode.

This implies the electrodynamic tether will not generate the current loops postulated by Stenzel and that current closure may in fact occur in the resistive E layer of the ionosphere as originally postulated. This is an interesting result since it lends support to the conclusion that the electrodynamic tether can be used a very low frequency transmitter with an antenna consisting of the current channels created by the tether in the ionosphere.

Appendix

A listing of the programs used to 1) pass data from the LeCroy DSO to a Macintosh computer and 2) calculate correlation functions are included on the next several pages. The data acquisition program is included as an example to anyone wishing to write similar code for passing data along the GPIB using a National Instruments interface board.

Data Acquisition Program

```
/*
This program reads data from channel 1 or channel 2 and stores the unprocessed data in a file called
RAW. The data is then converted to voltage values, using information stored in the DESCRIPT file, and
stored in a file named by the user.
The program reads in 1000 equally spaced data points starting from the left hand side of the DSO
screen. The first column of data in the user named output file  contains the time at which the data in
the second column was acquired.

    The program is working fine as of 4/26/93.
*/

#include <stdio.h>
#include <console.h>
#include <stdlib.h>
#include <decl.h>
#include <DeviceMgr.h>
#include <string.h>
#include <math.h>
#include <unix.h>
#include <fcntl.h>

int fadd,ladd,spp,count;
double sint;
float VGain;
main()
{


        int j,brd0,scope,mask,frmt;

        int desc[149];

        double tempp[1000],td;
        char ans[30],me[21],response[8],prvrsp;

        int ibrdf (int ud, char *flname);              /*..... NI-488 functions .....*/
        int ibsre (int ud, int v);
        int ibwrt (int ud, char *wrt, long cnt);
        int ibrd (int ud, char *rd, long cnt);
        int ibfind (char *bdname);
        int ibloc( int ud);
        int ibclr(int ud);
        int ibwait(int ud, int mask);
        int ibcmd( int ud, char *cmd, long cnt);

    printf("\f\n");
    printf("\t\t\tLeCroy 9400 control program.\n\n");

        brd0 = ibfind ("gpib0");
        scope = ibfind ("dev1");
        ibclr(scope);
```

```
        ibsre (brd0,1);


    response[0]='y';
    while(response[0]=='y'){
                    ibwrt(scope,"cfmt,l,byte,usho,comma",22L);


            /*      Tell the oscilloscope to send the waveform descriptor      */
                    printf("ENTER 2 character channel name: ");

                    scanf("%s",response);

                        printf("\nReading descriptor for channel %s.",response);
                                sprintf(me,"rd %s.de",response);
                                ibwrt(scope,me,8L);
                                BFWD(desc,scope);


/*  setup communication protocol. See page 7-8 for a description of format L,  pages 7-30, 7-31 for a description

 of the commands cmft, chdr, ctrl, cbls. */

                    if(response[1]=='1' || response[1]=='2'){
                        ibwrt(scope, "cfmt,L,byte,ufix",16l);
                        frmt=3;
                        }
                    else{
                        ibwrt(scope, "cfmt,L,word,ufix",16l);
                        frmt=5;
                        }

                    ibwrt(scope, "chdr off;ctrl cr;cbls -1",24l);


                    sprintf(me,"rd %s.da,%5d,1000",response,ladd/1000); ibwrt(scope,me,29l);
            /*..... read in the data points.....*/
                      td=sint*ladd/1000;
                      RDAT(desc,tempp,td,scope,frmt);



                    prvrsp=response[1];
                    ibloc(scope);
                    printf("\n\n\nRead in more data (y/n) ? ");
                    scanf("%s",response);
}

 printf(".....\t\tFINISHED\n\n");


        /*.....  END  .....*/  }
```

```
/*.....*/

/*..... FUNCTION DEFINITIONS .....*/ /*.....*/

/*..... get waveform descriptor .....*/

BFWD(d,skope)
   int d[];
   int skope;
{
   FILE *fd1;
   int i, c, j, k, _VGain, _vvgain, _voff, gainv, pdiv, pv, ps;
   char s;
   char temp[13], dbuff[3000];
   div_t gain;
   div_t div(int numer, int denom);
   float vvgain, voff;
   double tbase;
   double pow(double x, double y);

   /*      Read the information from the scope into the file DESCRIPT.
     Open the file for reading.                                    */

     ibrdf (skope, "descript");
     fd1=fopen("descript","r");

    /*      Scan the descriptor information stored in the file DESCRIPT
     into the character array DBUFF.                               */

     fscanf(fd1,"%s",dbuff);

/*   Read the descriptor information into the array DESC. The information
   is sent in the unsigned short format with the individual data bytes seperated by commas. The
following procedure reads the elements of the DBUFF array untill a comma is encountered. The
data that has been read is then converted to an integer value and stored in the DESC array.
   The comma in DBUFF is skipped and the process continues.      */

                    c=0;
      for(i=0; i<149; i++){
           j=0;
           s=' ';
           d[i]=0;

           while(s!=','){
                s=dbuff[c+j];
                temp[j]=s;
                j=j+1;

                     if(j==10){
```

```
                                        printf("\nPROBLEMS reading descriptor\n");
                                        /* just in case things foul up */
                                        exit(j);
                                        }
                        }

                c=c+j;

/*

Convert the ASCII characters in the TEMP array to integer format and put the result in DESC. The first
two runs through the i loop are ignored because they contain (1) the #L format specifier and (2) the
number of transferred bytes. This information is not needed.

*/

                for( k=0; k<j-1; k++){   d[i-2]=d[i-2]+(temp[k]-48)*pow(10,(j-2)-k);
                        }

                /*printf("d[%d]=%3d\n",i-2,d[i-2]);*/

                }


        /*.....*/

        /*.....*/
        /*      get fixed verticle gain         */
        /*              VGain                   */
        /* The verticle gain is stored in the desc
             array at position 0.               */


                _VGain=d[0];
                gainv = _VGain-22;  /* This is done so that gainv mod[3] =0 can be
                                                made to represent the number 5.
                                                */
                gain = div(gainv,3); VGain=5*pow(2,gain.rem)*pow(10,gain.quot-
                3);



        /*.....*/

        /*.....*/
        /*    get variable verticle gain  */
        /*              vvgain

           The verticle gain is stored in the desc
           array in position 1.

        */
```

```
                _vvgain=d[1];
    vvgain = .4 + _vvgain*.005;


 /*.....*/

 /*.....*/
 /*   get  verticle offset  */
 /*                voff

    The verticle offset is stored in the desc
    array as a 16 bit integer in positions 4 and 5.

 */

                _voff=256*d[4]+d[5];
                  voff = VGain*(-8 + _voff*.04);

 /*.....*/

/*     get  timebase  */
/*                tbase

    The time base is stored in the desc
    array in position 9.

 */

      gainv = d[9];
                  gainv = gainv-2;  /* This is done so that gainv mod[3]
                                       =0 can be made to represent the number 5. */
            gain = div(gainv,3);
              tbase = 5*pow(2,gain.rem)*pow(10,gain.quot-10);


 /*.....*/
 /*.....*/
/*     get  sampling interval  */
/*                sint

    The sampling interval is stored in the desc
    array in position 10.

 */

      gainv = d[10];
      spp=gainv;

                  if ( gainv>16&&gainv<37){
                        gainv = gainv-14;  /* This is done so that gainv mod[3] =0 can be
                                              made to represent the
                                              number 5. */
                        gain = div(gainv,3);
                        sint=10*pow(2,gain.rem+1)*pow(10,gain.quot10);}
```

```
                                        if(d[10]==16)
                                           sint=10e-9;

                                        if(gainv<16)
                                       gainv=999.999999999;

                    if ( gainv>58&&gainv<93){
                         gainv=gainv-57;
                         gain = div(gainv,3);
                         sint = 5*pow(2,gain.rem)*pow(10,gain.quot-7);


/*   pdiv
     Get the number of measured data points per division.  This information is      stored as a
 16 bit integer in positions 22 and 23 of the desc array*/

                                  pdiv = 256*d[22] + d[23];


/*     fadd
     Get the position of the first measured data point relative
     to the left-hand edge of the screen.
     This information is stored as a 16 bit integer in positions 24 and 25 of the      desc array
*/

                                  fadd = 256*d[24] + d[25];



/*     ladd
     Get the position of the last measured data point relative
     to the left-hand edge of the screen.
     This information is stored as a 16 bit integer in positions 26 and 27 of the      desc array
*/

                                  ladd = 256*d[26] + d[27];

/*     pv
     Get the "power of volts" used in constructing the generalized units used in      waveform
processing ( see page 10-15 ).
     This information is stored as a 16 bit integer in positions 36 and 37 of the      desc array
*/

                                  pv = 256*d[36] + d[37];



/*          ps
     Get the position of the last measured data point relative
     to the left-hand edge of the screen.
     This information is stored as a 16 bit integer in positions 38 and 39 of the      desc array                */

                             ps = 256*d[38] + d[39];
```

```
        /*.....*/
        /*   Print out optional discriptor data */

      printf(" \nDo you want to see the descriptor data (y/n)?\n");
              i=getchar();
              i=getchar();
    if(i=='y'){
                        printf("\n");
                        printf("..... verticle gain (V/div) = %3.3e\n", VGain);
                        printf("..... variable verticle gain = %3.3f\n", vvgain);
                        printf("..... verticle offset (V) = %3.3f\n"voff);
                        printf("..... time base  (sec) = %3.9e\n"tbase);
                        printf("..... sampling interval (sec)  = %3.9e\n", sint);
                        printf(".....number of measured points/div = %6d\n",pdiv);
                        printf(".....address of first point = %6d\n", fadd);
                        printf(".....address of last point = %6d\n", ladd);
                        printf(".....power of volts = %6d\n", pv);
                        printf(".....power of seconds = %6d\n\n", ps);
              }
       printf("done... ibcnt = %ld, ibsta = %d, iberr=%d\n\n", ibcnt, ibsta, iberr);

/*.....*/

}



        /* read data from the scope to the file called VOLT  */
RDAT(d,t,dt,skope,fmat)
int d[],skope,fmat;
double t[],dt;
{

int nbyte,k,i,fd4;
double avg,stor;
float dum;
char temp[8],fn[13], merl[18],**endptr;
FILE *fd3;

        /* open the output file used by CRICKET GRAPH to plot the data       */
              fn[12]='\0';
              printf("ENTER filename to save transformed data to: ");
              scanf("%s",fn);
              fd3 = fopen(fn,"w");

                printf(" reading data from oscilloscope\n");
                ibrdf(skope, "RAW");
                printf("# transferred data bytes = %ld status=%d, err=%d\n", ibcnt, ibsta, iberr);

                fd4=open("RAW",0);
/*     The first 7 bytes of data are #L<count>.  These are of no interest at
     this point so they are read and discarded.    */
                        nbyte=read(fd4, temp,7);

/*    Read the data from the ASCII file VOLT and convert them to
```

real values. Store these values in the TEMPP array for later use. Write the results to the file OUTPUT. Find the maximum, minimum and average values of the data.These will be used later for plotting histograms. */

```
                k=0;
                nbyte=read(fd4, merl,fmat);
        printf("        WRITING DATA TO OUTPUT FILE \n");
        if (spp<37)
            fprintf(fd3,"time (sec)\tvolts\r");
        if (spp>58)
            fprintf(fd3,"frequency (Hz)\tdbm\r");

        while (nbyte==fmat){

                stor=strtod(merl,endptr);


                if(fmat==3){
                    t[k] = VGain*((stor-128)/32 - ((256*d[4]+d[5])-
                                200)/25)*200/(d[1] + 80);
                      }
                  else{
                      t[k] = VGain*((stor-32768)/8192 - ((256*d[4]+d[5])-
                                200)/25)*200/(d[1] + 80);
                      }

                   /* see page 7-50 DOOM */

                     fprintf(fd3,"%e\t%f\r",dt*k,t[k]);

                  k=k+1;
                  nbyte=read(fd4, merl,fmat);
            }

    close(fd4);
    fclose(fd3);
    count=k;

}
```

Correlation Function Program

```
#include <console.h>
#include <stdlib.h>
#include <math.h>
#include <fcntl.h>

double SCON(char *strng);

main()
{

char  file1[8],file2[8],data1[15],data2[15];
double num1,num2,crscr,mean1,mean2;
int i,j,k,l,n,r;
FILE *fd1,*fd2,*fd3;

file1[8]='/0';
  printf("enter the name of the first file to open\n");
  scanf("%s",file1);
  fd1=fopen(file1,"r");

file2[8]='/0';
  printf("enter the name of the second file to open\n");
  scanf("%s",file2);
  fd2=fopen(file2,"r");

/* count the number of elements in the file*/
  i=0;
  while(fscanf(fd1,"%s",data1)>0){
      i=i+1;
      }
  rewind(fd1);
  printf("number of elements in file 1 = %i\n", i);
  n=i;

  i=0;
  while(fscanf(fd2,"%s",data1)>0){
      i=i+1;
      }
  rewind(fd2);
  printf("number of elements in file 2 = %i\n", i);
   n=(n-3)/2;
 /*n=(n-2)/2;*/

/*Scan in the first two time ticks for each file and compare their difference*/
/* First get rid of the column headers */

i=0;
/* 4 used to be 5*/
while(i<5){
fscanf(fd1,"%s",data1);
printf("%s\n",data1);
i=i+1;
}
```

```
i=0;
while(i<5){
fscanf(fd2,"%s",data2);
printf("%s\n",data2);
i=i+1;
}

fscanf(fd1,"%s",data1);
fscanf(fd2,"%s",data2);

if(strcmp(data1,data2)!=0){
  printf("\n\n\n\n\n\n\n\n\n\n\n\n\n%s\n",data1);
printf("%s\n",data2);
printf("\a\a\a");
  abort();
  }

rewind(fd1);
rewind(fd2);

/* calculate mean values */
/*  for FILE 1:      */
  i=0;
  while(i<3){
       fscanf(fd1,"%s",data1);
       i=i+1;
       }
  i=0;
  mean1=0;
  while(i<n){
      fscanf(fd1,"%s",data1);
      fscanf(fd1,"%s",data1);
      mean1=mean1+SCON(data1);
      i=i+1;
      }
  mean1=mean1/n;
  printf("mean1 = %f\n",mean1);

  rewind(fd1);

/*  for FILE 2:      */
  i=0;
  /* 2 or 3 */
  while(i<3){
       fscanf(fd2,"%s",data2);
       i=i+1;
       }
  i=0;
  mean2=0;
  while(i<n){
      fscanf(fd2,"%s",data2);
      fscanf(fd2,"%s",data2);
      mean2=mean2+SCON(data2);
      i=i+1;
      }
  mean2=mean2/n;
  printf("mean2 = %f\n",mean2);
```

```
  rewind(fd2);


i=0;
/* 3 or 4 */
while(i<4){
    fscanf(fd1,"%s",data1);
    fscanf(fd2,"%s",data2);
    i=i+1;
    }
 printf("START\n");


/* calculate cross correlation coefficients using the formula on page 298
  of Bendat and Piersol.                                          */
  fd3=fopen("output","w");

for(r=0;r<=(.75*n);r++){

     for(j=0;j<2*r; j++){
        fscanf(fd2,"%s",data2);
        }
    crscr=0;
    for(i=0;i<n-r; i++){
       fscanf(fd1,"%s",data1);
       fscanf(fd2,"%s",data2);
       crscr=crscr+(SCON(data1)-mean1)*(SCON(data2)-mean2);
      /* printf("i=%i,  %e   %e\n",i,SCON(data1),SCON(data2));*/
       fscanf(fd1,"%s",data1);
       fscanf(fd2,"%s",data2);
      }

   crscr=(1./(n-r))*crscr;
   printf("r=%i   cross correlation coefficient = %f\r", r,crscr);
   fprintf(fd3,"%i\t%e\r",r,crscr);
   rewind(fd1);
   rewind(fd2);
   i=0;
   /* 3 used to be 4*/
   while(i<4){
       fscanf(fd1,"%s",data1);
       fscanf(fd2,"%s",data2);
       i=i+1;
       }


}

fclose(fd3);
}


double SCON(char *strng)
{
int j,k,l,s;
double num;
```

```
j=strlen(strng);
k=strcspn(strng,".");
  l=0;
  s=0;
if(strng[0]=='-'){
  l=1;
  s=1;
  }
  num=0;
  while(l<k){
     num=num+pow(10,k-1-l)*(strng[l]-48);
     l=l+1;
     }
  l=0;
  while(l<(j-k-1)){
      num=num+pow(10,-(l+1))*(strng[l+k+1]-48);
      l=l+1;
     }
     if(s==1)num=-num;
return num;
     }
```

References

[1] Martinez-Sanchez, M., Hastings, D. E., "A systems study of a 100 kW electrodynamic tether", J. Astro. Sci., **35**, 1, 1987.

[2] *Plasma Contactor Research - 1989,* John D. Williams, NASA annual report for grant NAG 3-776, NASA CR-185212, February, 1990.

[3] Olsen, R. C. "Record charging event from the applied technology satellite 6", J. Spacecraft, **24**, 4, 1987.

[4] Parks, D. E. et al, "Threshold-determining mechanism for discharges in high-voltage solar arrays", J. Spacecraft, **24**, 4, 1987.

[5] Siskind, D. E., et al, "Interactions between the orbiting space shuttle and the ionosphere", Planet. Space. Sci., **32**, 7, 1984.

[6] Hwang, K. S., et al, "The emissions of broadband electrostatic noise in the near vacinity of the shuttle orbiter", 1987.

[7] Stone, N. H., et al, "Further observations of space shuttle plasma-electrodynamic effects from OSS-1/STS-3", Geophys. Res. Lett., **13**, 3, 1986.

[8] Katz, I., Davis, V. A., "Ram ion scattering caused by space shuttle v x B induced differential charging", J. Geophys. Res., **92**, A8, 1987.

[9] Greene, M., Wheelock, D., Baginski, M., "Electrodynamics of the getaway tether experiment", J. Spacecraft, **26**, 6, 1989.

[10] *The Collected Works of Irving Langmuir, Volume 3,* C. Guy Suits editor, Pergamon Press, New York, 1961, pp. 6.

[11] *The Oxide-Coated Cathode*, Phil. S. Wagener, Chapman & HAll, LTD., London, 1951, pp. 35.

[12] *Ionized Gases*, A. von Engel, Clarendon Press, Oxford, 1965, pp. 10.

[13] *Ionization Phenomena in Gases,* Gordon Francis, Butterworths Scientific Publications, London, 1960, pp. 134.

[14] *The Collected Works of Irving Langmuir, Volume 4,* C. Guy Suits editor, Pergamon Press, New York, 1961, pps. 29-32.

[15] Parker, L. W., Murphy, B. L., "Potential buildup on an electron-emitting ionospheric satellite", J. Geo. Res., **72**, 5, 1967.

[16] Wei, R., Wilbur, P. J., "Space-chargeLimited current flow in a spherical double sheath", J. Appl. Phys, **60**, 7, 1986.

[17] Iess, L., Dobrowolny, M., "The interaction of a hollow cathode with the ionosphere", Phys. Fluids B, **1**, 9, 1989.

[18] Levine, J. S., Crawford, F. W., " Probe measurements of double-layers in a pulsed discharge", J. Plasma Physics, **24**, 2, 1980.

[19] Block, Lars P., "Potential double layers in the ionosphere", Cosmic Electrodynamics, **3**, 1972.

[20] Montgomery, D., Joyce, G., "Shock-like solutions of the electrostatic Vlasov equation", J. Plasma. Phys., **3**, 1, 1969.

[21] Berstein, I. B., Greene, J. M., Kriskal, M. D., "Exact nonlinear plasma oscillations", Phys. Rev., **108**, 3, 1957.

[22] Van Kampen, N. G., "On the theory of stationary waves in plasmas", Physica XXI, 1955, pp. 949.

[23] Hershkowitz, N., "Review of recent laboratory double layer experiments", Sp. Sci. Rev., **41**, 1985.

[24] Carlqvist, P., "On the formation of double layers in plasmas", Cosmic Electrodynamics, **3**, 377, 1972.

[25] Block, L. P., "Double layers", in *Physics of the hot plasma in the ionosphere*, B. Hultqvist and L. Stenflo, Eds., Plenum Press, New York, 1975,pp. 229-249.

[26] Quon, B. H., Wong, A. Y., "Formation of potential double layers in plasmas", Phys. Rev. Lett., **37**, 21, 1976.

[27] *Advanced space propulsion and plasma contactor research*, Paul J. Wilbur, NASA annual report for grant NGR-06-002-112, NASA CR-175119, January, 1986.

[28] Hairapetian, G., Stenzel, R. L., "Observation of a stationary, current-free double layer in a plasma", Phys. Rev. Lett., **65**, 2, 1990.

[29] Chan, C., Hershkowitz, N., Payne, G. L., "Laboratory double layers with no external fields", Phys. Lett., **83A**, 7, 1981.

[30] Gerver, M. J., Hastings, D. E., Oberhardt, M. R., "Theory of plasma contactors in ground-based experiments and low earth orbit", J. Spacecraft, **27**, 4, 1990.

[31] Hastings, D. E., Blandino, J, "Bounds on current collection from the far field by plasma clouds in the ionosphere", J. Geophys. Res., **94**, A3, 1989.

[32] Hastings, D. E., "Theory of plasma contactors used in the ionosphere", J. Spacecraft, **24**, 3, 1987.

[33] Drell, S. D., Foley, H. M., Ruderman, M. A., "Drag and propulsion of large satellites in the ionosphere: An Alfven propulsion engine in space", J. Geo. Res., **70**, 13, 1965.

[34] Urrutia, J. M., Stenzel, R. L., "Anomalous currents to an electrode in a magnetoplasma", Phys. Rev. Lett., **57**, 6, 1986.

[35] Urrutia, J. M., Stenzel, R. L., "Transport of current by whistler waves", Phys. Rev. Lett., **62**, 3, 1989.

[36] Urrutia, J. M., Stenzel, R. L., "Modeling of induced currents from electrodynamic tethers in a laboratory plasma", Geophys. Res. Lett., **17**, 10, 1990.

[37] *Whistlers and Related Ionospheric Phenomena*, R. A. Helliwel, Stanford University Press, Stanford, CA, 1965.

[38] Stenzel, R. L., Urrutia, J. M., "Whistler wings from moving electrodes in a magnetized laboratory plasma", Geophys. Res. Lett., **16**, 5, 1989.

[39] Stenzel, R. L., Urrutia, J. M., "Currents between tethered electrodes in a magnetized laboratory plasma", J. Geo. Res., **95**, A5, 1990.

[40] Mather, J. W., Ahluwalia, H. S., "The geomagnetic field - an explanation for the microturbulence in coaxial gun plasmas", IEEE Trans. Plas. Sci., **16**, 1, 1988.

[41] Terry Sheridan, Ph.D. thesis, Dartmouth College, Hanover, New Hampshire, 1986.

[42] Brown, M. R., Sheridan, T. E., Hayes, M. A., "Reentrant cavity as a low power plasma source", Rev. Sci. Instrum., **57**, 12, 1986.

[43] *Klystrons and Microwave Triodes*, D. R. Hamilton, J. K. Knipp and J. B. H. Kuper, eds., MIT radiation Lab Series vol. 7, McGraw Hill, New York, 1948, pps 73-79.

[44] Buchsbaum, S. J., Mower, L., Brown, S. C., "Interaction between cold plasmas and guided electromagnetic waves", Phys. Fluids, **3**, 5, 1960.

[45] Rose, D. J., Brown, S. C., "Methods of measuring the properties of ionized gases at high frequencies. III. Measurement of discharge admittance and electron density", J. App. Phys., **23**, 9, 1952.

[46] Brown, S. C., "Microwave studies of gas discharge plasmas", Proceedings of the Second International Conference on the Peaceful Uses of Atomic Energy, 32, 394, CERN Scientific Information Service, Geneva, 1958.

[47] Brown, S. C., Rose, D. J., "Methods of measuring the properties of ionized gases at high frequencies. I. Measurements of Q", J. App. Phys., **23**, 7, 1952.

[48] *Plasma Diagnostics, Volume 1*, O. Auciello and D. L. Flamm eds., Academic Press, New York, 1989.

[49] Kuninaka, H., Kuriki, K., "Numerical analysis of interaction of a high-voltage solar array with the ionospheric plasma", J. Spacecraft, **24**, 6, 1987.

[50] Stone, N. H., et al., "Multiple ion streams in the near vacinity of the space shuttle", Geophys. Res. Lett., **10**, 12, 1983.

[51] Stenzel, R. L., Urrutia, J. M., "Laboratory model of a tethered balloon-electron beam current system", Geophys. Res. Lett., **13**, 8, 1986.

[52] *Plasma Waves,* D. G. Swanson, Academic Press, New York, 1989, pp. 53.

[53] *Handbook on Plasma Instabilities, Volume 1*, Ferdinand F. Cap, Academic Press, New York, 1976, pp. 102.

[54] Hastings, D. E., "Enhanced curent flow through a plasma cloud by induction of plasma turbulence", J. Geophys. Res., **92**, A7, 1987.

[55] Klozenberg, J. P., McNamara, B., Thonemann, P. C., "The dispersion and attenuation of helicon waves in a uniform cylindrical plasma", J. Fluid. Mech., **21**, 3, 1965.

[56] Hershkowitz, N., in *Plasma Diagnostics, Vol. 1*, pp. 113-184, O. Auciello and D. L. Flamm eds., Academic Press, New York, 1989.

[57] Kemp, R. F., Sellen, J. M., "Plasma potential measurements by electron emissive probes", Rev. Sci. Instrumen., **37**, 4, 1966.

[58] Yao, W. E., Intrator, T., Hershkowitz, N., "Direct indication technique of plasma potential with differential emissive probe", Rev. Sci. Instrum., **56**, 4, 1985.

[59] Smith, J. R., Hershkowitz, N., Coakley, P., "Inflection-point method of interpreting emissive probe characteristics", Rev. Sci. Instrum., **50**, 2, 1979.

[60] Benjamin, N., "High-impedeance capacitive divider probe for potential measurements in plasmas", Rev. Sci. Instrumen., **53**, 10, 1982.

[61] Roth, J. Reece, Krawczonek, W.M., " Paired comparison tests of the relative signal detected by capacitive and floating langmuir probes in turbulent plasma from 0.2 to 10 MHz", Rev, Sci. Inst., **42**, 5, 1971.

[62] Schmidt, J., A., "High impedance Langmuir probe", Rev. Sci. Instrum., **39**, 9, 1968.

[63] Stenzel, R. L., "High-frequency noise on antennas in plasmas", Phys. Fluids B, **1**, 7, 1989.

[64] Stenzel, R. L.,"Lower-hybrid turbulence in a nonuniform magnetoplasma", Phys. Fluids B, **3**, 9, 1991.

[65] Whelan, D. A., Stenzel, R. L., "Electromagnetic radiation and nonlinear energy flow in an electron beam-plasma system", Phys. Fluids, **28**, 3, 1985.

[66] Stenzel, R. L., Gekelman, W., "Magnetic field line reconnection experiments 1. Field topologies", J. Geophys. Res., **86**, A2, 1981.

[67] Stenzel, R. L., Gekelman, W., Wild, N., "Magnetic field line reconnection experiments 4. Resistivity, heating and energy flow", J. Geo. Res., **87**, A1, 1982.

[68] Lovberg, R. H., in *Plasma Diagnostic Techniques*, pp 65-111, R. H. Huddlestone and S. L. Leonard, eds., Academic Press, New York.

[69] Stenzel, R. L., "Antenna radiation patterns in the whistler wave regime measured in a large laboratory plasma", Radio Sci., **11**, 12, 1976.

[70] *The Art of Electronics*, P. Horowitz and W. Hill, Cambridge University Press, New York, 1981, pp. 288.

[71] Phillips, R. C., Turner, E. B., "Construction and calibration techniques of high frequency magnetic probes", Rev. Sci. Instrum., **36**, 12, 1965.

[72] Chan, C., Lonngren, K. E., Hershkowitz, N., "Electrostatic ion cyclotron instability driven by a defelected ion beam", Phys. Lett., **78A**, 1, 1980.

[73] *Theory of Plasma Instabilities, Vol. 1,* A. B. Mikhailovskii, Consultants Bureau, Plenum Publishing, New York, 1974, pg. 235.

[74] Stenzel, R. L., et al., "Directional velocity analyzer for measuring electron distribution functions in plasmas", Rev. Sci. Instrum., **54**, 10, 1993.

[75] Medicus, G., "Diffusion and eleastic collision losses of the "fast electrons" in plasmas", J. App. Phys., **29**, 6, 1958.

[76] Gekelman, W., Stenzel, R. L., "Ion sound turbulence in a magnetoplasma", Phys. Fluids, **21**, 11, 1978.

[77] Guyot, M., Hollenstein, Ch., "Experiments on potential gradients in a current-carrying plasma. I. Potential structures", Phys. Fluids, **26**, 6, 1983.

[78] *Measurement and Analysis of Random Data*, Julius S. Bendat, Allen G. Piersol, 1966, John Wiley & Sons, New York.

VITA

Richard Logan was born in 1962 in Brentwood, New York. He graduated with an AB degree from Cornell University in 1984. In September, 1984, Mr. Logan entered Northeastern University's graduate physics program, specializing in experimental particle physics. He spent some time at the European Center for Nuclear Research (CERN) and participated in the design and calibration of a muon chamber calibration system used on the L3 experiment. While in Boston, Mr. Logan worked part time at the Harvard-Smithsonian Center for Astrophysics as a computer specialist.

In 1987, Rich left Northeastern to work (briefly) in the optics industry and study classical mechanics. He enrolled in Georgia Tech's nuclear engineering program in the fall of 1988. While at Tech, Rich met Dr. Mike Hayes and the two of them developed a successful proposal (funded by NASA) to study the interaction of plasma contactors with the ionosphere. When Mike left the nuclear engineering program the following year, Rich independently continued the research. Since 1993, Rich has been working as a research scientist at Shonka Research Associates.

Dr. Logan would like to build a career either in experimental space physics or in semiconductor processing research. To this end, he has submitted proposals to the Small Business Innovative Research program to develop a high specific impulse ion thruster and to develop a small magnetic probe for measuring high frequency emissions from circuit boards.